

**STRUCTURAL DEVELOPMENT AND PALEOSEISMICITY  
OF THE HURRICANE FAULT, SOUTHWESTERN UTAH  
AND NORTHWESTERN ARIZONA**

**Geological Society of America  
2002 Rocky Mountain Section Annual Meeting  
Cedar City, Utah  
May 5 and 6, 2002**



*View to the northwest of a lava cascade over the Hurricane Cliffs near the Utah – Arizona border.*

**FIELD TRIP LEADERS**

**William R. Lund, Utah Geological Survey  
Wanda J. Taylor, University of Nevada at Las Vegas  
Philip A. Pearthree, Arizona Geological Survey  
Heidi Stenner, U.S. Geological Survey  
Lee Amoroso, Arizona State University  
Hugh Hurlow, Utah Geological Survey**

# **STRUCTURAL DEVELOPMENT AND PALEOSEISMICITY OF THE HURRICANE FAULT, SOUTHWESTERN UTAH AND NORTHWESTERN ARIZONA**

**Geological Society of America  
2002 Rocky Mountain Section Annual Meeting  
Cedar City, Utah  
May 5 and 6, 2002**

**William R. Lund, Utah Geological Survey  
Wanda J. Taylor, University of Nevada at Las Vegas  
Philip A. Pearthree, Arizona Geological Survey  
Heidi Stenner, U.S. Geological Survey  
Lee Amoroso, Arizona State University  
Hugh Hurlow, Utah Geological Survey**

## **INTRODUCTION**

The Hurricane fault is one of the longest and most active of several large, late Cenozoic, west-dipping normal faults in southwestern Utah and northwestern Arizona. Quaternary activity of the fault is indicated by the geomorphology of the high, steep Hurricane Cliffs, the result of fault slip, and by displaced Quaternary basalt flows, alluvium, and colluvium at many locations along its length. Extending from Cedar City, Utah, to south of the Grand Canyon in Arizona (figure 1), the 250-kilometer-long fault almost certainly ruptures in segments, as observed historically for other long basin-and-range normal faults (Schwartz and Coppersmith, 1984; Schwartz and Crone, 1985; Machette and others, 1992). Previous workers (Stewart and Taylor, 1996; Stewart and others, 1997; Reber and others, 2001) have suggested that major convex fault bends and zones of structural complexity are likely candidates for boundaries between present-day seismogenic fault segments and also provide evidence of fault linkage and the long-term structural development of the fault. Initial paleoseismologic investigations along the fault have suggested that some parts of the fault have ruptured more recently than others (Stenner and others, 1999; Lund and others, 2001; Amoroso and others, 2002).

Assessing the seismic hazard presented by the active Hurricane fault is important because southwestern Utah and adjacent areas of Arizona and Nevada are experiencing a now decades-long population and construction boom. A proposed pipeline from Lake Powell to the St. George basin, which would cross the Hurricane fault, could provide water for an additional 300,000 residents in southwestern Utah within the next 10 to 15 years. We have integrated recent paleoseismologic and structural studies along the Hurricane fault (Stenner and others, 1999; Lund and others, 2001; Reber and others, 2001; Amoroso and others, 2002) to more completely describe the fault's behavior through time and evaluate potential earthquake hazards.

This trip focuses on the results of the recent studies that provide insight into the Hurricane fault's long-term development and paleoearthquake history, and covers that part of the Hurricane fault between Diamond Butte in Arizona and Cedar City, Utah.

## **GEOLOGIC OVERVIEW**

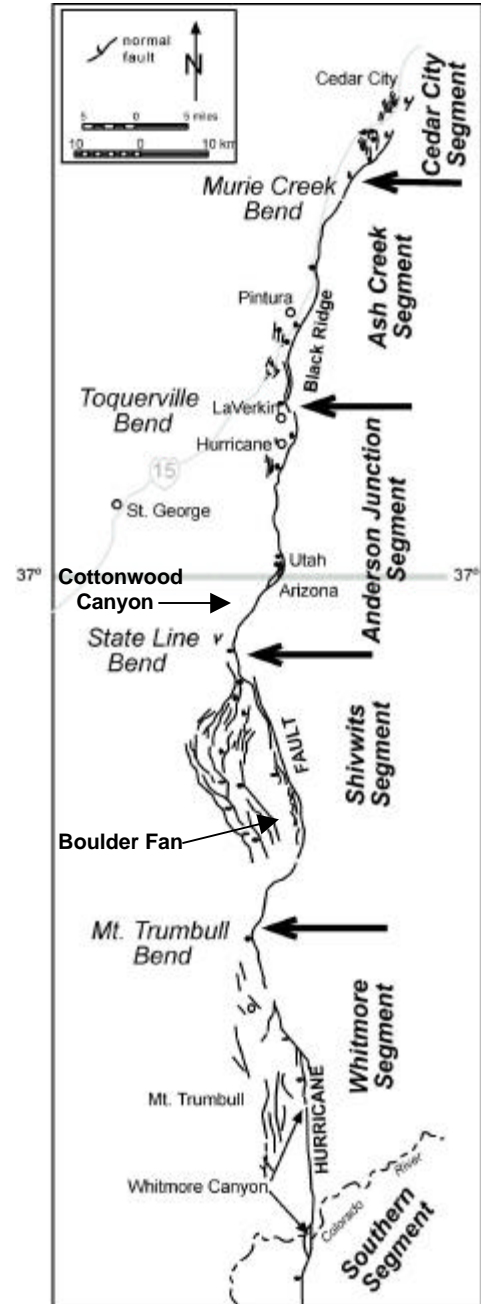
The Hurricane fault lies within the ~150-kilometer-wide structural and seismic transition zone between the Colorado Plateau and Basin and Range physiographic provinces. Within this transition zone, generally subhorizontal Paleozoic and Mesozoic strata of the Colorado Plateau

are displaced down-to-the-west by a series of generally north-striking normal faults. Although the Hurricane fault also strikes generally north-south, it includes distinct sections that strike northeast or northwest. These variations in strike produce a sinuous fault trace that, in map view, suggests the Hurricane fault is geometrically segmented.

In southwestern Utah, from Cedar City to the Arizona border, the Hurricane fault zone is the tectonic boundary between the Colorado Plateau and Basin and Range (Arabasz and Julander, 1986). In northwest Arizona, the Hurricane fault is 50 kilometers east of the Grand Wash fault, which is considered the tectonic boundary (Mayer, 1985). Huntoon (1990) considers the normal faults in northwestern Arizona and southwestern Utah to be located along Precambrian normal faults that were later reactivated (in the reverse sense) during Laramide compression and uplift. These fault zones activated again, to a lesser degree, during late-Tertiary high-angle extension (Spencer and Reynolds, 1989), and to a greater degree during the Pliocene and Quaternary as normal faults (Menges and Pearthree, 1989).

The steep Hurricane Cliffs represent a fault-line scarp that closely follows the trace of the Hurricane fault and records the displacement across the structure. Total displacement varies along strike with the largest displacements in the north and the smallest in the south. The Hurricane fault's trend cutting across the Colorado Plateau – Basin and Range Province boundary near the border may explain a displacement of more than 2,500 meters in Utah as compared with 250-400 meters in Arizona (Stewart and others, 1997). Previous studies have documented displaced Quaternary basalt flows (hundreds of meters) and late Quaternary unconsolidated alluvial and colluvial deposits (meters to tens of meters) (Hamblin, 1963, 1965a, 1970a, 1970b, 1984; Anderson and Mehnert, 1979; Pearthree and others, 1983; Menges and Pearthree, 1983; Anderson and Christenson, 1989; Hecker, 1993; Stewart and Taylor, 1996). Estimates of displacement across the Hurricane fault have varied widely, ranging from a low of 1,400-4,000 feet (Kurie, 1966) to a high of 12,000-13,000 feet (Dutton, 1880). Kurie (1966) attributed the wide range in estimates to the failure of many workers to recognize the significance of major fold structures related to the Cretaceous to Eocene Sevier orogenic belt (Armstrong, 1968), which predate and parallel the trace of the Hurricane fault over much of its length in Utah. Anderson and Mehnert (1979) attribute the displacement discrepancies to the inclusion, or lack thereof, of near-fault deformation associated with the younger tectonics.

Along the route of this field trip, the Hurricane fault displaces strata ranging in age from Permian to Quaternary (figure 2). The Paleozoic and Mesozoic strata record depositional environments ranging from marine and marginal marine to terrestrial. Deposited by wind and



**Figure 1. The Hurricane fault and proposed fault segments.**

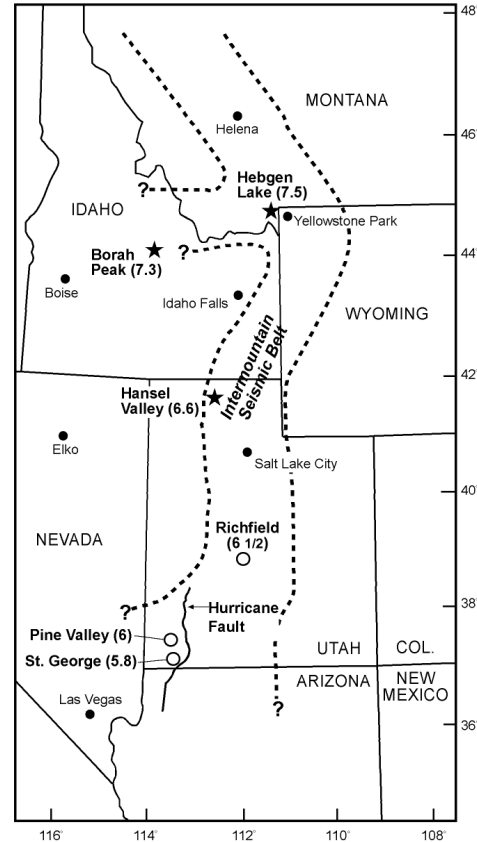
Age	Unit	Thickness (m)	Rock Type	
Q	alluvium, colluvium & fluvial units	0-70		
	basalt	0-90		
Plio	Sevier River or Muddy Creek Fm. / unnamed sed unit.	0-90		
Eocene	Tuffs & andesites - Page Ranch Volcs, Quichapa Gp., Isom tuffs, Needles Range Gp., Bullion Cyn, Osiris Tuff, Mt Dutton Fm., Brian Head, etc	0-1110		
Paleocene	Cedar Breaks / Wasatch / Claron Fms.	120-430		
	+/-Pine Hollow Fm.	0-120		
	+/-Canaan Peak Fm.	0-305		
Cretaceous	Iron Springs Formation	80-215		
Jurassic	Camel Fm	520-700		
	Triassic	Navajo Sandstone (main body)	90-370	

Age	Unit	Thickness (m)	Rock Type	
Triassic	Moenvave Fm	Springdale SS Mbr	18-35	
		Whitemore Pt Mbr	0-20	
		Dinosaur Cyn Mbr	25-120	
	Chinle Fm	Petrified Forest Member	80-120	
		Shinarump Member	0-50	
	Moenkopi Fm	upper red member	~150	
		Shnabkaib Member	~100	
		middle red member	~90	
Virgin Limestone		~40		
Permian	Kaibab Limestone	75-260		
		+/- White Rim SS	0-60	
	Toroweap Formation	30-150		
	Hermit Shale	0-30		
	Queantoweap/ Esplanade / Coconino Sandstone	300-380		
	+/- Pakoon Fm.	0-90		
Penn	Callville Limestone	60-275		

**Figure 2. Summarized and generalized stratigraphy for the entire Hurricane fault region, compiled and modified from Hintze (1980, 1988) and authors' data.**

flowing water, the terrestrial sedimentary rocks along the field trip route are generally colored distinctive red tones and have been differentially eroded to form massive, near-vertical cliffs such as those seen in Zion National Park. The approximately 20-million-year-old Pine Valley laccolith crops out west of I-15 in the Pine Valley Mountains (Cook, 1953; McDuffie and Marsh, 1991), north of St. George, Utah, and late Cenozoic cinder cones and basalt flows are common along the fault. Quaternary deposits along the fault consist of steep colluvial deposits mantling the lower Hurricane Cliffs, steep alluvial fans emanating from smaller drainages along the cliffs, and fans, terraces and channels associated with the few larger drainages that breach the cliffs.

The Colorado Plateau/Basin and Range Transition Zone is coincident with part of the Intermountain seismic belt (Smith and Sbar, 1974; Smith and Arabasz, 1991; figure 3), although this belt of earthquake epicenters becomes broader and more poorly defined from north to south. Surface rupture has not occurred along the Hurricane fault historically, but the area does have a pronounced record of seismicity. At least 20 earthquakes greater than M 4 have occurred in southwestern Utah over the past century (Christenson and Nava, 1992; figure 4). The largest events were the M 6.3 Pine Valley earthquake in 1902 (Williams and Trapper, 1953) and the M 5.8 St. George earthquake in 1992 (Christenson, 1995). The Pine Valley earthquake is pre-instrumental and poorly located, and therefore not attributable to a recognized fault. However, the epicenter is west of the surface trace of the Hurricane fault, so the earthquake may have occurred on that fault at depth. Pechmann and others (1995) tentatively assigned the St. George earthquake to the Hurricane fault. The largest historical earthquake in northwestern Arizona was the 1959 M 5.7 Fredonia, Arizona earthquake (Dubois and others, 1982). Since 1987 northwestern Arizona has experienced more than 40 events with  $M \geq 2.5$ , including the 1993 M 5.4 Cataract Canyon earthquake (Lay and others, 1994) between Flagstaff, Arizona, and the Grand Canyon (Arizona Earthquake Information Center, Arizona Earthquakes 1830 - 1998; <http://vishnu.glg.nau.edu/aeic/azcat.txt>).



**Figure 3. The Intermountain seismic belt showing major historical earthquakes and the Hurricane fault.**

## STRUCTURAL STUDIES

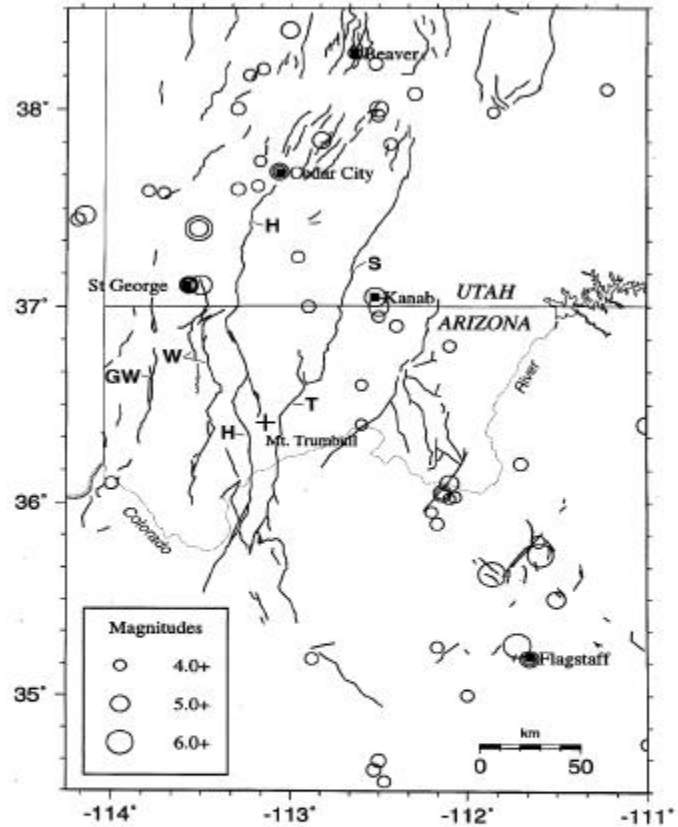
The sinuosity of the trace delineates the geometric segments along the Hurricane fault. A geometric segment is a portion of a fault that has a constant strike or a systematically and continually varying strike that results from a gently curved fault. Along normal faults, the curves of geometric segments are generally concave toward the hanging wall. From south to north, the geometric segments along the Hurricane fault are the Southern, Whitmore, Shivwitz, Anderson Junction, Ash Creek, and Cedar City segments (figure 1). We are currently investigating whether the Anderson Junction geometric segment should be divided into two geometric segments near Hurricane, Utah.

Geometric segments are separated by geometric segment boundary zones (GSBZ), which tend to have relatively sharp changes in strike. Along normal faults, GSBZ generally form bends, called salients, that are convex toward the hanging wall. In the area of this field trip, four GSBZ are present along the Hurricane fault: the Mt. Trumbull bend, the State line bend, the Toquerville bend, and the Murie Creek bend (figure 1). In addition, a possible GSBZ lies near the town of Hurricane, Utah. We interpret the GSBZ to be sites where fault segments linked.

### Structural Linkage Models

In the first stage of the evolution of a segmented fault, originally isolated faults grow toward each other by radial propagation. Eventually, if the fault spacing is small enough, the stress fields in the fault tip regions interact causing the fault tips to curve toward each other (Burgmann and others, 1994; Willemsse, 1997; Willemsse and Pollard, 2000). In cases where the fault tips overlap,

a relay ramp forms between the propagating faults in the overlap zone (Larsen, 1988; Peacock and Sanderson, 1994; Trudgill and Cartwright, 1994; Childs and others, 1995; Walsh and others, 1999). In the second stage, the propagating fault segments can physically connect to form a through-going fault, which is called "hard" linkage (Trudgill and Cartwright, 1994; Young and others, 2001). A marked change in strike typically characterizes the linkage zone (figure 5). Fault growth by segment linkage implies that the length of the fault increases dramatically when the faults join (figure 5) (Segall and Pollard, 1980; Pollard and Aydin, 1984; Peacock and Sanderson, 1991; Cowie and Scholz, 1992a, 1992b; Dawers and others, 1993; Jackson and Leeder, 1994; Cartwright and others, 1995, 1996; Schlische and Anders, 1996). In the third stage, deformation is localized on the through-going fault (Cowie and others, 1995; Cowie, 1998; Gupta and others, 1998; Young and others, 2001). The Hurricane fault is completely hard linked in the area of this field trip.



**Figure 4. Historical earthquakes and Quaternary faults in southwestern Utah and northwestern Arizona. H = Hurricane fault, W = Washington fault, GW = Grand Wash fault, S = Sevier fault, and T = Toroweap fault.**

The development of isolated or linked faults may be interpreted using displacement–distance profiles, graphs used to illustrate changes in displacement along a fault (Pollard and Segall, 1987; Walsh and Watterson, 1987; Peacock and Sanderson, 1991; Cowie and Scholz, 1992a; Burgmann and others, 1994; Peacock and Sanderson, 1996). Naturally occurring faults exhibit variations in displacement along strike that differ from predictions based on simple linear or power-law models (Peacock and Sanderson, 1996). This variability may result from fault interaction and linkage, fault bends, lithologic variations, and fault propagation rate variations (Peacock, 1991; Burgmann and others, 1994; Peacock and Sanderson, 1996). The average displacement gradient on a displacement–distance profile is steeper in a zone of interacting faults and the locus of maximum displacement of each fault shifts toward the interacting tip (Peacock and Sanderson, 1991, 1994; Willemse and others, 1996; Willemse, 1997).

If geometric bends are sites of segment linkage, then displacement gradients may be recorded near the bend on displacement - distance profiles providing that two assumptions apply: (1) slip on the original isolated faults was less near the ends than near the center, and (2) the linkage zones remain asperities at which slip is more difficult than elsewhere or the release of elastic strain concentrated around the original fault tips has not yet driven slip in the linkage zones to equalize with the rest of the fault. To illustrate displacement variations near linkage zones with geometric bends, Taylor and others (2001) generated synthetic displacement - distance profiles for three different styles of hard linkage: underlapping, overlapping, and fault



capture (figure 5). The profiles allow comparison of the observed total displacement at various positions along a fault to idealized map view examples of each type of linkage. The offsets across the faults are summed in areas of overlap. Where underlapping faults linked, displacement decreased at the bend because fault tip zones have less displacement than the middle regions of a fault (figure 5a). The minimum, which is at the center of the displacement decrease, is relatively sharp. Where overlapping faults linked at a bend relatively near both fault tips, displacement decreased, but a bench formed in the displacement-distance profile in the area of original overlap (figure 5b). The along-strike length of the bench is proportional to the length of fault overlap. Where faults linked by segment capture, either a decrease or increase could occur with a significant displacement gradient on one side of the site of linkage and little or no appreciable displacement gradient, or a plateau, on the opposite side (figure 5c). The significant gradient occurred in the area of overlap. The plateau occurred along the fault or segment that remained relatively static and that was captured. The plateau would be relatively constant (horizontal) if the linkage site is within the zone where fault slip is relatively constant, typically the central one-third of the fault. A slope in the plateau suggests a displacement gradient along the captured fault. The gradient may have existed prior to linkage. Alternatively, the gradient may have formed during post-linkage slip. Post-linkage slip is not illustrated in figure 5. The point of transition between the plateau and the gradient occurred near the site where the tip of the propagating fault intersected the relatively static fault.

Total displacement versus distance patterns around salients are consistent with at least four of the GSBZ in the Hurricane fault being sites of segment linkage. A through-going fault surface and displacement minima are present at these GSBZ (see Stop 1-3). Therefore, we suggest that the GSBZ at the Mt. Trumbull, State Line, Toquerville, and Murie Creek bends, are sites where fault tips (at which displacement is zero) linked. In addition, the post-linkage displacement history is not great enough to have erased the minima.

Post-linkage displacement can have a variety of effects on subsequent fault history. The elastic strain build up may drive additional slip in the linkage zone, which would cause an increase in post-linkage slip rates near the linkage zone. The modeled tendency for faults to maintain a constant length to displacement ratio that approaches a power law relationship could increase or decrease slip rates at appropriate sites along the fault. In general, the step-wise length increase during linkage will increase slip without increasing fault length after linkage. In addition, the large bends created during linkage may prove unstable and new fault splays may be generated that effectively straighten the fault. Therefore, the presence of a geometric salient that is a site of segment linkage cannot be used as a simple predictor of subsequent fault history without data on post-linkage slip.

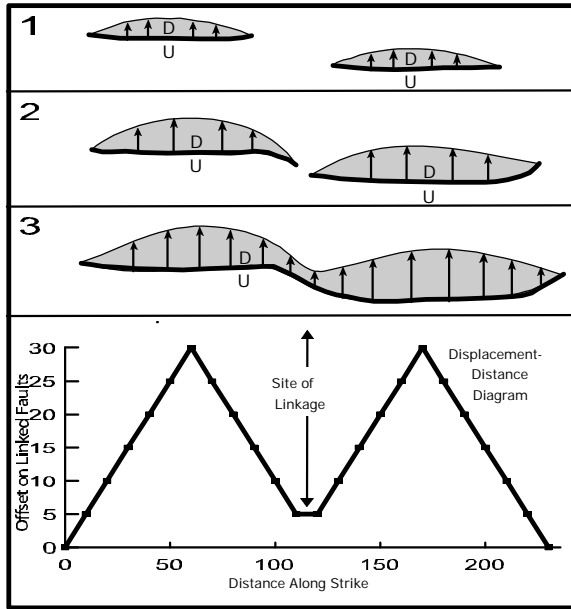
### **Reactivation of Older Structures**

In structural studies, it is common to consider whether younger faults reactivate older structures. In the case of linked and segmented faults, such as the Hurricane fault, such a consideration is complicated by two factors: (1) the variations in strike along the length of the fault, and (2) the possibility that different older structures may have been reactivated by different segments (i.e., different original faults).

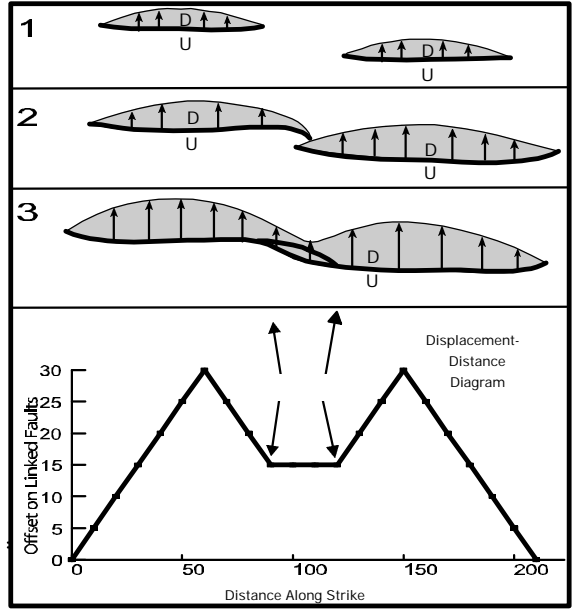
Much of the Ash Creek segment lies near subhorizontal to gently plunging upright open folds that formed during the Mesozoic Sevier orogeny. Two of these folds are most popularly called the Pintura anticline and the Kanarra anticline. The trend of these folds generally parallels the strike of much of the Ash Creek segment. However, the fault does not lie along the core of either fold or the likely location of the intervening syncline. The similarities in fault segment strike and dip and the fold axial surfaces suggests the possibility that along the Ash Creek segment the fault reactivated an axial planar cleavage or fracture. The Hurricane fault appears to depart from this trend at the Toquerville bend.

South of the Toquerville bend, the strike of the Anderson Junction geometric segment veers away from the trend of the Sevier-related folds, including the Virgin anticline. The trend of the Virgin anticline is more northeasterly than the strike of most of the fault segment. Whether this geometric segment reactivates another pre-existing structure is difficult to assess at this time, largely due to levels of exposure.

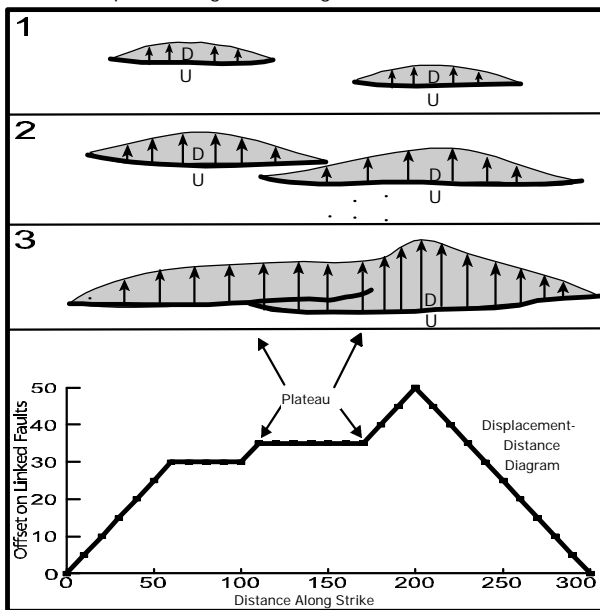
A. Linkage of Underlapping Fault Segments



B. Linkage of Overlapping Fault Segments



C. Fault Capture Along Connecting Faults



**Figure 5. These conceptual models show map view patterns (upper) and displacement vs. distance graphs (lower) for idealized cases of (A) linkage of underlapping faults, (B) linkage of overlapping faults and (C) fault capture. The map patterns show three sequential stages in the development of linkage (1, 2 and 3). The heavyweight lines represent the fault traces. The lightweight line represents the slip distribution projected into map view. The arrows qualitatively show displacement vectors projected into map view. The displacement (offset) – distance diagrams show patterns of offset predicted around sites where different types of linkage took place. Underlapping fault linkage produces a sag in the diagram, while overlapping fault linkage produces a bench. Fault capture produces a plateau. These graphs represent situations where the post-linkage magnitude of slip around the linkage site is relatively small in comparison to the total displacement. Modified from Taylor and others (2001).**



The long northern sections of both the Shivwitz and Southern geometric segments strike generally subparallel to Middle Proterozoic faults. Normal faults about 1.1 billion years in age exposed in the Grand Canyon strike northwest (Timmons and others, 2001). Some of these faults were reactivated during the Laramide orogeny. The parallelism suggests the possibility that sections of the Shivwitz and Southern geometric segments reactivated these older faults. However, additional data and analysis are needed to further evaluate this suggestion.

### **Linkage and Quaternary Displacements**

Because of segment linkage, it is possible to form faults that are too long to rupture during a single earthquake. Thus, a question arises: Are post-linkage earthquakes confined to the original segments or do earthquake ruptures cross original segment boundaries? To date, various data sets and publications present conflicting alternatives. Walsh and Watterson (1991) suggested that structural linkage implies kinematic linkage. dePolo and others (1991) used empirical data to suggest that large magnitude earthquakes can rupture across GSBZ, but relatively small magnitude earthquakes are unlikely to do so. Mansfield and Cartwright (2001), using analog models, suggested that linked faults tend toward a long-term consistency in the displacement pattern along strike. However, on time scales that are short relative to the entire growth history of the fault, component segments may have independent activity and displacement, often for long time periods after hard linkage. Other studies show variations or other influences on the mechanics during and after linkage (Cowie and Roberts, 2001; Shipton and Cowie, 2001; Maerten and others, 2002). Given the paleoseismic data described below, we suggest that the Ash Creek and Anderson Junction geometric segments probably acted as independent rupture segments in the recent past. Whether the Shivwitz geometric segment is also an earthquake rupture segments is uncertain. Without further data we cannot exclude the possibility that recent ruptures have been located along segments of the fault defined by factors other than geometry.

### **Structural Conclusions**

1. The sinuosity of the trace of the Hurricane fault indicates that the fault is geometrically segmented. It consists of at least six geometric segments from south to north: Southern, Whitmore, Shivwitz, Anderson Junction, Ash Creek, and Cedar City. The segments are separated by the Mt. Trumbull, State Line, Toquerville, and Murie Creek bends.
2. We suggest that fault linkage occurred at the bends. Along the State Line bend linkage occurred by fault capture. Along the Toquerville bend linkage of underlapping faults occurred.
3. The orientations of some sections of the geometric segments may be controlled by older structures that were reactivated. Much of the Ash Creek segment parallels nearby Sevier-age folds. Long sections of the Southern and Shivwitz geometric segments parallel Middle Proterozoic normal faults exposed near the Grand Canyon.
4. The available data suggest that the Toquerville and Murie Creek geometric bends may still be an earthquake rupture boundary. However, additional data are needed for greater certainty of this interpretation. Existing paleoseismic data do allow certain conclusion about whether the State Line geometric bend is still an earthquake rupture boundary.

### **PALEOSEISMIC STUDIES**

The Hurricane fault has long been recognized as a potential source of large earthquakes in southwestern Utah and northwestern Arizona, but a general lack of definitive evidence for latest Pleistocene or Holocene surface rupture has made assessing the seismic hazard presented by the Hurricane fault problematic. Detailed paleoseismic investigations conducted over the past several years have begun to illuminate the recent history of surface-rupturing

earthquakes along the fault zone. We summarize the results of these investigations in this section.

### Previous Workers

In addition to its structural characteristics, geologists have long been interested in the amount and timing of displacement on the Hurricane fault. Huntington and Goldthwait (1904, 1905) first introduced several important ideas regarding the Hurricane fault, including: (1) the fault partially follows an older fold and thrust belt, (2) displacement decreases from north to south, (3) much of the southern escarpment has retreated eastward from the trace of the fault, suggesting a long period of quiescence or long recurrence interval, and (4) offset has been episodic through time. Averitt (1964) prepared a chronology of post-Cretaceous geologic events on the Hurricane fault. Hamblin (1963, 1970a, 1987) studied late Cenozoic basalts along and near the fault in southwestern Utah and northwestern Arizona. His observations regarding displaced basalt flows resulted in several papers on the tectonics and rate of slip on the Hurricane fault (Hamblin, 1965a, 1965b, 1970b, 1984; Hamblin and Best, 1970; Hamblin and others, 1981). Anderson and Mehnert (1979) reinterpreted the history of the Hurricane fault, refuting several key elements of Averitt's (1964) fault chronology. They also provided a much smaller estimate of total net vertical displacement across the fault in Utah.

Several seismotectonic studies have been conducted along or near the Hurricane fault. Earth Sciences Associates (1982) mapped generalized surficial geology and photo lineaments along the fault and trenched scarps and sites of photo lineaments that cross U.S. Soil Conservation Service (now Natural Resources Conservation Service) flood-retention structures in southern Utah. Based on historical seismicity and existing geologic data, they estimated an average return period of 1,000-10,000 years for large, surface-faulting earthquakes (M 7.5) on the Hurricane fault. Menges and Pearthree (1983) conducted reconnaissance field investigations of the Hurricane fault in Arizona. They suggested that several portions of the fault ruptured as recently as the early Holocene or latest Pleistocene. Anderson and Christenson (1989) compiled a 1:250,000-scale map of Quaternary faults, folds, and selected volcanic features in the Cedar City 1°x2° quadrangle based on existing data and reconnaissance field work. The apparent absence of young fault scarps in unconsolidated deposits along the fault in Utah led them to conclude that a surface-faulting earthquake probably had not occurred there in the Holocene. They noted that a lack of Holocene activity on the fault seems inconsistent with the high Quaternary slip rate derived from displaced Quaternary basalts (Anderson and Mehnert, 1979; Hamblin and others, 1981). Hecker (1993) included the Hurricane fault in her 1:500,000-scale compilation of Quaternary tectonic features in Utah and assigned a probable age of late Pleistocene (10,000 - 130,000 years) to the time of most recent deformation. A structural analysis by Schramm (1994) of a complex portion of the Hurricane fault near the Toquerville, geometric bend, (figure 1) showed that movement on the fault there is predominantly dip-slip with a slight right-lateral component. Stewart and Taylor (1996), and Stewart and others (1997) defined a structural and possibly a seismogenic (earthquake) boundary at the large geometric bend in the Hurricane fault near Toquerville, which they called the Toquerville geometric bend. Fenton and others (2001) recently investigated basalt flows and alluvial landforms displaced by the Hurricane and Toroweap faults in the western Grand Canyon region. They concluded that both structures have been active through the Quaternary and that much of the development of the Inner Gorge of Grand Canyon can be attributed to relative uplift across these faults.

Christenson and Deen (1983) and Christenson (1992) reported on the engineering geology of the St. George, Utah area and discussed seismic hazards associated with the Hurricane and other Quaternary faults in the area. Christenson and others (1987) and Christenson and Nava (1992) included the Hurricane fault and other potentially active faults in southwestern Utah in their reports on Quaternary faults and seismic hazards in western Utah, and earthquake hazards in southwestern Utah, respectively. Williams and Tapper (1953) discussed the earthquake history of Utah including the 1902, M 6.3 Pine Valley earthquake. Christenson (1995) provided a comprehensive review of the 1992, M<sub>L</sub> 5.8 St. George earthquake, which likely occurred on the Hurricane fault. Stewart and others (1997) included a review of seismicity and seismic hazards in southwestern Utah and northwestern Arizona in their review of the

neotectonics of the Hurricane fault. Pearthree and Bausch (1999) inferred that seismic hazard in northwestern Arizona is moderate based on historical seismic activity and the presence of many Quaternary faults.

### **Utah Geological Survey/Arizona Geological Survey Cooperative Paleoseismic Study**

To more accurately evaluate the seismic hazard presented by the Hurricane fault to southwestern Utah and northwestern Arizona, the Utah Geological Survey (UGS) and Arizona Geological Survey (AZGS) conducted two National Earthquake Hazard Reduction Program-funded cooperative studies (Pearthree and others, 1998; Lund and others, 2001) of the Hurricane fault to acquire data on long-term fault slip rates and on the magnitude, timing, and location of past surface-faulting earthquakes. The UGS investigated the paleoseismicity and long-term slip history of the northern portion of the fault (proposed Ash Creek and Anderson Junction segments) in Utah. The AZGS studied the southern part of the Anderson Junction segment and the adjacent Shivwitz segment to the south to better understand the geologic controls of earthquake rupture on the Hurricane fault in Arizona.

#### **Utah Study**

For approximately 80 kilometers the trace of the Hurricane fault trends generally north-south through southwestern Utah. Displaced Quaternary basalt flows and alluvial and colluvial deposits indicate a significant rate of Quaternary fault activity. The UGS proposed to excavate trenches across fault scarps formed on unconsolidated deposits to characterize the size, timing, and rate of late Quaternary faulting, and to calculate long-term slip rates from displaced basalt flows.

Fault scarps are formed on unconsolidated deposits at six sites along the Utah portion of the fault (figure 6). The preferred UGS trench site at Coyote Gulch is on private property and was unavailable for study. Trenching at Shurtz Creek, the best alternative site, encountered large boulders that prevented exposing the fault zone. The remaining sites had similar geologic constraints or access problems, so the UGS refocused on dating young alluvium along the fault at three locations along the Ash Creek segment. The alluvium at the two northern sites (Middleton and Bauer; figure 6) is not faulted, while the sediments at the southern site (Coyote Gulch) are displaced. Radiocarbon ages from detrital charcoal recovered from the unfaulted alluvium at the Bauer and Middleton sites were 330-525 cal yr. B.P. and 1,530-1,710 cal yr. B.P., respectively. Charcoal from the faulted alluvium at Coyote Gulch gave an age of 1,055-1,260 cal yr. B.P. The fact that the sediments at Coyote Gulch are faulted and those at the Bauer and Middleton sites are not, show that the most recent surface-faulting earthquake (MRE) at Coyote Gulch did not extend north to the other two sites, indicating the likely presence of a seismogenic boundary between Coyote Gulch and the Bauer and Middleton sites. The most likely location for a boundary is at a right bend in the fault north of Coyote Gulch at Murie Creek. The proposed new northern fault segment is named the Cedar City segment and is a minimum of 13 kilometers long. The redefined Ash Creek segment is about 32 kilometers long. If the segment boundary is indeed a consistently maintained seismologic boundary, then based on those lengths and on limited displacement-per-event data, rupture of the Cedar City segment could produce a M 6.5 earthquake and rupture of the Ash Creek segment could produce a M 6.9-7.1 event.

Displaced Quaternary basalt flows at several locations along the Hurricane fault in Utah provide good evidence for rates of long-term slip on the fault. Determining long-term slip rates using the displaced flows required correlating the flows across the fault using trace-element geochemistry and new geologic mapping, dating correlative flows using  $^{40}\text{Ar}/^{39}\text{Ar}$  dating techniques, and evaluating near-fault deformation using a combination of paleomagnetic vector analysis and geologic mapping.

Geochemical data identified four locations in Utah where displaced basalts are correlative across the Hurricane fault: two on the Anderson Junction segment, one at the proposed boundary between the Anderson Junction and Ash Creek segments (Toquerville geometric bend), and one on the Ash Creek segment (figure 7). A fifth basalt site is 12 kilometers east of the fault in Cedar

Canyon and consists of a basalt remnant that occupies the ancestral channel of Coal Creek high on the north canyon wall. The basalt flow displaced Coal Creek, forcing the stream to incise a new channel and leaving the basalt remnant stranded high above the present stream. Coal Creek grades to Cedar Valley and crosses the Hurricane fault at the mouth of Cedar Canyon. Fault movement controls the stream base level and therefore, the stream-incision rate is a proxy for slip on the fault.

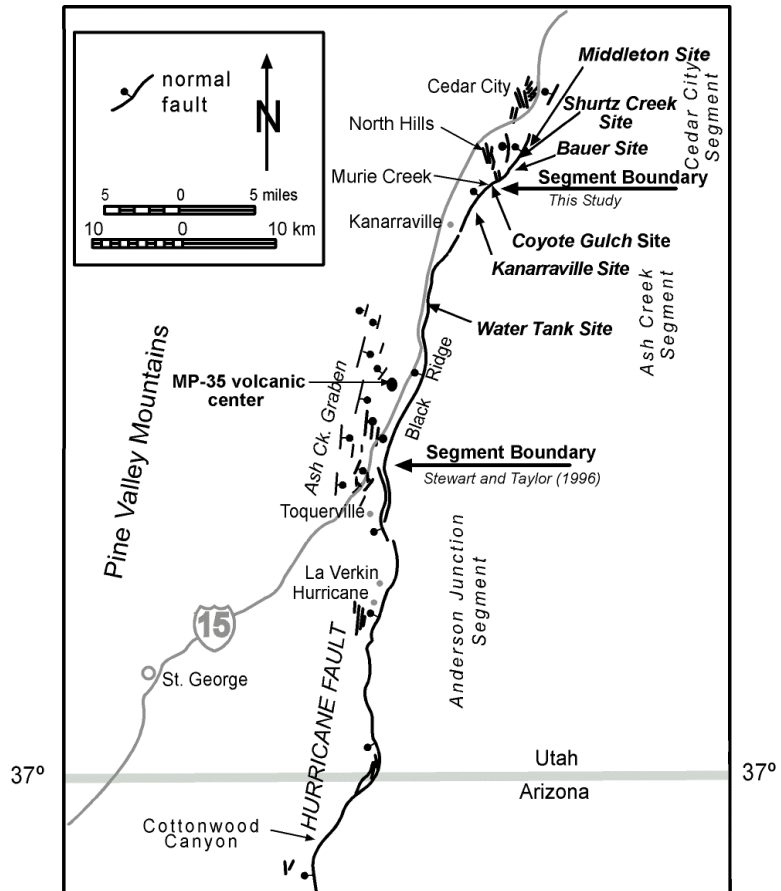
The new long-term slip rates for the Hurricane fault in Utah range from 0.21 to 0.57 mm/yr (table 1) and generally increase from south to north along the fault. Additionally, slip increases markedly to the north across the suspected Ash Creek/Anderson Junction segment boundary. Although little change in long-term slip rate is apparent across the proposed Ash Creek/Cedar City segment boundary, slip rates reported for segmented

faults elsewhere in the western United States indicate that a seismogenic boundary could still be present (Machette and others, 1992). A comparison of the new long-term slip rates with late Quaternary rates determined for several locations in Utah shows that slip has slowed on the Hurricane fault in Utah over the past approximately one million years. We conclude that the average recurrence for surface-faulting earthquakes on the fault segments in Utah is now several thousand to more than ten thousand years.

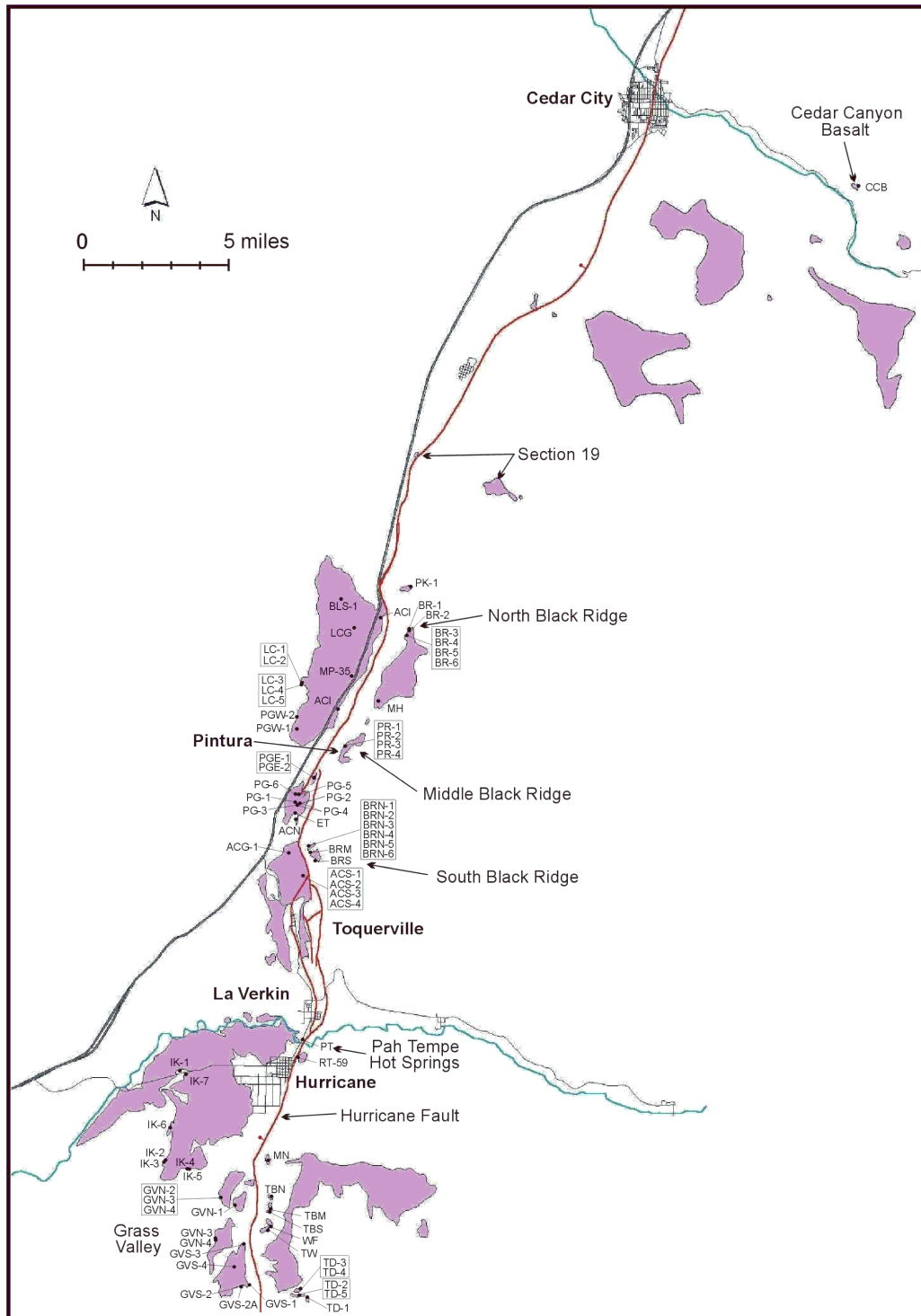
Considering the three potential seismogenic segments in Utah, the newly proposed Cedar City segment has gone the longest without a surface-faulting earthquake. The proxy slip rate available for the Cedar City segment closely approaches that of the adjacent Ash Creek segment, which has had a Holocene surface-faulting earthquake. Given its long-term record of activity and the general absence of geologically young fault scarps indicative of recent surface faulting, the Cedar City segment is considered the most likely location for the next surface faulting on the Hurricane fault in Utah.

### Arizona Study

Studies to characterize the late Quaternary rupture history of the southern Anderson Junction and Shivwitz segments of the Hurricane fault included: geologic and geomorphic mapping, scarp profiling, soil profile analysis, cosmogenic isotope dating, trenching, and geochemical correlation and dating of a displaced basalt flow. Detailed studies were conducted



**Figure 6. Hurricane fault in southwestern Utah showing sites with scarps formed on unconsolidated alluvium. Ash Creek graben and the MP-35 cinder cone are also shown.**



**Figure 7. Quaternary basalts associated with the Hurricane fault in Utah and geochemical, paleomagnetic, and radiometric sample sites. Locations where displaced basalt could be geochemically correlated across the fault include: Grass Valley, Pah Tempe Hot Springs, South Black Ridge, and North Black Ridge. The Cedar Canyon basalt site is shown east of Cedar City.**

**Table 1. Slip rates derived from displaced basalt flows along the Utah portion of the Hurricane fault.**

Location	Slip Rate mm/yr	Time Period Ma	Segment	Comments
Grass Valley	0.44	1.0	AJ	Higgins (2000) <sup>40</sup> Ar/ <sup>39</sup> Ar ages
Pah Tempe Hot Springs	0.21	0.353	AJ	
S. Black Ridge	0.45	0.81	AJ/AC	Proposed segment boundary
N. Black Ridge	0.57	0.86	AC	
Section 19	0.37-0.51	1.08	CC	Ages from Anderson and Mehnert (1979)
Cedar Canyon	0.53	0.63	CC	Surrogate rate – from stream downcutting

on the Anderson Junction segment/section just north of the State Line geometric bend GSBZ and in the southern part of the Shivwitz segment/section. In both of these areas, there are obvious fault scarps formed in late Quaternary alluvium and colluvium along the base of the Hurricane Cliffs. Quaternary units displaced by the fault include the Moriah Knoll basalt and late Pleistocene to early Holocene (?) alluvial and colluvial deposits. Late Quaternary slip-rate estimates using soil analysis, cosmogenic isotope dating, and carbonate-rind-thickness to approximate surface-age, and scarp profile modeling vary from <0.1 to 0.6 mm/yr, but most fall in the range of 0.1 to 0.3 mm/yr (Stenner and others, 1999; Amoroso and others, 2002). Geochemical data and geologic mapping (Billingsley, 1994b) show that the Moriah Knoll basalt flow was erupted on top of the Hurricane Cliffs, flowed across a structurally complex part of the fault zone, and subsequently was displaced by faulting. A new <sup>40</sup>Ar/<sup>39</sup>Ar age estimate establishes the age of the basalt at 0.83± 0.06 Ma. There has been about 200 meters of cumulative displacement across several faults since the flow was extruded, resulting in a long-term slip rate for the Shivwitz segment of about 0.24 mm/yr.

The Arizona Geological Survey (AZGS) excavated trenches at two sites in Arizona, the Cottonwood Canyon site (two trenches) on the southernmost part of the Anderson Junction segment, and the Boulder Fan site (one trench) on the southern part of the Shivwitz segment (figure 1). At Cottonwood Canyon the AZGS excavated the Q1 trench across a low fault scarp with less than 1 meter of displacement formed on an early Holocene (?) alluvial terrace. The trench exposed a 2-meter-wide fault zone, and stratigraphic and structural relations showed that a single surface-faulting earthquake probably occurred 8-15 thousand years ago. A second trench excavated across a 5-meter-high scarp formed on a late Pleistocene terrace surface about 25 meters south of the Q1 trench did not reveal any further information about late Quaternary fault behavior, as burial of older fault-related sedimentary units in the fault hanging wall by younger alluvial deposits precluded direct observation of evidence for older surface-faulting earthquakes in the trench.

The possibly Holocene MRE for the southern Anderson Junction segment resulted in a 60- centimeter displacement at Cottonwood Canyon. The event was at least a M 6.5, and may have been small compared to previous events at the site. Based on a 30- to 35-kilometer-length, the proposed Anderson Junction segment could produce a M 6.8-6.9 event.

At the Boulder Fan site on the Shivwitz segment, the AZGS excavated a single trench across a scarp formed on a large, Pleistocene alluvial fan that is an estimated 15,000-33,000 years old. The fan surface there is displaced about 4.5 meters. The scarp shows little evidence of erosion and likely represents multiple surface-faulting events. Stratigraphy in the trench consisted of debris-flow deposits in the footwall, and fault-scarp colluvium, fissure-fill deposits,

slope-wash deposits, and a framework gravel deposit in the hanging wall. Two colluvial-wedge deposits are evidence of two surface-faulting earthquakes. Secondary geologic relations indicate that total slip for the two events is 4.3 to 4.7 meters. Retro-deformation analysis suggests that the MRE produced about 2.5 to 3 meters of vertical displacement. Detrital charcoal recovered from fissure-fill material at the base of the MRE colluvial wedge had an age of 9,300 ±1,070, -430 cal B.P., which is considered close to the age for the MRE at this site.

A MRE single-event maximum surface displacement of 2.5 meters along the southern Shivwitz segment gives an estimated moment magnitude of 7-7.1. Using an estimated segment length of 57 kilometers, rupture of the Shivwitz segment is capable of producing M 6.8-7 events.

## Summary and Conclusions

The UGS/AZGS studies of the Hurricane fault provide new information critical to earthquake hazard assessment in southwestern Utah and northwestern Arizona. In summary, their new results show:

1. Long-term slip rates on the Hurricane fault in Utah and Arizona range from 0.21 to 0.57 mm/yr and generally increase from south to north indicating that for the past approximately one million years, the north end of the Hurricane fault has been its most active part.
2. Differences in long-term slip rates appear to be incremental across previously suspected fault segment boundaries, lending support to the presence of a seismogenic boundary at the Toquerville GBBZ between the proposed Anderson Junction and Ash Creek segments and the State Line GBBZ between the Anderson Junction and Shivwitz segments. The data are also permissive, but not necessarily supportive, of another seismogenic boundary farther north at a right bend in the fault near Murie Creek.
3. Slip rates determined from displaced late Pleistocene and Holocene alluvial and colluvial deposits along the fault in Utah are lower (<0.01 - 0.3 mm/yr) than the long-term rates (-0.4 - 0.6 mm/yr) and show that slip on the Hurricane fault has slowed there (generated fewer surface-faulting earthquakes) in more recent geologic time. This decrease in activity helps explain the sparse distribution of young fault scarps on unconsolidated deposits at the base of the high, steep Hurricane Cliffs in Utah. This slowing may have begun more than 350,000 years ago as evidenced by the 0.21 mm/yr slip rate for the Anderson Junction segment, determined from the displaced basalt flow at Pah Tempe Hot Springs. On the Shivwitz section of the Hurricane fault in Arizona, long-term (0.24 mm/year determined for the Moriah Knoll basalt) and late Quaternary slip rate estimates are not demonstrably different. Late Quaternary slip rate estimates for the Shivwitz, Anderson Junction, Ash Creek, and Cedar City segments are similar (0.1 to 0.3 mm/yr).
4. Based on our trench investigations, the MRE on the southern part of the Shivwitz segment occurred about 8,900 to 10,400 cal B.P., and it involved at least 2 meters of surface displacement. The MRE on the southern part of the Anderson Junction segment probably occurred in the early Holocene and involved less than 1 meter of surface displacement. The MRE on the Ash Creek segment occurred in the late Holocene more recently than 1,260 cal. B.P. Timing of the MRE on the proposed Cedar City segment is prior to 1,530 cal B.P. How much prior is unknown, but the absence of young scarps on the Cedar City segment argues for a considerable period of time since the last surface-faulting earthquake.
5. The most recent surface-faulting earthquakes on the Ash Creek and Anderson Junction segments are different in time, demonstrating that the two adjacent proposed segments last ruptured independently. Both segments must be considered active and capable of generating additional large earthquakes in the future. The rupture lengths of the MREs on the Anderson Junction and Shivwitz segments are poorly constrained at this time. The MRE on the Anderson Junction segment may have ruptured only the southern part of the segment with relatively little displacement. Alternatively, much or the entire segment may have ruptured, with evidence of the rupture only being clearly preserved at

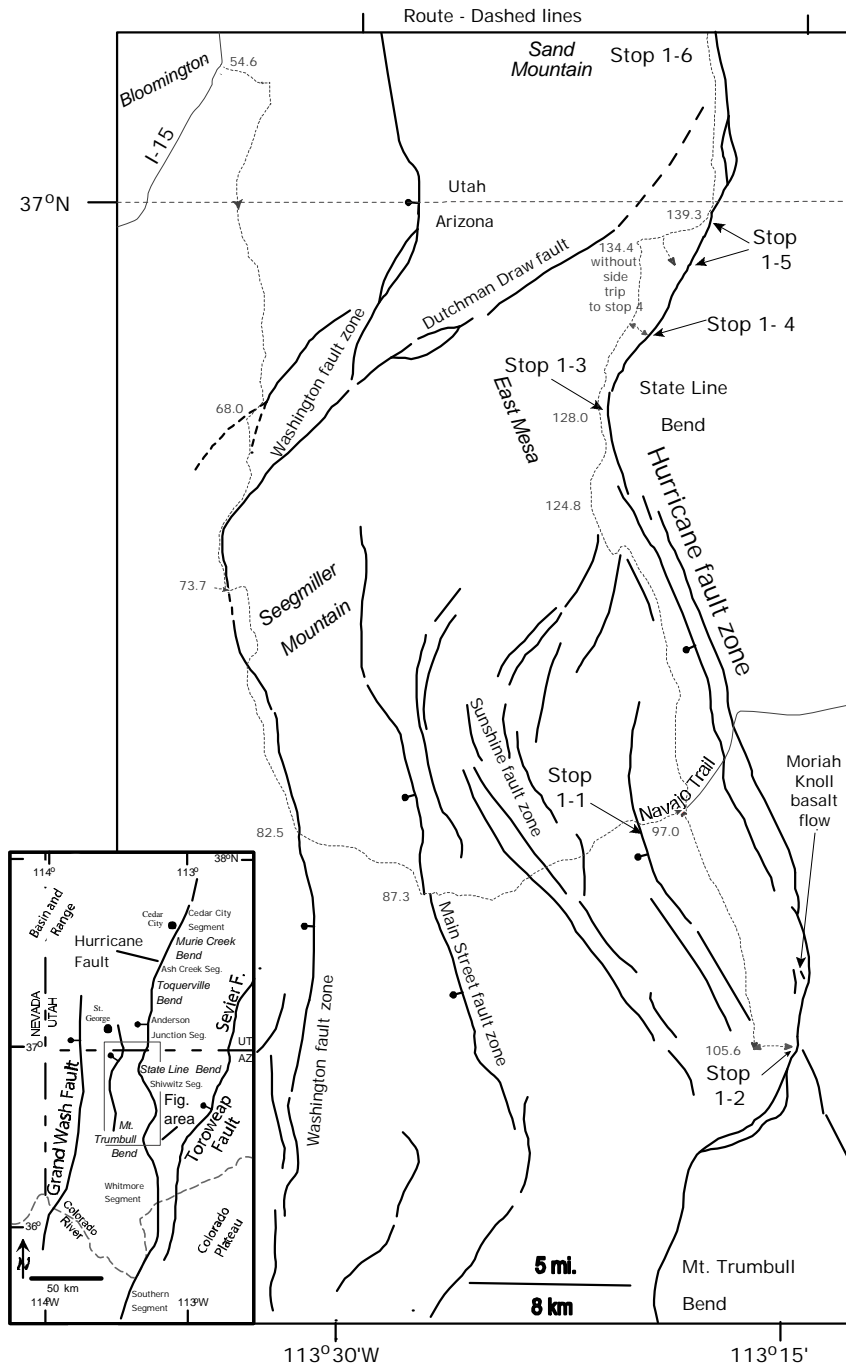


- the southern end. At least the southern part of the Shivwitz section ruptured about 10 thousand years ago. On the southern Shivwitz section, we found no evidence of rupture of mid- to late-Holocene deposits or landforms (including stream thalweg profiles). Because of the wide spacing between trenches and the uncertainty in the age estimates, we cannot rule out the possibility that the youngest faulting recorded on the Shivwitz and southern Anderson Junction segments occurred in one large earthquake.
6. The presence of faulted late Holocene alluvial-fan deposits at Coyote Gulch on the Ash Creek segment, and the absence of evidence for young faulting along the fault north of that point, argues for a third fault segment in Utah with a seismogenic segment boundary possible at the right bend in the fault at Murie Creek. We have named this proposed new northern segment the Cedar City segment.
  7. The decrease in slip rates from early to late Quaternary time along the Hurricane fault in Utah translates into longer recurrence intervals between large surface-faulting earthquakes. The average recurrence interval for surface faulting on the Hurricane fault's Utah segments is probably several thousand to possibly more than 10,000 years.
  8. Based on 2.75 meters of single-event displacement at Coyote Gulch, the MRE on the Ash Creek segment had an estimated moment magnitude of M 6.9-7.1. Based on an estimated segment length of 13 kilometers, the Cedar City segment is capable of producing up to M 6.5 events. Using ~0.6 meters of displacement recorded at Cottonwood Canyon, the most recent Anderson Junction rupture was likely at least M 6.5. Based on a 30-35 kilometer length, the Anderson Junction segment could produce M 6.8-6.9 events. Based on the ~2.5 meter single-event displacement at the Boulder Fan, the MRE estimated moment magnitude for the rupture on the Shivwitz section is M 7 – 7.1.

# FIRST DAY ROAD LOG

## The Shivwitz and Southern Anderson Junction Segments Hurricane Fault Zone, Arizona and Utah

Day 1 Stop and Route Map



**Figure 8. Day 1 Route Map.** The dashed line shows the route of our trip on Day 1. Some key mileage values are shown along the route (note that the map begins at mileage 54.6 at Bloomington; I-15 exit #4). Heavy weight lines represent faults. Words in italics are geographic locations noted in the road log. Inset shows trip map in a regional context.

# FIRST DAY ROAD LOG

## The Shivwitz and Southern Anderson Junction Segments Hurricane Fault Zone Arizona and Utah

On the first day of this two-day field trip, we will examine the Shivwitz and the southern part of the Anderson Junction segments of the Hurricane fault in Arizona and Utah. The trip will depart from the Southern Utah University parking lot at 200 South and 1150 West Streets in Cedar City, Utah, and will proceed directly to the Utah/Arizona border south of St. George, Utah. From there we will continue via dirt roads into the Arizona Strip to our first stop along the Navajo Trail, which provides an overview of the Shivwitz segment. It is an approximately 2.5 hour drive from Cedar City to the first stop. We will next proceed to the Boulder Fan trench site and examine direct stratigraphic evidence for two paleo-earthquakes on the Shivwitz segment, the youngest probably being earliest Holocene in age. The remainder of the day will be spent traveling northward along the fault on the Temple and Honeymoon Trails, examining evidence of the Hurricane fault's long-term structural development, the proposed boundary between the Shivwitz and Anderson Junction segments at the State Line geometric bend, the Cottonwood Canyon trench site on the Anderson Junction segment, a proposed trench site at Rock Canyon, and basalt flows, some of which cascaded over the Hurricane Cliffs, and others of which are displaced hundreds of meters across the fault. We will end the first day in Hurricane, Utah.

The six stops today provide information that allowed us, at least in part, to draw six main conclusions. (1) The Hurricane fault is geometrically segmented. (2) Fault linkage occurred at the State Line bend. The linkage style was fault capture. (3) Long-term slip rates on the Hurricane fault range from 0.21 to 0.57 mm/yr. On the Shivwitz section in Arizona, long-term (0.24 mm/year determined for the Moriah Knoll basalt) and late Quaternary slip rate estimates are not demonstrably different. (4) Increases in long-term slip rates appear to be incremental across previously suspected fault segment boundaries, lending support to the presence of a seismogenic boundary at the State Line GBBZ between the Anderson Junction and Shivwitz segments. (5) Based on our trench investigations, the most recent surface-faulting earthquake (MRE) on the southern part of the Shivwitz segment occurred about 8,900 to 10,400 cal. B.P. Each faulting event involved at least 1.5 meters of surface displacement, suggesting that they were associated with large earthquakes that ruptured much or the entire Shivwitz segment of the Hurricane fault. The MRE on the southern part of the Anderson Junction segment probably occurred in the early Holocene, and may have been a smaller event.

### Mileages

#### Inc. Cum.

0	0	Begin trip in parking lot at Southern Utah University near corner of 200 South and 1150 West streets. <b>Turn left (N)</b> onto 1150 West. Note that it will take about 2.5 hours to reach the first stop.
0.2	0.2	<b>Turn left (W)</b> at intersection of 1150 West and Center Streets. Proceed across freeway overpass.
0.3	0.5	<b>Turn right (N)</b> onto College Way (1650 West) at stop sign.
0.3	0.8	<b>Turn right (E)</b> onto 200 North at the stop light.
0.3	1.1	<b>Turn right (S)</b> onto I-15 on ramp.
0.8	1.9	At 11:00 the Green Hollow landslide is visible. It is a large late Pleistocene landslide extending from valley floor to ridge crest.

- 1.0 2.9 Providence Center Lighthouse on right (W). Constructed in 2000, this lighthouse has proven to be a major safety improvement for Cedar City, which has not experienced a single shipwreck since the lighthouse went into operation.
- 1.7 4.6 Another large, late Pleistocene landslide extending to the valley floor on the left (E).
- 0.1 4.7 Hurricane fault to left (E) near base of Hurricane Cliffs.
- 0.4 5.1 Quaternary basalt in road cut.
- 1.1 6.2 North Hills on left (E), which is a faulted anticline that deforms the Tertiary Claron Formation, Tertiary conglomerate, and Quaternary basalt.
- 4.2 10.4 At 9:00 (E) along the base of the Hurricane Cliffs is the active strand of the Hurricane fault. Here, the stratigraphic section in the footwall is overturned. The hanging wall is comprised of alluvium. We will visit this area tomorrow (STOP 2-6). For the next several miles I-15 will parallel the trace of the Hurricane fault. Also note the New Harmony Hills on the right (W) at about 1:00.
- 3.1 13.5 Great Basin drainage divide (near freeway overpass), leave the Great Basin and enter the Colorado River drainage.
- 1.0 14.5 To the left (E), the Hurricane Cliffs expose the grayish tan Permian Kaibab Formation. The Kaibab lies in the limb of an anticline that formed during the Sevier orogeny.
- 2.4 16.9 To the left (E), young fault scarps are generally absent along the Hurricane fault. The gravel quarry here is periodically monitored for fault exposures.
- 0.1 17.0 Nice exposures of the Hurricane fault at 9:00. The tan unit is the Permian Kaibab Formation (footwall) that is juxtaposed against the red Shnabkaib Member of the Triassic Moenkopi Formation (hanging wall).
- 1.0 18.0 To the left (E) the Hurricane Cliffs expose the Moenkopi Formation. The Pine Valley Mountains lie to the right (W) at 2:00.
- 1.4 19.4 Pass I-15 off ramp to the Kolob Canyons entrance to Zion National Park. Permian Kaibab Formation exposed in Hurricane Cliffs to the left (E).
- 1.8 21.2 At 2:00, Quaternary basalt of the informally named New Harmony basalt field.
- 1.0 22.2 At 3:00, Ash Creek Reservoir, I-15 forms the dam for this unused reservoir. At 11:00 along the skyline, Quaternary basalt crops out at the top of Black Ridge (Hurricane Cliffs).
- 0.6 22.8 Quaternary basalt in this road cut is geochemically and geochronologically the same as the basalt on the skyline in the footwall of the Hurricane fault. We will stop here tomorrow (STOP 2-5, I-15 Exit 36) to discuss the relation between the basalts and the Hurricane fault in more detail.
- 0.8 23.6 At 9:00, the hummocky topography of a landslide is visible on the flank of Black Ridge. The Triassic Chinle Formation is failing and carrying Quaternary basalt with it. Also, you are still looking at the east limb of a Mesozoic anticline.

- 2.9 26.5 At 9:00, large fault scarps are formed in unconsolidated deposits and bedrock near the base of the Hurricane Cliffs. Following cliffs to the south, more scarps are visible.
- 1.5 28.0 Pass exit 31.
- 1.2 29.2 Look toward 10:00 to see a graben expressed topographically in Quaternary basalt.
- 0.6 29.8 The hill at 11:00 is comprised of Tertiary quartz monzonite of the Pine Valley laccolith.
- 0.7 30.5 To the right (W), at 3:00, the Tertiary Claron Formation (orange and white) crops out below more of the Pine Valley laccolith.
- 1.0 31.5 At 9:00 on the skyline are the radio towers where we will be about mid-day tomorrow (Stop 2-4). The towers are on the south end of Black Ridge.
- 1.0 32.5 Pass exit 27 to Toquerville. Here, I-15 diverges from the trace of the Hurricane fault. The fault bends east and the freeway continues generally south. This is Anderson Junction and the Toquerville geometric bend.
- 1.3 33.8 Red beds on the right (W) at 3:00 are Jurassic Navajo Sandstone. The Pine Valley laccolith crops out in the distance near the skyline.
- 0.6 34.4 At 11:00 is the nose of the north-plunging part of the doubly plunging Virgin anticline, a large fold related to the Mesozoic Sevier orogeny.
- 0.7 35.1 At 2:00 is the historic Silver Reef mining district with the reddish Kayenta Formation and Navajo Sandstone exposed in the near distance. The Silver Reef mining district is noted for its uncommon occurrence of ore-grade silver chloride (cerargyrite or horn silver) in sandstone, unaccompanied by obvious alteration or substantial base-metal ores. The principal mining activity in the district extended from 1876 to 1888 with lessee operations through 1909. The district produced about 8 million ounces of silver prior to 1910.
- 1.1 36.2 We are now driving parallel to the west flank of the Virgin anticline. The Shinarump Conglomerate Member of the Triassic Chinle Formation forms the resistant dip slope. The Triassic Moenkopi Formation crops out on the left (E). We are driving in a strike valley in the Petrified Forest Member of the Chinle Formation.
- 3.1 39.3 In the near distance at 3:00 the Moenkopi Formation crops out. In the background is the Jurassic Navajo Sandstone.
- 0.3 39.6 At 9:00, Quail Creek cuts through and forms a gap in the west limb of the Virgin anticline.
- 1.0 40.6 The Triassic Petrified Forest Member of the Chinle Formation crops out at 10:00.
- 0.9 41.5 Alluvial fans are visible in the low foothills at 3:00. This area is designated as desert tortoise habitat.
- 1.0 42.5 Conglomerate in road cut is a Tertiary deposit that contains mostly clasts of quartz monzonite from the Pine Valley laccolith. Hurlow (1998) interpreted this

deposit as debris-flow material derived from the steep southern and southeastern slopes of the Pine Valley Mountains.

- 2.2 44.7 At 12:00 is Washington Black Ridge. The road cut exposes the Washington basalt flow occupying the now inverted ancestral channel of Grapevine Wash. This is the most mafic of the flows in the St. George area. Best and others (1980) dated it at  $1.7 \pm 0.1$  Ma. The basalt is strongly jointed and has been quarried for building stone (Biek, 1997).
- 1.0 45.7 The hill at 11:00 is Shinob Kaib Butte, type section of the Shnabkaib Member of the Triassic Moenkopi Formation. The Shnabkaib Member is characterized by the “bacon slab” appearance of its alternating red and white strata. The Shinarump Member of the Chinle Formation, here a coarse, well-cemented pebbly sandstone, caps the butte.
- 0.8 46.5 Cross the Washington fault. The Washington fault is a 42-mile-long, down-to-the-west, high-angle normal fault that trends north-south through northern Arizona and southern Utah. Displacement on the Washington fault decreases to the north. It reaches a maximum of about 2,200 feet six miles south of the Utah/Arizona border, is approximately 1,600 feet at the border, and about 700 feet at this location, where the fault begins to bifurcate and quickly die out to the north (Higgins, 1998).
- 0.2 46.7 At 12:00 is the St. George basin. At 2:00, Quaternary basalt flows that were erupted from volcanoes located near the base of the Pine Valley Mountains.
- 2.3 49.0 At 2:00 is the doubly plunging Washington Dome, one of three such domes along the Virgin anticline.
- 0.8 49.8 At 12:00 is Middleton Black Ridge. The road cut exposes the Middleton basalt flow, which occupies a now inverted valley in the Jurassic Kayenta Formation (Willis and Higgins, 1995). The Middleton flow is about 200 feet above the Virgin River and has been dated at  $1.5 \pm 0.1$  Ma by Best and others (1980).
- 1.4 51.2 At 3:00, two levels of basalt flows are visible on West Black Ridge. The lower basalt flow is home to the St. George airport and is  $^{40}\text{Ar}/^{39}\text{Ar}$  dated at approximately 1.23 Ma (Willis and Higgins, 1995). Below the flow, red siltstone outcrops of the Jurassic Dinosaur Canyon Member of the Moenave Formation dip northward on the mostly talus-covered hillside. The higher, and thus older, basalt flow that caps West Black Ridge is  $^{40}\text{Ar}/^{39}\text{Ar}$  dated at 2.34 Ma. Note the well-formed columnar jointing. West Black Ridge is an outstanding example of inverted topography, wherein former stream channels tributary to the Virgin River now stand high above the surrounding landscape.
- 2.8 54.0 At 12:00, in the road cut the Triassic Shinarump Conglomerate overlies the upper red member of the Moenkopi Formation. This gap was cut by the Virgin River where it exits the St. George basin.
- 0.3 54.3 Cross the Virgin River.
- 0.3 54.6 **Take Exit 4 into Bloomington.**
- 0.3 54.9 Traffic circle. **Drivers exercise caution here, even the locals have trouble with this thing.** Follow around to the left and exit on Brigham Road, under the freeway.

- 0.2 55.1 Drive east on Brigham Road. At 9:00 is an excellent exposure of the Shnabkaib and upper red members of the Moenkopi Formation. The unit capping the ridge is the Shinarump Conglomerate Member of the Chinle Formation.
- 1.7 56.8 **Turn right** at intersection with River Road. Proceed south toward Arizona and the Moenkopi Terrace.
- 3.7 60.5 Utah/Arizona state line. Beyond this point we will be entering the infamous Arizona Strip, note that in Utah, unlike Arizona, we mostly provide paved roads for field trips. You will come to appreciate that fact as today's trip bumps and grinds on and on. We are traveling through low relief terrain eroded into the Moenkopi Formation. This area is partially covered by Quaternary alluvial deposits, including young deposits along active washes and eroded remnants of terraces and alluvial fans (Billingsley, 1993a).
- 2.1 62.6 At 9:00, Pine Valley laccolith at the skyline.
- 0.4 63.0 The high ridge to the southwest is Mokaac Mountain, a large ridge composed of Moenkopi Formation capped by late Tertiary basalt (Hamblin, 1970a). Much of the slopes of Mokaac Mountain consist of large Quaternary landslides (Billingsley, 1993a).
- 0.6 63.6 A strand of the Washington fault zone, a major, down-to-the-west normal fault, is at the base of steep, linear cliffs formed in resistant beds of the Kaibab and Toroweap Formations at about 12:00. The Washington fault zone extends from the town of Washington, Utah, southward for about 60 kilometers into Arizona. In this area, the Washington fault zone consists of two generally northeast-trending strands. The western strand, which is most apparent from this vantage point, has been named the Mokaac fault (Billingsley, 1993a). Paleozoic rocks are displaced by about 200 to 400 meters across the Mokaac fault zone in this area, with displacement increasing to the northeast. Total displacement across the main strand of the Washington fault zone to the east is 100 to 600 meters, also generally increasing to the north through this area. Surface exposures of the Washington fault zone indicate that it is very high angle, and it has been interpreted as a reverse fault (Billingsley, 1993a) or high-angle normal fault (Billingsley and Workman, 2000). Quaternary activity on the Washington fault zone in Arizona has not been studied in detail, but late Quaternary alluvium and colluvium is displaced several meters at a number of localities (Billingsley, 1993a) and the linear, steep escarpments associated with portions of the fault zone suggest substantial Quaternary activity (Menges and Pearthree, 1983; Pearthree, 1998).
- 0.9 64.5 Where the West Stays Wild sign. You may well see no people on the field trip route in Arizona, and thus you should not venture out without plenty of gas, food, water, and good maps.
- 1.1 65.6 A low ridge of the Virgin Limestone Member of the Moenkopi Formation crops out at 11:00-12:00.
- 2.4 68.0 The road crosses the Mokaac fault in this area, although the fault zone is not exposed.
- 0.5 68.5 You are on a block between the two strands of the Washington fault zone. The main (eastern) strand of the fault zone is at the base of the large escarpment straight ahead.



- 1.2 69.7 The road roughly parallels the main strand of the Washington fault zone for a couple of miles. Kaibab Formation crops out in upper cliffs. The Harrisburg Member of the Kaibab Formation is eroded, whereas the Fossil Mountain Member is a resistant cliff-forming unit. Red and yellow units lower in the cliff are in the Toroweap Formation (Billingsley, 1993a).
- 0.7 70.4 We are driving mainly in the Harrisburg Member of the Kaibab Formation, and locally in the overlying Moenkopi Formation; equivalent units on the upthrown side of the fault are high above us. Total vertical displacement across the Washington fault zone here is about 300 meters (Hamblin and Best, 1970; Billingsley, 1993a).
- 1.4 71.8-71.9 Exposures of steeply dipping colluvial deposits in road cuts indicate we are quite close to the fault zone, but are probably still on the downthrown side of the fault.
- 0.7 72.6-72.9 The road probably crosses the Washington fault zone several times through this interval.
- 0.5 73.4 Exposure of the Fossil Mountain Member of the Kaibab Formation indicates that we are now driving on the upthrown side of the fault.
- 0.3 73.7 Top of the long uphill grade in a pass at the base of Quail Hill. The Washington fault zone continues southeastward from this point, and we will cross it several more times.
- 0.2 73.9 There is a radio tower on top of Seegmiller Mountain at 12:00. The mountain is capped by a basalt flow over the Moenkopi Formation. Reynolds and others (1986) dated the flow at 2 to 3 Ma (K-Ar), Wenrich and others (1995) dated it at 4 to 5 Ma (K-Ar), and Downing and others (2001) at 3.5 to 4.2 Ma ( $^{40}\text{Ar}/^{39}\text{Ar}$ ).
- 0.6 74.3 Take right (main) fork at junction, left fork goes to Seegmiller Mountain.
- 0.9 75.2 Exposure of white and red Moenkopi Formation capped by Tertiary basalt at 8:00-9:00.
- 0.9 76.1 We are still roughly paralleling the Washington fault zone on the upthrown side of the fault.
- 0.9 77.0 We cross the Washington fault zone somewhere in this vicinity. The ridgeline to the left of the road is capped with the Seegmiller Mountain basalt, which is displaced about 100 meters here. Displacement of underlying Triassic strata is similar, implying that displacement on the Washington fault zone began less than 4 million years ago (Billingsley, 1993a; Downing and others, 2001).
- 0.8 77.8 The Shivwitz Plateau dominates this view to the south. The Shivwitz Plateau is the hanging-wall block of the Hurricane fault and the footwall block of the Grand Wash fault to the west. The Grand Wash fault and its associated cliffs form the western margin of the Colorado Plateau at this latitude. The Shivwitz Plateau is cut by a number of normal faults with much less displacement than either the Grand Wash or Hurricane faults, including the Washington fault zone.
- 0.5 78.3 To the northeast, several ridges are associated with multiple strands of the Washington fault.

- 4.9 79.2 BLM sign identifying Wolf Hole Valley. This tiny basin is on the downthrown side of the Washington fault. The low escarpment in the distance at 10:00-11:00 is the continuation of the upthrown side of the Washington fault. The high plateau to the west is Wolf Hole Mountain, which consists of Moenkopi Formation capped by late Tertiary basalt flows. Billingsley (1993a) obtained a K-Ar date of  $3.1 \pm 0.4$  Ma from a basalt atop Wolf Hole Mountain. Near this location, Wolf Hole, Arizona, now defunct, formerly consisted of a post office and general store to serve ranchers on the Arizona Strip. Edward Abbey listed Wolf Hole, Arizona as his home address.
- 0.4 79.6 Three small knobs (Mustang Knolls) at 2:00-3:00 are capped by basalts over the Moenkopi Formation.
- 0.6 80.2 Continue straight at T intersection with Black Mountain Road.
- 0.1 80.3 The upthrown block of the Washington fault is evident at 9:00, where there is about 60 meters of total displacement (Hamblin and Best, 1970; Billingsley and Workman, 2000).
- 2.3 82.6 Bear left at Y intersection and quickly cross the Washington fault.
- 0.7 83.3 High point in the road at Wolf Hole Pass with views to the east and south. The high escarpment in the distance at 12:00-1:30 is the Hurricane Cliffs. The plateau above the escarpment is the Uinkaret Plateau. The high, broad mountain on the Uinkaret Plateau in the far distance to the southeast is Mt. Trumbull, the remnant of an early Quaternary volcano. Left of Mt. Trumbull is Antelope Knoll, another Quaternary volcano. Diamond Butte at 1:00-1:30 is composed of Moenkopi Formation capped by basalt dated by Billingsley (1993b) at  $4.3 \pm 0.6$  (K-Ar). Extensive Pliocene basalts capping buttes and mountains on or around the margins of the Shivwitz imply that the land surface was generally formed on the Moenkopi Formation in the early Pliocene. In most places, Moenkopi deposits have been completely removed and the surface of the Shivwitz Plateau is now formed on the underlying Kaibab Formation. Erosion of the Moenkopi Formation must have provided abundant sediment to the Colorado River system over the past few million years. The road here is very close to the contact between the Permian Kaibab Formation to the north and the Triassic Moenkopi Formation to the south. In this area, the Moenkopi Formation filled a Triassic paleovalley carved into the Kaibab Formation (Billingsley, 1991).
- 2.1 85.4 We are driving through eroded Kaibab and Moenkopi rocks.
- 0.6 86.0 Bear right at Y intersection as you enter Main Street Valley. Main Street Valley is bounded on the east by an obvious escarpment associated with the principal strand of the Main Street fault. Total displacement across this eastern fault ranges from about 50 to 120 meters. Quaternary deposits and basalts are displaced in a few locations, but no detailed studies have been completed on this fault zone. Portions of the west side of the valley are also fault-bounded, and this part of the fault system has been labeled the Main Street graben (Menges and Pearthree, 1983; Billingsley, 1993c).
- 0.6 86.6 Cattle guard.
- 0.7 87.3 **Turn left onto Navajo Trail** and proceed east across the principal Main Street fault strand.

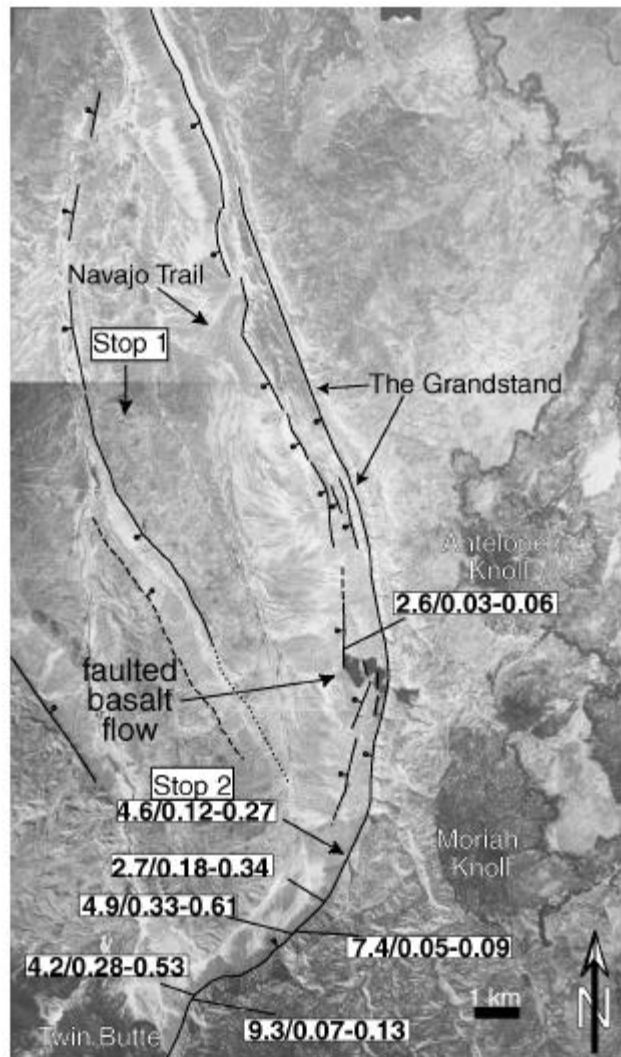
- 0.3 88.6 We are now driving on the Harrisburg Member of the Kaibab Formation. The knoll in the far distance at 12:00 is Antelope Knoll.
- 2.5 91.1 Hurricane Cliffs are visible in the distance at 12:00. The Fossil Mountain Member of the Kaibab Formation crops out in the lower parts of this valley. This is a prominent cliff-forming unit that you will see high up in the footwall of the Hurricane fault.
- 0.5 91.6 We cross the Sunshine fault as we emerge into a valley. The Sunshine fault has generated an escarpment at the southwestern margin of this valley; total displacement is about 110 to 130 meters, down-to-the-east (Billingsley, 1993c). The Sunshine fault is likely an east-dipping normal fault, antithetic to the Hurricane fault. It has the most linear and impressive escarpment of the secondary faults associated with the Hurricane fault. The road is on a young alluvial fan that is not displaced by the Sunshine fault. In the valley to the east there are several low scarps that are probably related to west-dipping normal faults.
- 0.7 92.3 Part of the Hurricane Cliffs escarpment is visible from 11:00-3:00. The Hurricane fault is at base of the escarpment. If the lighting is right, you may be able to see some low fault scarps formed in colluvium at the base of the cliffs that record late Quaternary displacement on the fault. The Pine Valley Mountains north of St. George, Utah, can be seen at 9:00-10:00.
- 0.4 92.7 A structurally complex portion of the Shivwitz section of the Hurricane fault, including the Navajo Trail crossing and the Grandstand, is visible from 11:00-1:00. We will discuss this area from Stop 1-1.
- 0.3 93.0 Keep straight on the Navajo Trail at the intersection with the Sunshine Trail.
- 0.2 93.2 This modest escarpment is associated with another minor, west-dipping fault strand. The road climbs across rocks of the Moenkopi Formation that filled a paleovalley in the Kaibab Formation; Kaibab Formation crops out at the top of the ridge.
- 0.6 93.8 A smaller west-dipping fault with a steep and linear scarp is visible in the near distance.
- 1.0 94.8 The ridgeline in the middle distance at 9:30-10:00 is capped with late Tertiary basalt dipping moderately towards the Hurricane fault.
- 0.5 95.3 Large stock tank and causeway at the crossing of Hurricane Wash.
- 0.2 95.5 Cross low escarpment associated with a west-dipping fault. Basalt-capped Diamond Butte is visible at 2:00.
- 0.2 95.7 Axis of the rollover Hurricane monocline is somewhere in this vicinity (Billingsley, 1993d). Park on the south side of the road; walk ~100 meters south of road to the top of a low hill (Stop 1-1). This hill is capped by a thin layer of alluvium (Billingsley, 1993d) that was probably part of an alluvial fan associated with a relict course of Hurricane Wash. It is likely that some combination of displacement on the fault zone immediately to our west and associated drainage capture altered the course of Hurricane Wash to its present position.

**STOP 1-1. Overview of the Shivwitz segment of the Hurricane fault.** (Grandstand 7.5' quadrangle, T38N, R10W, section 1)

From this vantage we can see much of the Shivwitz segment of the Hurricane fault. Down-to-the-west displacement across the Hurricane fault has resulted in the formation of the Hurricane Cliffs, the prominent escarpment that dominates our view to the east (figure 9). The Hurricane Cliffs separate the higher Uinkaret Plateau to the east from the Shivwitz Plateau on which we are standing. The obvious volcanic cone in the distance above the Hurricane Cliffs is Antelope Knoll, one of several Quaternary eruptive centers on the footwall of the Hurricane fault. Stop 1 is on the monocline in the hanging wall where strata on the downthrown side dip toward the fault. This increase in dip toward the fault likely results from reverse drag flexure due to decreasing fault dip at depth (Hamblin, 1965b; Billingsley and Workman, 2000).

The Hurricane Cliffs escarpment exposes Permian marine carbonates and marine to continental clastic rocks of the Toroweap and Kaibab Formations (Sorauf and Billingsley, 1991). The Harrisburg Member of the Kaibab Formation is at the top of the escarpment; in many places, it has retreated from the escarpment. The highest steep cliff is formed in the Fossil Mountain Member of the Kaibab Formation. Lower in the cliffs the Toroweap Formation consists of the slope-forming Woods Ranch member, the cliff-forming Brady Canyon member, and the slope-forming Seligman member (where exposed at the base of the cliffs). Coarse, very poorly sorted colluvium covers much of the slope-forming units, especially the Seligman Member. Because of the structural complexity of the Hurricane fault zone immediately across the valley from this vantage point, you may see all or parts of this sequence repeated several times.

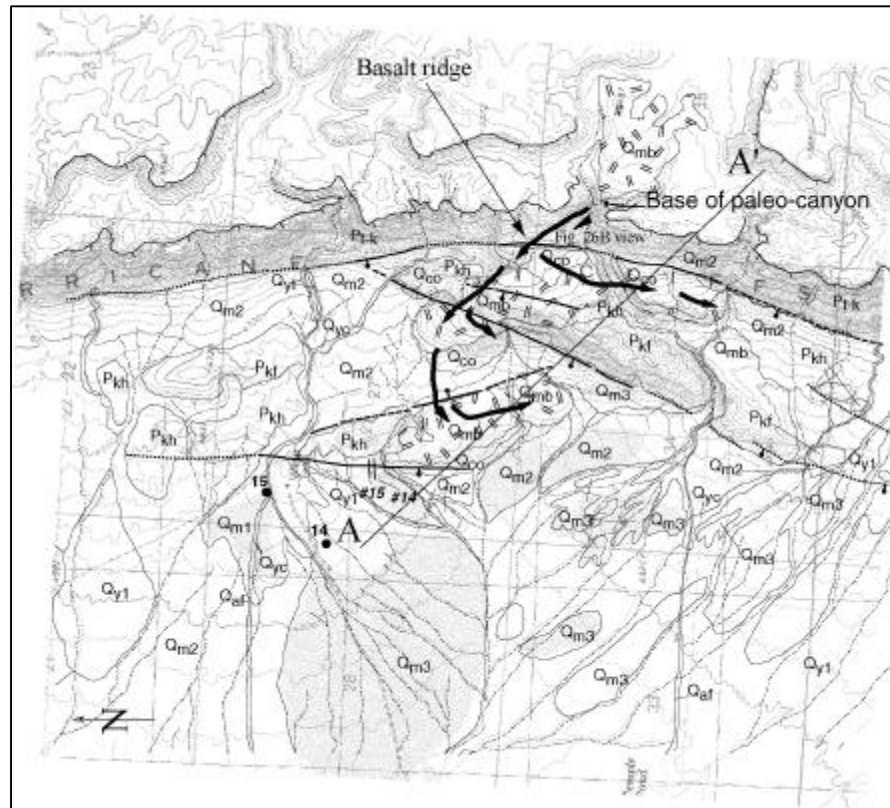
Most of the Shivwitz segment is a large structural embayment between two prominent convex fault bends. On the hanging wall at the northern end of the Shivwitz segment you can see a prominent east-sloping



**Figure 9. Mosaic of NASA high-altitude aerial photography of the Shivwitz section of the Hurricane fault zone showing fault traces and results of slip rate estimates. Faults are dashed where approximate or inferred, dotted where concealed. Field trip stops and features discussed in the text are labeled. Also shown is a compilation of the vertical surface displacement observations and slip rates estimated from scarp morphologies (surface offset in meters, slip rate range in mm/yr). We determined a slip rate of 0.1 to 0.3 mm/yr using similar methodology at Cottonwood Canyon 25 kilometers to the north of this portion of the Shivwitz section (Stenner and others, 1999). The basalt flow displaced by the Hurricane fault originated from Moriah Knoll.**

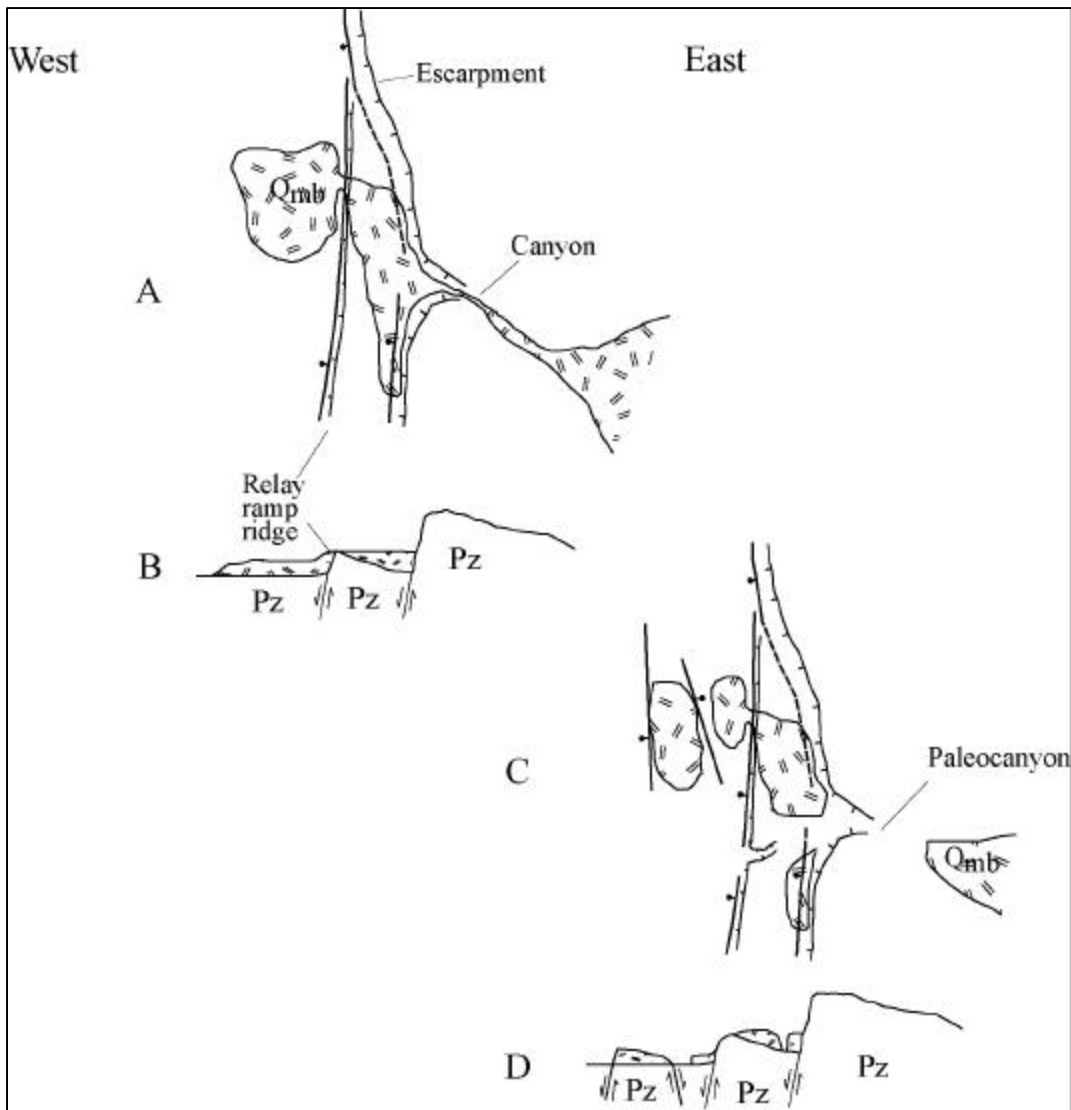
butte, where beds of the Triassic Moenkopi Formation are capped with late Tertiary basalt and all are tilted toward the Hurricane fault. This butte is at a major convex bend in the trace of the Hurricane fault; this is the approximate location of the State Line geometric bend and the site of field trip Stop 1-3. Immediately northeast of our overlook, the gravel road of the Navajo Trail can be traced up to the Hurricane escarpment, where it ascends the surface of a ruptured relay ramp between overlapping strands of the Hurricane fault. The Grandstand, seen south of the Navajo Trail, is a zone of multiple fault strands associated with a left stepover.

To the southeast, we can see the Moriah Knoll basalt where it flowed across the escarpment (figure 10). The Moriah Knoll volcano erupted this basalt on top of the escarpment; the basalt then flowed down a valley cut into the early escarpment, across several fault strands,



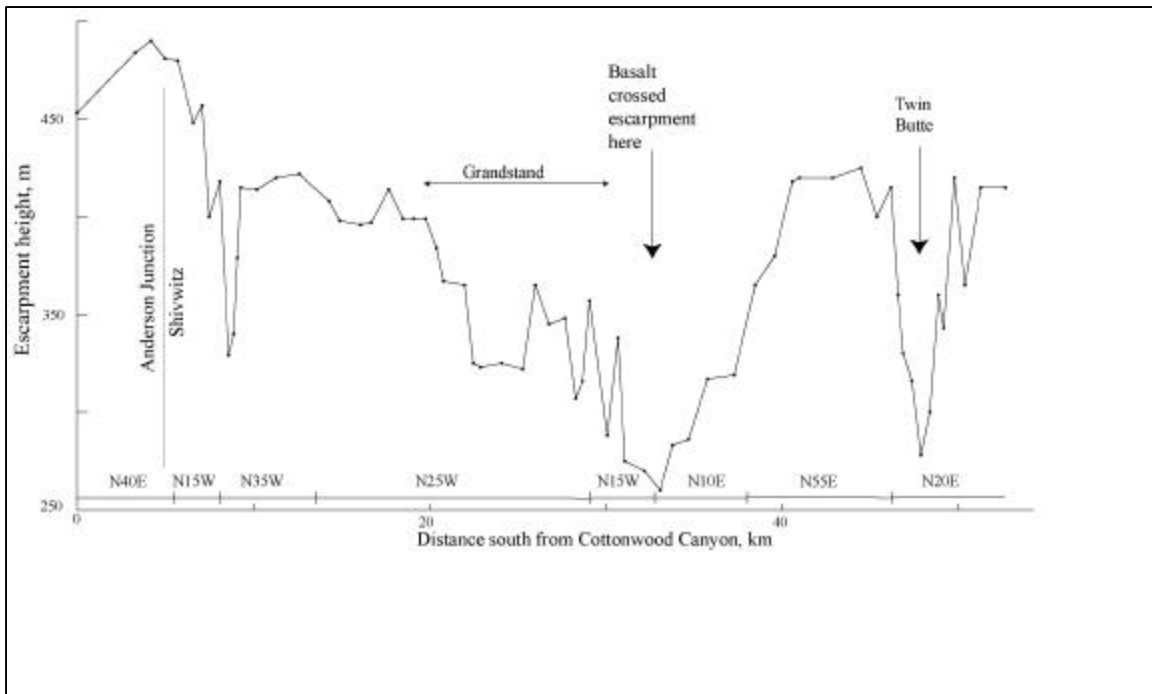
**Figure 10. Geologic map showing the relation of the faults to the Moriah Knoll basalt flow (Amoroso and others, 2000). The basalt filled the space between the main escarpment and the Pkf ridge until the ridge was overtopped and the basalt flowed farther west. The basalt flow directions, estimated from flow thickness, are shown by heavy black arrows.**

and onto the hanging wall. From map relations it appears that the basalt flowed south along a developing relay ramp, accumulated against the relay ramp ridge, over-topped the ramp to the west and flowed down onto the hanging wall (figure 11). Several fault strands have subsequently displaced the flow. We correlated various exposed remnants of the Moriah Knoll basalt across the fault using XRF geochemical correlation. A sample collected from the flow in a paleocanyon on the footwall gave a  $^{40}\text{Ar}/^{39}\text{Ar}$  date of  $0.83 \pm 0.06$  Ma. Total displacement across the basalt is an estimated 200 meters, yielding a minimum long-term slip rate of about 0.24 mm/yr (Amoroso and others, 2002). We can see another convex portion of the fault far to the south at the basalt-capped mesas of Twin Butte, and to the west, Diamond Butte. These buttes preserve remnants of the easily eroded Moenkopi Formation on the hanging wall because of the resistant cap of late Tertiary basalt.



**Figure 11. Sketches illustrating fault development history at the basalt flow. Faults are shown with stem and ball on downthrown side, dashed faults indicate possible lower displacement on the fault due to fault overlap. Teeth point down steep escarpment slopes. A) During emplacement of the basalt, the relay ramp must have dipped eastward to trap much of the basalt flow between the base of the escarpment and the relay ramp. B) East-west cross-section through A. Once sufficient basalt had been emplaced, the ridge was overtopped and the flow moved further west and ponded against the relay ramp. C) Basalt flow after being offset by several strands of the fault, and eroded from the paleocanyon. The western fault strands may have been present at time A/B but were not topographic barriers. D) The basalt between the ramp ridge and the escarpment has been incised by the present drainage, and both flow remnants west of the relay ramp are now tilted toward the east.**

Changes in fault strike and escarpment height suggest that the Moriah Knoll basalt locale is another geometric boundary and might be a segment boundary. The fault strike changes from N20°E north of Twin Butte, to N15°W at the basalt locale; to N35°W south of the State Line geometric bend (figure 12). The escarpment is 470 meters high at the State Line geometric bend. To the south near Twin Butte, the escarpment is 450 meters high. The escarpment height is lowest (250 m) where the Moriah Knoll basalt crossed the fault zone. The faults seen in the fault development figure are rotational faults. The eastern fault shows increasing displacement to the north, and the fault to the west has increased displacement to the south (Billingsley, 1994a). We suggest that the minimum in escarpment height at the Moriah Knoll basalt is related to fault



**Figure 12. Variation in escarpment height along the Hurricane Cliffs for the Shivwitz section. The x-axis is the distance along the escarpment, and the strike of the Hurricane fault is shown at the bottom of the figure. The Shivwitz - Anderson Junction segment boundary is at kilometer 5, approximately where the fault strike changes 55 degrees. Note the broad decrease in elevation where the basalt crossed the escarpment is also where the fault strike changes 25 degrees. Differences in escarpment height reflect the general variation in total slip on the section.**

geometry. The basalt flowed down the relay ramp between these faults where total displacement decreases and stress is distributed over several fault strands in the area (Zhang and others, 1991). The next stop, the Boulder Fan trench site, is another part of the fault where hard linking along the fault zone has isolated a smaller fault strand. Movement on this fault strand may have created a zone of weakness to form the embayment in the cliffs southeast of the Boulder Fan.

Return to the vehicles and proceed east on the Navajo Trail.

- 0.8 96.5 Rocks of the Moenkopi Formation crop out on the left side of the road here. These sediments filled a northeast-trending Triassic paleovalley (Billingsley, 1993d).

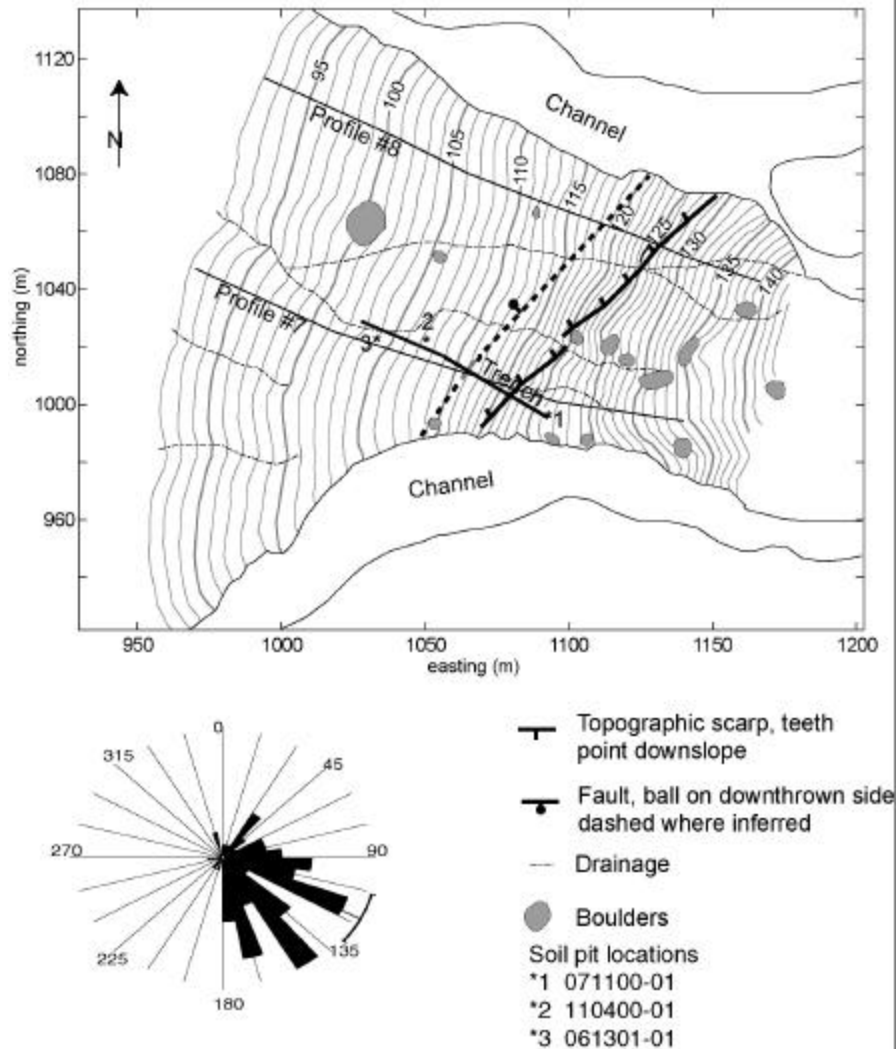


- 0.5 97.0 **Turn right** onto small dirt road. As we ascend a short incline, we are climbing onto older Quaternary fluvial deposits (Billingsley, 1993d) laid down by a stream that flowed northward in this valley along the Hurricane Cliffs.
- 0.4 97.4 The hummocky part of the Hurricane Cliffs at 11:00-12:00 is where the Moriah Knoll basalt flowed across the Hurricane fault zone. The Temple Trail traverses the Hurricane Cliffs on the Moriah Knoll basalt. Mormon pioneers constructed this trail to bring large Ponderosa pine logs from Mt. Trumbull to St. George, where they were used as roof beams in the construction of the Church of Latter Day Saints temple. The trail up the basalt flow is not passable by motor vehicles.
- 0.2 97.6 After we descend off of this low ridge to the south, we are driving on low terraces and the flood plain of a sizable, unnamed north-flowing tributary of Hurricane Wash.
- 0.9 98.7 Gate.
- 2.3 101.0 Another gate. Go right at Y intersection.
- 0.2 101.2 The Boulder Fan trench site is visible in the middle distance at 12:00. The large rockfall boulder on the fan is responsible for its name. Twin Butte is visible on the hanging wall of the Hurricane fault at 2:00.
- 0.3 101.5 A drilling rig is visible in the middle distance at 2:00. This is called the Dutchman Prospect, and it is being drilled into a surface anticline between the Hurricane and Sunshine fault zones. Potential source rocks are Paleozoic and Precambrian shales. Drilling began in 1998 using an old-fashioned cable tool rig. Because of hard drilling and lack of progress, the rig was converted to rotary drilling. As of mid-2001, the hole depth was about 3,200 feet.
- 1.0 102.5 Fault scarps along the base the Hurricane Cliffs are quite apparent at 11:00, especially when the sun is low in the sky. Alluvial fault scarps that record the past few faulting events are very common along the base of the cliffs from this area south to Twin Butte. These scarps are formed in steep late Quaternary alluvial fans or colluvial slope deposits composed of rather coarse, poorly sorted gravels. Morphologic analyses based on diffusion modeling suggest an early Holocene to late Pleistocene age for these fault scarps (Amoroso and others, 2002). The south-dipping Moriah Knoll basalt surface in the relay ramp is at 9:00. The basalt obviously flowed south along the relay ramp, but it also has likely been tilted southward because of increasing fault displacement to the south subsequent to its eruption.
- 0.5 103.0 Go through gate.
- 1.0 104.0 Boulder Fan and trench are in view at 11:00. The drainage cutting into the cliffs south of the Boulder Fan is the location of a secondary fault trace that continues for a few kilometers behind the main trace.
- 0.4 104.4 Proceed through gate at Merchant Tank. The U.S. Fish and Wildlife Service released a number of juvenile condors into the wild atop this section of the Hurricane Cliffs in 1999 as part of efforts to ensure the survival of this largest North American bird species. The birds remained in the area through most of 2000, but eventually flew off to join their colleagues in the eastern Grand Canyon area. It is rumored that they left either because the geology is more interesting or the pickings are better in Grand Canyon.

- 1.2 105.6 **Turn left** onto a dirt track, follow it toward Sheep Pockets Reservoir (a large stock tank), proceed around the tank to the left and follow the track up an increasingly steep alluvial fan to the base of the cliffs.
- 1.0 106.6 Park near the large boulder.

**STOP 1-2. Boulder Fan trench.** (Russell Spring 7.5' quadrangle, T37N, R9W, section 15).

This stop is near the apex of the Boulder Fan where we excavated a 70-meter-long trench across the Hurricane fault (figure 13). Topographic profiles across the fault scarp show 4 to 4.6 meters of far-field vertical surface displacement of the fan surface. Based on calibrated carbonate rind measurements, we estimate the age of the alluvial fan surface to be late

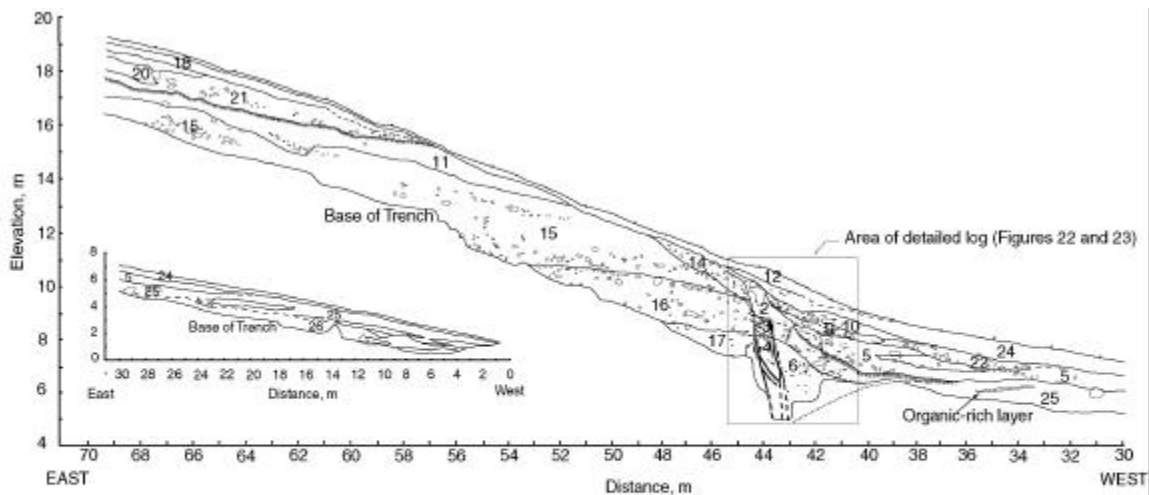


**Figure 13. Detailed topographic map of the Boulder Fan, one-meter contour interval. The trench is on the southern part of the fan. The framework fluvial unit (Unit 5) seen in the trench was deposited in a back-tilted area on the hanging wall after the MRE. The results of 80 measurements of clast imbrication of Unit 5 indicate a source direction of  $117^{\circ} \pm 11^{\circ}$  (95% confidence interval).**

Pleistocene (15 to 75 ka; Amoroso and others, 2002). This trench revealed fairly complex stratigraphy in the hanging wall associated with fault deformation, rotation of strata adjacent to the fault, and erosion of the fault scarp. We believe there is solid evidence for two faulting events since deposition of the fan sediment; the youngest event occurred about 10 thousand years ago. Each faulting event involved at least 1.5 meters of surface displacement, suggesting that they were associated with large earthquakes that ruptured much or all of the Shivwitz segment of the Hurricane fault.

### Trench Stratigraphy and Structure

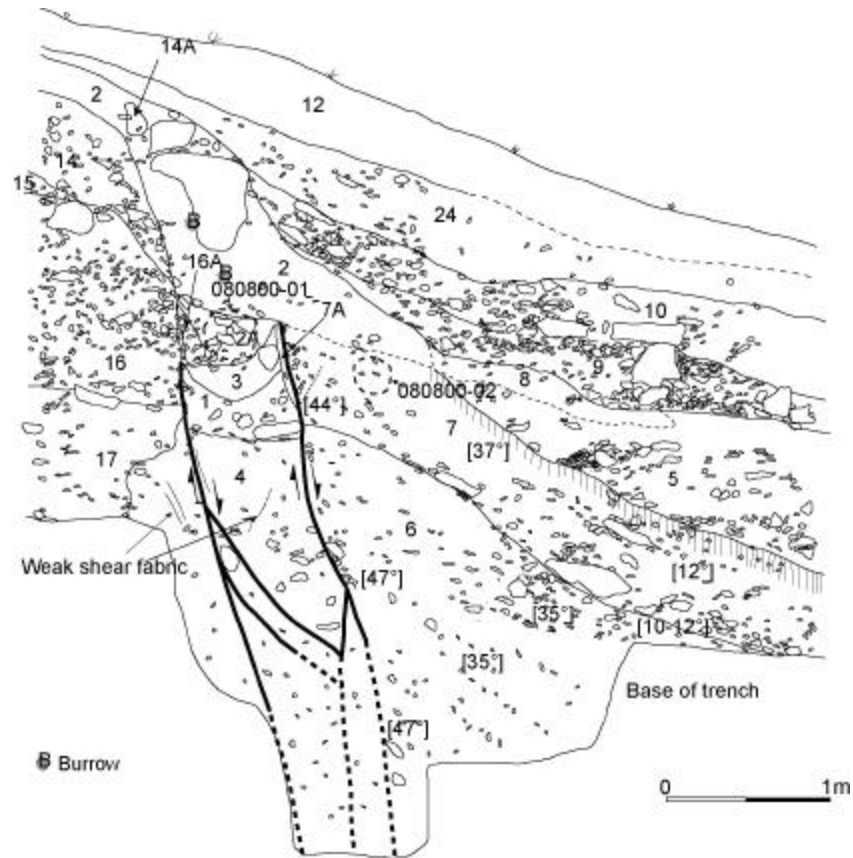
Deposits exposed in the trench record deformation in the past two faulting events and the erosion and deposition that occurred at the fault scarp in response to the faulting. Thus, we may use these deposits to interpret the recent history of the Hurricane fault at this site. The stratigraphy in the footwall consists of a series of ~0.5- to 3-meter-thick debris-flow deposits and minor framework gravels that are probably water-lain deposits (figure 14; see Amoroso and others [2002], for more complete discussion of the fault trench). The debris-flow materials are clayey to silty sand, pebbles, cobbles, and some boulders, primarily matrix supported. Stratigraphic relationships in the hanging wall are more complex. Beginning at the bottom, they consist of: (1) debris-flow deposits that we correlate with the uppermost strata exposed in the footwall (Unit 25), (2) a mystery unit against the fault zone (Unit 6) that probably is correlative with the debris-flow deposits of Unit 25, but might represent the oldest colluvial package derived from the fault scarp, (3) poorly sorted and weakly stratified colluvium derived from the fault scarp after the penultimate event (PUE; Unit 7), (4) a colluvial wedge derived from the scarp formed in the most-recent event (MRE; Unit 2), (5) a framework fluvial gravel also derived from the scarp after the MRE (Unit 5), and (6) a mantle of fine-grained slope colluvium that likely has a significant eolian component (Units 24 and 12).



**Figure 14. Log of the south wall of the Boulder fan trench. The lower portion of the trench is shown in the inset. Alluvial-fan deposits on the footwall consist of a series of debris flows with a thin veneer of slope-wash materials. Units adjacent to the fault in the hanging wall were derived from the degrading fault scarp; farther from the scarp, we observed pre-faulting fan deposits. Soil development on the surface of the penultimate wedge (Unit 7) appears to have obscured the basal contact with Unit 25. The buried soil zone in Unit 25 (between 34 and 36 m marks), and clast fabric of the eastern part of that unit (between 30 and 36 meter marks) show that these surfaces have tilted back toward the fault. We observed no antithetic faulting or tectonic fissures west of the fault zone.**

Structural relations of the fault zone shown in figure 15 are relatively subtle. The eastern fault is marked by weak shear fabric in Unit 17 against Unit 4 and by several rotated and broken

clasts. It appears to have experienced most of the movement during the MRE. The western bounding fault is clearly defined by shear fabric and an accumulation of additional soil carbonate low in the trench. The zone of cemented and sheared gravels between the faults may be a small graben that formed during the penultimate event. These faults were zones of preferential water infiltration suggested by the enhanced carbonate accumulation in Units 4 and 17, as well as roots of living plants that followed the fault zone to a depth of 4 meters below the ground surface. The western fault had an estimated 15-25 centimeters of movement in the MRE, based on the displacement of Unit 7A compared to Unit 7. Based on the limited upslope extent of the penultimate event (PUE) wedge (Units 7 and 7A), it is likely that most or all of the displacement in the PUE occurred on the western fault.

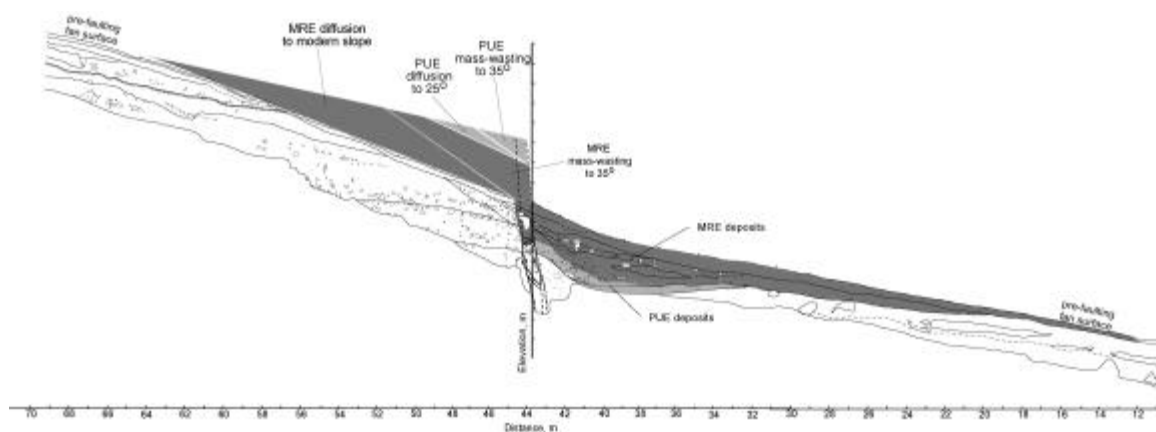


**Figure 15. Detail of the fault zone in the Boulder Fan trench. We deepened the trench at the fault zone to further investigate the nature of the faulting and expose more of Unit 6. Unit 6 is depicted as a debris-flow unit that shows the effects of fault drag. Alternatively, Unit 6 may be evidence of a third event.**

Most of the sediment exposed at the base of the scarp was deposited after the MRE (about 37 m<sup>2</sup> of the trench area; see table 2). The colluvial wedge associated with the MRE (Unit 2) was apparently deposited against an eroded free-face (Units 14 and 16 and on top of fissure-fill material (Units 2A and 3). The large boulder in Unit 2 probably fell during the MRE or was derived from degrading of the free-face immediately after the MRE. The basal contact of Unit 2 with the penultimate wedge (Unit 7) is locally indistinct, perhaps due to erosion of the top of the penultimate wedge. The upper stratigraphic units exposed in the hanging wall consist of framework gravels (Unit 5) that filled a trough along the base of the scarp, and a mantle of fine-grained material derived from the scarp. Closer to the scarp, Unit 5 appears to have been buried

below slope colluvium (Unit 24), a slump or debris flow (Unit 22), and fluvial deposits. Although the sedimentology of the framework gravels suggest that they might have been deposited by a stream flowing along the scarp, clast imbrication measurements show they were transported downslope across the fault (figure 13). A bulk sample from a fissure fill at the base of the most recent surface-faulting earthquake (MRE) colluvial wedge yielded 3 milligrams of unidentifiable charcoal and 2 milligrams of sagebrush charcoal. This sample was collected because such locations have been interpreted as providing the closest minimum limiting age of the rupture (McCalpin and Nelson (1996). Lawrence Livermore National Laboratory (Center for Accelerator Mass Spectrometry, Livermore, CA) analyzed the organic material and reported a radiocarbon age of  $9,910 \pm 210$  yr BP for the MRE. The corrected 2- $\sigma$  calendar age of the sample is 8,870 to 10,370 cal B.P. This date is probably a reasonable age estimate for the MRE, as the dated material is rather delicate and it is likely that the fissure filled very soon after surface rupture.

Deposits associated with the PUE (Unit 7) are much less extensive than the MRE deposits. They consist primarily of matrix-supported, weakly stratified fault scarp colluvium that displays an increase in clast number and size downslope. McCalpin and others (1993) observed a similar change in the scarp derived colluvium fabric at the fault scarp produced by the 1983 Borah Peak earthquake, where they noted that proximal parts of the wedge are more matrix rich than the distal portion. Many of the larger clasts of Unit 7 are aligned with the long axis pointing downslope, and there is some imbrication of clasts in the medial and distal part of the wedge. Soil development at the top of Unit 7, manifested by enhanced soil carbonate and clay accumulation, implies a significant hiatus between the PUE and the MRE. The lower contact between Units 7 and 6 is clear, but the contact between Unit 7 and the pre-faulting fan surface (Unit 25) farther west is subtle and probably not completely exposed in the trench. A dark, slightly organic-rich horizon that may be a burned layer exists between the 34 and 36 meter marks (figures 14 and 16); it may be at the contact between Units 25 and 7, or it may be within Unit 25. Uncertainty regarding the base of Unit 7 leads to some uncertainty in the size of the colluvial wedge associated with the PUE (about 3.5 to 6 m<sup>2</sup> of the trench area).



**Figure 16. Trench log showing relations between scarp erosion and deposits observed in the Boulder Fan trench. Wedges on the footwall are approximations of the material eroded from the scarp after the PUE (light shading) and the MRE (dark shading). In this example, throw in the PUE and MRE was 2.5 and 3.5 meters, respectively. The same shading pattern shows the areas of deposits associated with the PUE and MRE interpreted from the trench log. The location of the base of the PUE wedge is uncertain and probably not completely exposed, and the near-surface horizon in the MRE wedge probably has a substantial eolian component. Nonetheless, there is a close correspondence between the areas eroded from the scarp and the actual observed deposits in this scenario.**

Unit 6 is likely a debris-flow deposit that is correlative with Unit 25, but the possibility that it is a third colluvial wedge cannot be completely excluded. The clast fabric dip is somewhat less

than the penultimate wedge (Unit 7), which likely represents discordance between the dip of the original fan sediments and the overlying colluvial wedge as it accumulated. Support for correlation of Unit 6 with Unit 25 includes evidence of fewer clasts of 10 to 25 centimeters (long axis) in Unit 6 than in Unit 7. The depositional fabric of Unit 6 steepens from 35 degrees to 47 degrees near the fault; this is likely the result of normal fault drag. If Unit 6 is a colluvial wedge, it is at least 2 meters thick next to the fault as no obvious base to Unit 6 is exposed in the trench. Ostenaar (1984) observed in other trench investigations that colluvial wedge thickness was approximately half of the free-face height. The colluvial wedge interpretation for Unit 6 implies ~ 4 meters of throw across the fault zone in a possible third faulting event and at least 8 meters of cumulative throw at the fault zone since fan deposition. Rather sharp reverse-drag deformation of the hanging wall near the fault would be required to make space for the thick colluvial wedge. The principal problem with this interpretation is that the contact between Units 6 and 7 dips about 35 degrees to the west, and therefore cannot have been rotated to the east by any significant amount. Thus, all of the near-fault reverse drag occurred in the hypothetical first event, and none in the PUE or MRE. If Unit 6 is correlative with Unit 25, then this steep contact implies that fairly sharp normal drag exists immediately adjacent to the fault zone. This normal drag is superimposed on longer wavelength reverse drag to account for the decreasing dip of the top of Unit 25 between the 15- and 40-meter marks.

### **Paleoearthquake Scenarios**

The fault-related stratigraphy in the trench provides some clues regarding the size and timing of the two surface ruptures that have occurred since deposition of the Boulder Fan. Immediately after a surface rupture, the fault scarp in alluvium erodes rapidly by processes of mass wasting until it reaches the angle of repose. Depending on the size of the scarp and the erodibility of scarp material, it might take decades to centuries to remove a scarp free-face (Wallace, 1977). The scarp subsequently erodes more slowly by diffusive slope processes (Nash, 1980; Hanks and others, 1984). We can estimate the amount of material eroded from the footwall by these processes in various displacement and scarp erosion scenarios using some simple graphical analyses. The fault zone marks the approximate transition between erosion and deposition on the scarp, so most or all of the material that is eroded from the footwall is deposited immediately downslope on the hanging wall, forming the fault-related deposits that we recognize in fault trenches. Using the trench log, we can compare predictions of the amount of material eroded from the footwall with the amount of material that has been deposited on the hanging wall.

We modeled several displacement scenarios to estimate the amount of material eroded from the upper half of the scarp in two faulting events (figure 16; see Amoroso and others, 2002, for more complete discussion of the modeling). All scenarios account for about 6 meters of total throw at the fault zone. In any reasonable scenario, erosion of the scarp to its modern form after the MRE generated a much larger wedge of colluvial deposits than erosion to a similar slope after the PUE. As the scarp crest migrates upslope on an existing fault scarp, a much larger slice of the footwall must be removed by erosion to decrease the scarp slope. This is consistent with our trench interpretation, in which the area of PUE deposits is 10 to 20 percent of the area of the MRE deposits (table 2). Moreover, the size of the PUE wedge indicates that displacement in the PUE could not have been any larger than the MRE. Something like 2.5 to 3 meters of throw in the PUE and subsequent erosion of the scarp to about 25 degrees predicts the size of Unit 7 quite well, and 3 to 3.5 meters of throw and erosion to the modern slope fits the size of post-Unit 7 deposits fairly well. There appears to be a modest excess of mass in the post-MRE deposits (~2 to 4 m<sup>2</sup>), which may be the result of eolian input. The sizes of the PUE and MRE deposits can also be fit fairly well with a small PUE (2 meter throw) and a more eroded scarp (20°). In either case, it appears that the MRE was as large as or larger than the PUE.

Fairly large alluvial fault scarps are preserved intermittently along much of the Shivwitz segment, but this is the only locality where we have detailed information about the size and ages of young faulting events. The displacements we have inferred for paleoseismic events at the Boulder fan suggest that two large earthquakes occurred in the past few tens of thousands of years. Given the size of the surface displacements at the Boulder fan, it is reasonable that the earthquakes involved much of the entire Shivwitz segment. Morphologic analyses of fault scarps on the southern part of the Shivwitz segment suggest that this part of the segment ruptured in the

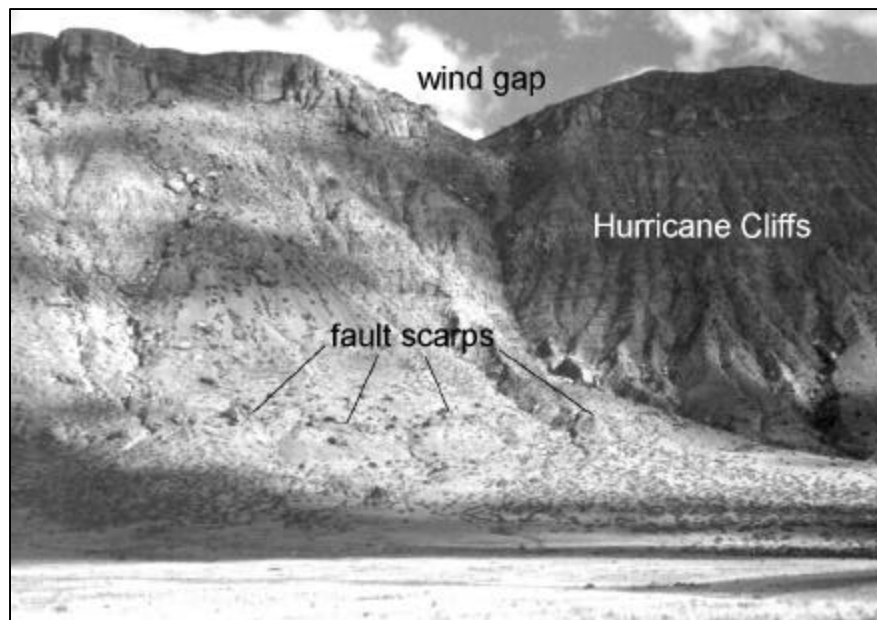
**Table 2. Predicted and measured colluvial deposits for the Boulder Fan trench. All scenarios account for 6 meters of throw at the fault. "PUE erosion" refers to the scarp slope prior to the MRE. The amount of material eroded from the scarp after a faulting event is a function of throw in the event, the slope of the surface above the fault scarp, and how long the scarp is eroded. Measured wedge areas were determined from the trench log. The maximum area for the PUE was estimated using the dark organic layer as the base of the PUE colluvium and extrapolating beneath the floor of the trench. The maximum area for the MRE includes the fine-grained surface layer. Because the slope above the MRE scarp was greater than the original fan slope, much more material must have been eroded to achieve a 20 to 25 degree scarp slope. This resulted in the formation of a much larger colluvial package, which is consistent with what we observed in the trench. The amount of material deposited after the PUE (<6.5 m<sup>2</sup>), excludes many of the displacement and erosion possibilities. Three displacement and erosion scenarios that fit the observed deposits in the trench are shown in bold font.**

Modeled Erosion Scenarios				Measured Wedge Areas			
Scenario	PUE erosion	Event	Throw (m)	Wedge Area (m <sup>2</sup> )	Event	Min. Area (m <sup>2</sup> )	Max. Area (m <sup>2</sup> )
1	25°	<b>PUE</b>	<b>2.5</b>	<b>4.1</b>	PUE	3.5	6.5
		<b>MRE</b>	<b>3.5</b>	<b>36.1</b>			
2		<b>PUE</b>	<b>3.0</b>	<b>6.0</b>	MRE	22.5	37.9
		<b>MRE</b>	<b>3.0</b>	<b>34.5</b>			
3		PUE	3.5	7.9	Total	26.0	44.4
		MRE	2.5	32.1			
4	20°	PUE	3.5	13.9			
		MRE	2.5	27.0			
5		PUE	3.0	10.2			
		MRE	3.0	29.7			
6		PUE	2.5	7.3			
		MRE	3.5	33.0			
7		<b>PUE</b>	<b>2.0</b>	<b>4.5</b>			
		<b>MRE</b>	<b>4.0</b>	<b>35.5</b>			

latest Pleistocene or early Holocene, probably in the same event recorded in the trench (Amoroso and others, 2002). We know very little about the age of the MRE on the northern part of the Shivwitz segment, however. As we discussed at Stop 1-1, there is an extensive zone of fault complexity a few kilometers north of the Boulder Fan from the Moriah Knoll basalt to the Navajo Trail, and this is also an area of minimum escarpment height. These factors suggest that the Shivwitz segment could be further subdivided (see Menges and Pearthree, 1983) and that parts of the segment may rupture independently. At this time, the total length of the MRE on the Shivwitz segment is poorly constrained and we do not have sufficient evidence to evaluate the long-term seismologic behavior of the segment.

Return back the way you came in, turn right onto main track and retrace your path north to the Navajo Trail. We will now be driving along the Shivwitz segment of the Hurricane fault for about 15 miles.

- 3.3 109.9 Take main left road at small Y intersection.
- 0.3 110.2 Gate.
- 0.6 110.8 Bear right at road junction.
- 1.4 112.2 Bear left at road junction.
- 0.1 112.3 Gate. Continue straight ahead.
- 3.8 116.1 **Bear right at Y intersection** onto graded gravel road. You are now on the Navajo Trail.
- 0.3 116.4 **Turn left** off the Navajo Trail onto smaller road (Temple Trail). We are now on a thin Pleistocene alluvial deposit over the Moenkopi Formation. If the lighting is right, you should be able to see late Quaternary fault scarps along the base of the Hurricane Cliffs as we descend toward the valley bottom. Fault scarps are particularly apparent on steep alluvial fans below the prominent notch or wind gap in the top of the cliffs north of the Navajo Trail. Scarps just north of the small drainage that comes down from the wind gap are as much as 25 meters high, but because the fan slopes are so steep, surface displacements are more like 7 to 10 meters (figure 17).



**Figure 17. Photo showing fault scarps at the base of the Hurricane Cliffs north of the Navajo Trail. Scarps in the sunlight are as much as 25 meters high, but because of the steep far-field slopes, surface displacement is about 10 meters.**

- 1.1 117.5 For the next few miles, we will chiefly be on Holocene valley bottom deposits and distal alluvial-fan deposits. Slightly higher areas are covered with relict valley-floor deposits that are likely Pleistocene in age. Bedrock exposures along the wash are the lower and middle members of the Moenkopi Formation, including



the relatively resistant Virgin Limestone Member (Billingsley, 1992a). The Toroweap and Kaibab Formations crop out in the Hurricane Cliffs to the east. The Kaibab Formation crops out in hills to the west. There is a nice view of some of the structural complexity of the Hurricane fault zone in the Navajo Trail area at 2:00.

- 1.0 118.5 Units dipping east into the Hurricane fault in a rollover monocline are evident at 1:00.
- 0.6 119.1 Pass through gate. At 12:00 we can see the apex of the State Line geometric bend; the back-tilted Hurricane Wash basalt is visible to the left (W).
- 1.4 120.5 Continue straight at Y intersection.
- 0.7 121.2 Fairly sharp east dip of beds of the Harrisburg Member of the Kaibab Formation in a rollover monocline is visible at 12:00-1:00.
- 0.7 121.9 Light-colored scars on the Hurricane Cliffs at 3:00-4:00 indicate locations of recent debris flows. Boulderly debris-flow lobes and levees are very common on Holocene fans along the Hurricane Cliffs, so debris flows are obviously a very important mechanism for moving material from the cliffs onto the adjacent piedmont.
- 0.2 122.1 At this point we begin to see deep arroyos that have formed along Hurricane Wash. Arroyos typically have fairly flat bottoms and nearly vertical sides as they initially develop. Arroyos propagate upstream through a series of headcuts (essentially waterfalls) where flow is concentrated and pours into the arroyos. During floods, headcuts may migrate hundreds of meters upstream. As arroyos mature, they become wider and eventually the sides become less steep. Similar arroyos have formed in many places in the Southwest in the past 120 years or so. As in the situation we see here, arroyos typically have formed where valley bottoms were covered with relatively fine sediment and channels were small and discontinuous. Concentration of flow in these areas by natural or anthropogenic causes, combined with floods, caused accelerated erosion of the fine valley bottom fill. The steep walls and headcuts in this system indicate that it is actively eroding upstream in the modern valley bottom. We will be following (and avoiding) this arroyo system for the next several kilometers.
- 0.2 122.3 As was noted earlier, strata of the Kaibab Formation are tilted unusually steeply toward the Hurricane fault in a rollover monocline at 9:00-10:00. Just to the north, this monocline is probably faulted (Billingsley, 1992b).
- 0.5 122.8 Coarse, fresh deposits on a tributary alluvial fan cross the road here. These deposits may represent the distal end of a debris flow that began on the Hurricane Cliffs.
- 0.1 122.9 Gate. The arroyo is about 30 meters to the west; to the east, steep alluvial/colluvial deposits are evident along the lower part of the Hurricane Cliffs.
- 0.5 123.4 Temple Trail sign. The Temple Trail followed the valley bottom from the Moriah Knoll basalt to Black Rock Canyon to the north.
- 1.4 124.8 **Keep right** and stay on Temple Trail. The left fork joins the Sunshine Trail, which may eventually be followed to St. George, Utah.
- 0.8 125.6 Headcut on a tributary wash is next to road. **Bear right.**

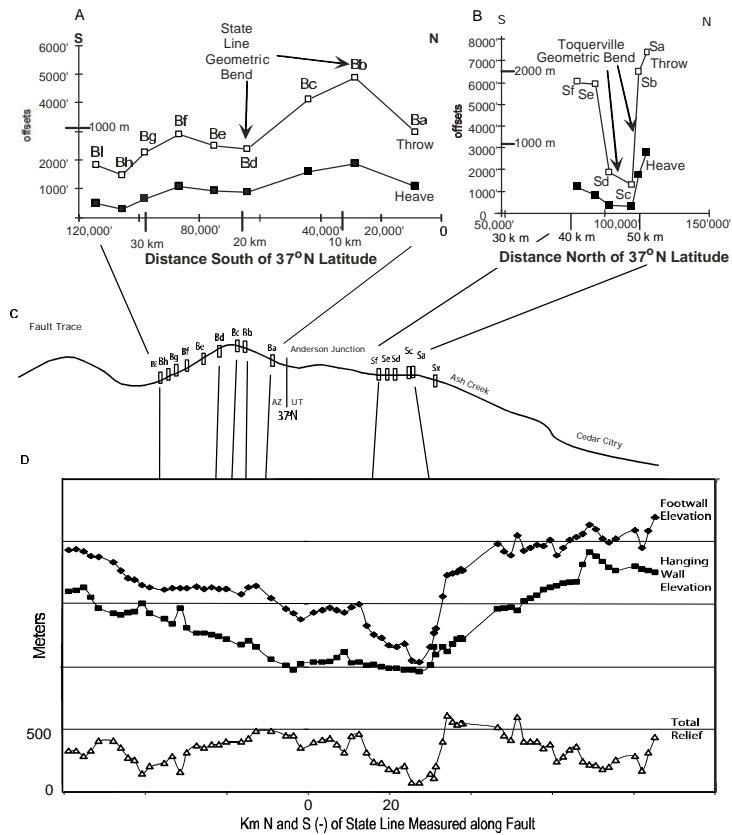
- 0.3 125.9 Numerous small arroyos to the right of the road. The road is migrating to the west to avoid the headcuts. At the base of the Hurricane Cliffs you can see steep alluvial fans and colluvial slopes with fairly large, eroded fault scarps developed on them.
- 0.2 126.1 Cross a sizable tributary wash.
- 0.2 126.3 Shinarump Conglomerate, at the base of the Triassic Chinle Formation, crops out on the left side of the road here.
- 0.2 126.5 The track formerly followed the left (west) bank of Hurricane Wash through this area, but it was washed out in the late 1980s. The track now crosses Hurricane Wash several times and circumvents the washed out stretch by traversing dissected alluvial fans on the east side of the wash. The next several kilometers of the route are rough and steep – 4-wheel drive is strongly recommended. See, you thought I was kidding about Arizona's rough roads.
- 0.5 127.0 Bear left at fork.
- 0.2 127.2 Cross Hurricane Wash. You are now back on the "road" that has existed for many decades. It climbs to a bench on the Hurricane Wash basalt, which has recently been dated at  $5.2 \pm 0.15$  (Ar/Ar; Downing and others, 2001). The road has not been maintained very recently and is steep and rough.
- 3.3 128.3 Park just beyond the gate. Walk to top of knoll to the north.

**STOP 1-3. State Line Bend.** (Rock Canyon 7.5' quadrangle, T41N, R10W, section 34).

At this stop, we are standing on Quaternary basalt near the apex of the State Line geometric bend, a relatively abrupt bend in the trace of the Hurricane fault. This salient parallels the visible bend in the cliffs, which lie to the east and south. (figure 18). The State Line geometric bend lies between the Shivwits geometric segment to the south and the Anderson Junction geometric segment to the north. The Hurricane Cliffs form the fault-line scarp on the footwall of the fault. The butte to the northwest is East Mesa.

The Paleozoic units exposed in the cliff near here lie in the footwall. Recognition and identification of these units is critical in determining the total stratigraphic separation on the fault segments north and south of this bend as well as at the bend. The units are, from lowest to highest, the Permian Esplanade Sandstone, which is a red, white, or tan sandstone near the base of the cliffs; the Permian Hermit Shale, which is a red, brown, and white siltstone to sandstone; the Permian Toroweap Formation, which contains three members: a lower unit of interbedded gray, yellow, and brown sandstone, siltstone, and dolomite (Seligman Member); a middle gray limestone cliff (Brady Canyon Member); and an upper gypsiferous unit of gray siltstone and light-red siltstone to sandstone (Woods Ranch Member); and near the top of the cliffs, the Permian Kaibab Formation with a lower gray cherty limestone (Fossil Mountain Member) and an upper red and gray unit of interbedded limestone, sandstone, and siltstone with white gypsum. More complete descriptions of these units are available with the quadrangle map for this area (Billingsley and Workman, 2000) and in Sorauf and Billingsley (1991).

We interpret the State Line geometric bend as the zone of linkage between the Shivwits and Anderson Junction geometric segments for several reasons. (1) The general fault strike changes across the State Line geometric bend. Just south of the bend, the Shivwits segment strikes  $\sim N30^{\circ}W$ . Just to the north of the bend, the Anderson Junction segment strikes  $\sim N25^{\circ}E$ . (2) The number of fault strands in the two segments differs. The Shivwits segment, just to the south, contains several fault strands exposed in both the bedrock footwall and the Quaternary deposits. Several of these faults appear to link and form relay ramps, evidence of strain transfer.



**Figure 18.** This figure summarizes the relations between changes in fault geometry, total displacement and elevation along the Hurricane fault from the Mt. Trumbull bend (salient) to the southern part of the Cedar City segment. (A) Displacement (offset) vs. distance graph along the State Line geometric bend. Note that the pattern most closely resembles that of fault capture (cf. Figure 5). (B) Displacement (offset) vs. distance graph along the Toquerville geometric bend. Note that the pattern most closely resembles that of linkage of underlapping faults (cf. Figure 5). (C) Map of the trace of the Hurricane fault. The salients at the State Line and Toquerville geometric bends are of different shapes and widths (measured normal to the general fault strike). The width probably reflects the original spacing between the linked faults. (D) Graph of distance vs. relief, footwall elevation and hanging wall elevation. Note that the changes in elevation mimic the changes in displacement at the State Line and Toquerville bends. Elevation may serve as a proxy for the total displacement pattern in locations where total offset cannot be determined.

In contrast, the Anderson Junction segment is more structurally simple. To the north, the Anderson Junction segment, contains one main strand near the Hurricane Cliffs with a few young scarps exposed in the Quaternary deposits. The few footwall faults present in the southern Anderson Junction segment have relatively minor offset and limited length. (3) The numbers and orientations of minor faults and folds also change at the bend (Billingsley and Workman, 2000). (4) The total displacement changes around the bend (figure 18). A minimum in total displacement exists slightly south of the bend apex. This pattern is consistent with that created by linked faults where the northern fault propagated more quickly than the southern fault and eventually captured the southern fault (figure 5). We can see an artifact of this displacement change in the elevation of the Triassic Chinle Formation in the hanging wall relative to the Paleozoic units in the footwall (described below). The elevation of the Chinle Formation is higher near the apex of the salient than along the fault sections to the north and south, which

corresponds to a decrease in stratigraphic separation at the bend. These multiple data sets allow us to interpret that the Anderson Junction and Shivwits segments linked by fault capture.

In cases where a large amount of the total slip occurred at a linkage zone after linkage, the fault may be driven by the release of elastic strain to increase slip rates at the bend. This process would effectively erase the displacement minimum near a linkage site. Because the displacement minimum still exists at the State Line geometric bend, it appears that the largest percentage of the slip at this bend took place prior to linkage. However, the Hurricane fault is a through-going fault in this area, which indicates that there was some post-linkage slip at the bend.

Another displacement minimum in the displacement-distance profile occurs along the Shivwits segment (figure 18) several miles south of the State Line geometric bend. Near this displacement minimum, the number of apparent fault strands and splays decreases and the displacement plateau slopes. A slope in the plateau suggests that a displacement gradient existed along the captured fault. However, it is also possible that the gradient formed during post-linkage slip. This minimum may reflect linkage of a smaller fault within the segment, displacement transfer via relay ramps containing folds, or post-linkage slip.

Various Quaternary deposits crop out along the base of the Hurricane Cliffs and in the fault's hanging wall. These deposits lack preserved fault scarps near the apex of the bend, but they, or similar deposits, are faulted north and south of the bend. These sedimentary deposits include small alluvial fans, talus, alluvium, landslide deposits, colluvium, and gravel terraces largely in the hanging wall. Many of these deposits are the debris-slope and wash-slope facies associated with the degradation of the Hurricane fault escarpment.

Quaternary igneous rocks include mafic lava flows and a small pluton that intrudes them. The hill to the west consists of mafic extrusive rocks and contains at least four distinct flows that are separated by agglomerates. The flows are fine grained and contain varying amounts of plagioclase and olivine phenocrysts.

Two flows from the basalt field in this area are dated. One sample is from East Mesa a few kilometers to the northwest at 36.9°N, 113.363°W. This flow cascaded over the boundary fault of a graben within the basalt field (Downing and others, 2001). The graben is in the hanging wall of the Hurricane fault. Based on  $^{40}\text{Ar}/^{39}\text{Ar}$  dating, the basalt is  $5.16 \pm 0.14$  Ma (Downing and others, 2001). However, this date represents a total gas age because the data lacked both a plateau and an isochron. Wenrich and others (1995) dated a second sample from East Mesa located at 36.902°N, 113.417°W. That sample yielded a date of  $1.4 + 0.25$  Ma using the K/Ar method.

Walk along the road to the south and then cross the wash on the east toward the mafic rocks that lie near the fault. The vertical columnar joints are associated with the pluton. This intrusion may plug a volcanic vent that was the source for some of the basalt flows in this region. The pluton or plug also has plagioclase and olivine phenocrysts, but is granular and coarser grained than the flows. Maureen Stuart (unpublished data from UNLV XRF laboratory, 1995) analyzed samples from the four flows and the plug for major and trace element contents; they are all subalkaline tholeiitic basalt.  $^{40}\text{Ar}/^{39}\text{Ar}$  dating of this intrusion is in progress. Because of erosion along the east side of the intrusion, the timing of intrusion emplacement relative to movement along the Hurricane fault is equivocal. However, some flow directions in the basalt to the west are toward the east-southeast (and the Hurricane Cliffs) and no basalt crops out on the footwall directly to the east. This relationship suggests that at least some of the fault escarpment existed prior to eruption of the basalt flows and that the basalt flowed toward a topographic low along the fault.

Proceed north along dirt road.

0.7 129.0 Rocks of the Kaibab Formation crop out at 1:30-2:00 in front of the main escarpment across Hurricane Wash. The lower part of the main escarpment consists of the Toroweap Formation. This Kaibab block was probably displaced down-to-the-west by a minor fault or a landslide off of the cliffs.

1.0 130.0 We are driving over a fairly extensive, relatively young terrace of Hurricane Wash.

- 0.1 130.1 Drive up onto a Pleistocene terrace of Hurricane Wash.
- 0.1 130.2 Intersection with a power line road. Continue straight north.
- 0.4 130.6 We are driving near the interface between alluvial fans deposited by tributary drainages that head on the cliffs and a relict Pleistocene terrace of Hurricane Wash.
- 0.4 131.0 Gate.
- 0.2 131.2 Bear right.
- 0.5 131.7 Park on the side of the road and walk to left (west) of road ~35 meters to the top of a low hill. The hill is the eroded remnant of a Pleistocene terrace of Hurricane Wash. To the northeast along the Hurricane Cliffs, we can see a zone of multiple faults and structural complexity where the Honeymoon Trail ascends the cliffs. Farther to the north, we can see a relatively young Quaternary basalt that was erupted on the footwall and cascaded over the escarpment. The large canyon to the east-southeast is Cottonwood Canyon.

Turnoff to right and follow rough, winding track if you want to drive up to the mouth of Cottonwood Canyon (0.7 miles each way).

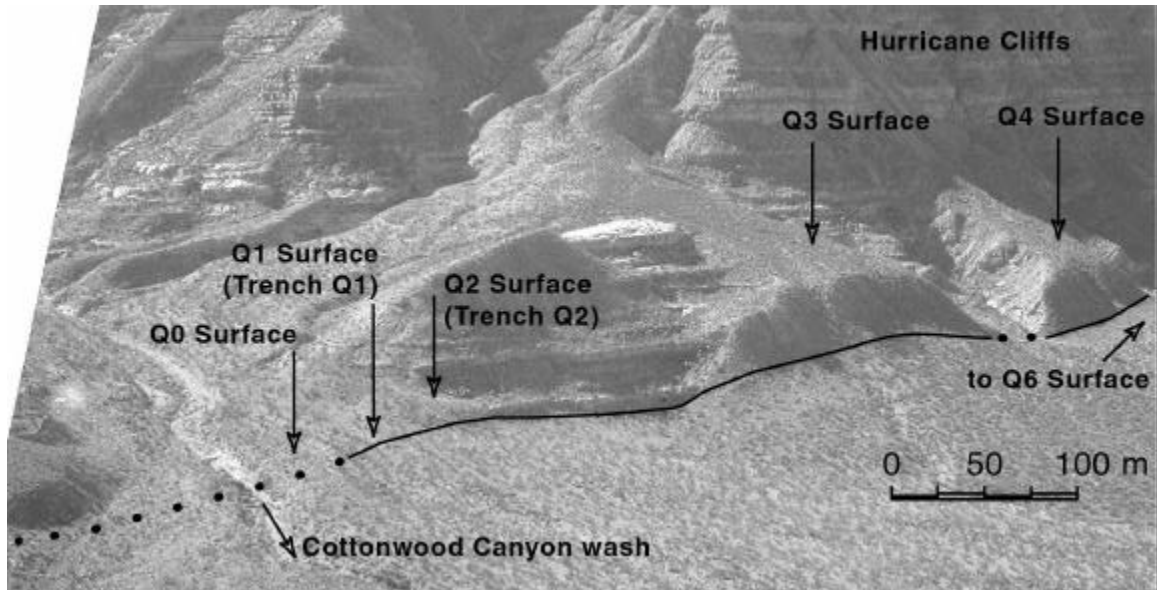
**STOP 1-4. Cottonwood Canyon Trench Site Overlook** (Rock Canyon 7.5' quadrangle, T41N, R10W, section 14)

At this stop about 6 kilometers south of the Utah/Arizona border we will view the mouth of Cottonwood Canyon, where Cottonwood Wash has incised through the Hurricane Cliffs. Near the mouth of this canyon, the late Quaternary activity of the Hurricane fault is beautifully recorded in a stair-step sequence of fault scarps formed in different-aged alluvial fans and terraces (figure 19). The alluvial surfaces are each remnants of deposits that were graded to a unique base level during the late Quaternary period. The Hurricane fault displaces five of these surfaces by increasing amounts with increased surface age; the larger fault scarps record multiple rupture events during the late Quaternary. In addition to the larger fault scarps, there is a low fault scarp that records the displacement during the MRE along this part of the fault, which probably occurred between 8 and 15 thousand years ago. We calculated a preferred late Quaternary slip rate of 0.15-0.3 mm/yr (18.5-20 m in 70-125 kyr) for this area of the Hurricane fault. This slip rate is based on displacements measured from topographic profiles across the fault scarps and estimates of surface ages from the qualitative assessment of soil development (primarily assessing carbonate development) and geomorphic profile modeling of a fault scarp to estimate the time over which it formed.

**Faulted and Unfaulted Alluvial Surfaces**

We identified several young, unfaulted terraces at the mouth of Cottonwood Canyon and five faulted alluvial surfaces south of Cottonwood Wash. These units are differentiated by: (1) the relative elevation of the upthrown portion of the unit above adjacent active stream channels, (2) soil development, (3) the presence of undulations and degree of dissection into their surfaces, and (4) fault scarp height. The degree of soil development increases with increasing unit elevation. Figure 20 is a topographic map of the Cottonwood Canyon mouth area and displays the spatial relations between four of the units.

Soil-profile development provides the basis for estimating the ages of the faulted units in this area. We examined the soils developed on surfaces Q3, Q2, Q1, and Q0 (figure 20). We found that surface Q3 has stage III carbonate morphology (Birkeland, 1984), Q2 has stage II morphology, Q1 has stage I morphology, and Q0 also has stage I morphology, but shows less development than surface Q1. Based on these carbonate morphologies, and comparing them and other soil characteristics (soil structure, color) to soils of the Desert Project in New Mexico,



**Figure 19. Oblique aerial photograph of the mouth of Cottonwood Canyon looking southeast.**

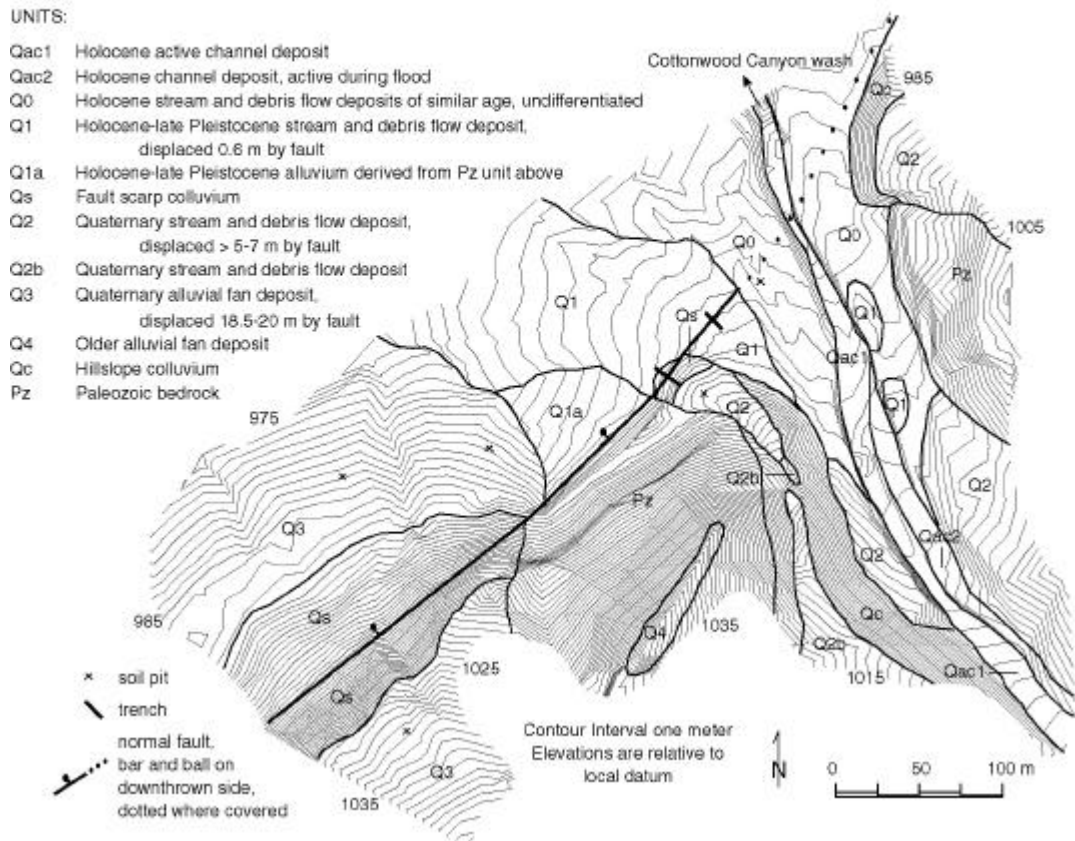
where the soils have developed in a similar climate and have estimated numerical ages (Gile and Grossman, 1979; Gile, 1994), we estimate the surface ages as follows: Q3 at 70-125 ka, Q2 at 20-50 ka, Q1 at 8-15 ka, and Q0 at 2-6 ka. To the south of surface Q3 is another faulted alluvial fan, Q4. We interpret Q4 to be intermediate in age between Q2 and Q3 based on its relative elevation. Farther south along the fault, is a steep colluvial landform, surface Q6. The Q6 colluvial apron grades to about the same elevation as Q3 and has recorded the same displacement as Q3, so we interpret it to be of similar age as surface Q3. Geomorphic profile modeling of the Q6 landform, using the technique described in Hanks (2000), yields results consistent with a conservative formation age of 70-210 thousand years for the scarp.

We estimated the vertical displacement across the Hurricane fault for the five faulted alluvial surfaces near Cottonwood Canyon from topographic profiles and from trench exposures of two of the surfaces. Surface Q6 and Q3 record 18.5-20 meters of vertical displacement. The downthrown equivalent of the Q4 surface has been buried by younger material so the 10-meter displacement measured for it is a minimum. The downthrown equivalent of surface Q2 has also been buried by younger material (of ~Q1 age) by more than 2 meters, as observed in a trench exposure, yielding a minimum net displacement of 7 meters for the surface. Fault displacement of the Q1 terrace surface is less than 1 meter.

### **Fault Trenches**

A 14-meter-long trench across surface Q1 exposed the deformation resulting from the MRE at Cottonwood Canyon (figure 21). Two fault strands reach to within 10-25 centimeters of the surface, displacing unconsolidated fluvial gravel and debris-flow deposits 37 centimeters down-to-the-west. Hanging-wall fault drag accommodates additional deformation, to yield a total of 58-60 centimeters of net vertical displacement across the 2-meter-wide fault and deformation zone.

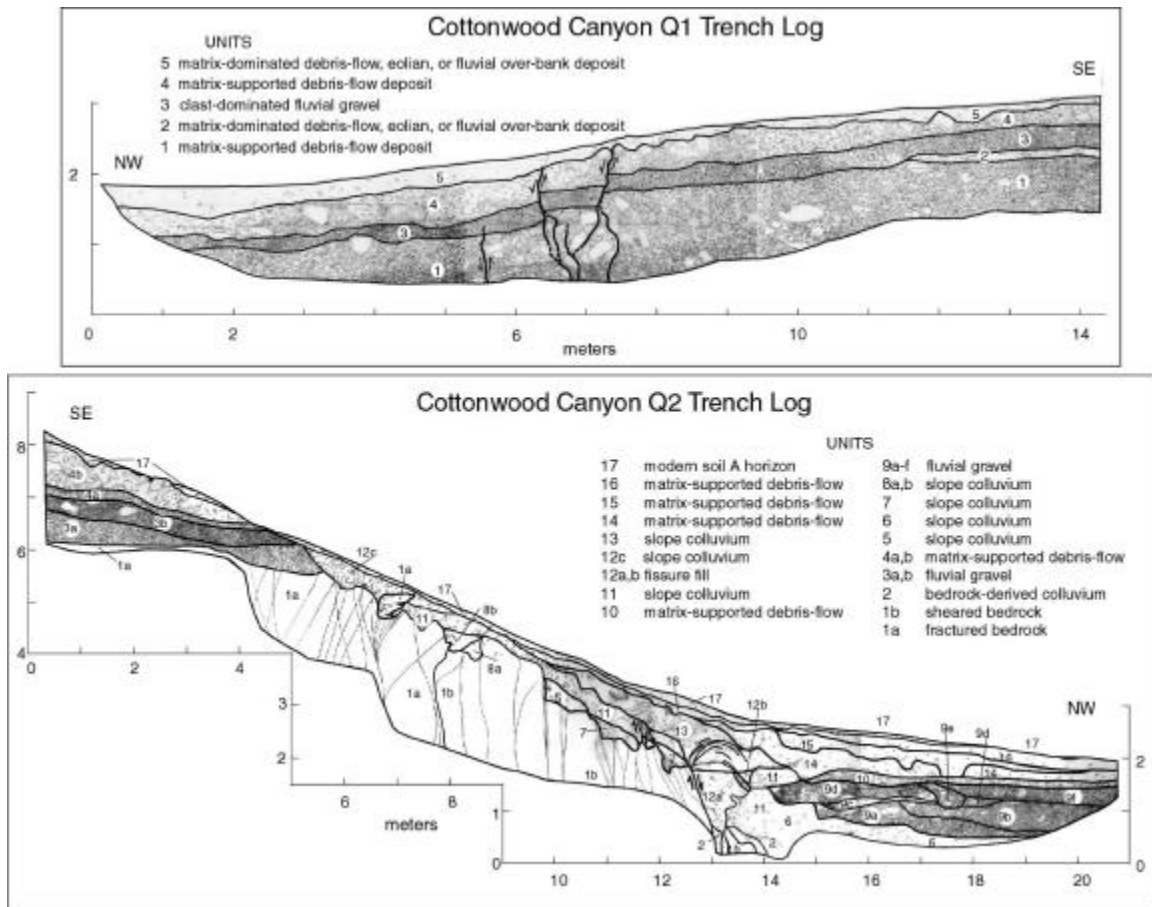
A silt-dominated deposit of debris-flow, fluvial overbank, or eolian origin caps the Q1 terrace surface and is the youngest unit exposed in the trench (Unit 5) (see Stenner and others, 1999, for detailed descriptions of trench units). Unit 5, from 10- to 50-centimeters-thick, is about twice as thick on the hanging wall side of the fault zone. Unit 5 was either (1) deposited after MRE faulting and the increased hanging-wall thickness is a result of increased deposition at the base of the MRE scarp, (2) deposited before the MRE, faulted, and then reworked across the



**Figure 20. Detailed topographic and geologic map of the south side of Cottonwood Canyon. Increasing displacement of older surfaces is evident. Trenches are in units Q1 and Q2.**

scarp to accumulate at the base, or (3) is eolian, and the oldest part of the unit is faulted with deposition continuing to accumulate more thickly in the swale formed against the scarp. The lower contact of Unit 5 does not have distinct displacement steps across the fault strands, suggesting that erosion began smoothing out the rupture topography before deposition of the uppermost unit. Alternatively, the lower contact of Unit 5 could be faulted, a possibility if displacement across the northwestern strand of the fault zone was distributed instead of discrete, and if the discrete displacement across the southeastern fault strand was obscured due to the presence of two large cobbles at the Unit 4/5 contact. A sub-vertical fabric observed in the lower part of Unit 5, above the fault strands, is consistent with the unit either being faulted or that post-event settling occurred above the fault zone subsequent to deposition. We believe that Unit 5 most likely post-dates the MRE.

Unit 4 is a poorly sorted, debris-flow gravel displaced by faulting. The 20- to 50-centimeter-thick, matrix-supported Unit 4 does not appear to have developed a significant soil before deposition of Unit 5, and we use the lack of a buried soil horizon to conclude that the time between deposition of Units 4 and 5 was possibly hundreds of years but not likely thousands of years. The three units underlying Unit 4 all show the same amount of vertical displacement across the fault zone, indicating that they have experienced the same faulting history.



**Figure 21. Logs for the trenches at Cottonwood Canyon. We found evidence for a single faulting event involving about 0.6 meters of vertical displacement in the Q1 trench. We concluded that the Q2 trench did not expose units in the hanging wall that are equivalent to the alluvial units in the footwall. The Q2 terrace surface has likely been buried on the hanging wall indicating a displacement of at least 7 meters.**

A second trench exposed faulting through the 5-meter-high scarp in the Q2 surface, about 25 meters southwest of the Q1 trench (figure 20). The trench revealed a 9-meter-wide zone of faulting in Paleozoic bedrock and overlying fluvial and debris-flow alluvium and colluvial units (figure 21). Deformation from the MRE, as seen in the Q2 trench, produced a 1-meter-wide fissure at the interface between bedrock and alluvium. We believe the top of Unit 11 was likely the ground surface at the time of the MRE, based on a fault strand that terminates at the contact between Units 11 and 13 and stratigraphic relations above the fissure (figure 21). Unit 11 is a matrix-dominated deposit present only on the cumulative fault scarp, and is likely colluvium deposited as the scarp eroded. We correlated Unit 11 across the MRE fissure, but at that location the unit lies in a convex-down part of the scarp, which together with the unit's limited extent, makes measurement of net vertical displacement by projecting the unit across the fault imprecise. We believe the net displacement recorded in the Q1 trench to be more robust, but we estimate that the MRE resulted in approximately 0.35-1.15 meters of net displacement on the Q2 fault scarp. We established the Q2 measurement by projecting the lower contact of Unit 11 across the MRE fissure and across steps in the contact along the cumulative scarp to the east (figure 21). One such step in Unit 11 is 3-4 meters east of the fissure, with a maximum possible MRE vertical slip of 0.8 meters. Unit 13, a matrix-dominated sandy silt colluvium, lies down-



slope from this step. Unit 13 is similar in grain size and texture with the fissure-fill material (Unit 12a), and together they form a colluvial package of material eroded from the fault scarp and re-deposited in the fissure and across the lower scarp. Not all of the Unit 13 material necessarily came from MRE-formed scarp(s), but may also have come from other units higher in the cumulative scarp that eroded after the MRE in a continual process to smooth out the 5-meter-high fault scarp. Arcuate fractures within Unit 13 appear to originate at the main slip plane of the MRE fissure, and are possibly related to post-event compaction of the loose fissure-fill material.

The trench did not expose the down-faulted equivalent of the Q2 terrace surface, which is likely buried by alluvium of the Q1 alluvial fan/terrace (figure 20). Units 9, 10, and possibly 14 and 15 are part of the sediment package of Q1 age that buried the down-faulted Q2 surface. The Q2 trench was 2 meters deep across the 5 meter scarp, therefore unless erosion removed the Q2 surface from against the scarp before the Q1 material buried it, the minimum vertical displacement of the Q2 surface is 7 meters.

We dated one piece of charcoal from the Q2 trench at the lower contact of Unit 13 above the filled fissure, but we do not consider the resulting radiocarbon age of 870 14C yr B.P. as representative of Unit 13. There is significant deposition above the sample site, and the charcoal-bearing unit correlates laterally with units on which a soil has developed, suggesting more than 1 thousand years of elapsed time. More likely, the charcoal sample was emplaced by bioturbation. Without other datable material, we used soil development to estimate the age of the Q1 surface and to constrain the timing of the last ground-rupturing earthquake. We estimate that the faulted Q1 surface has an age of 8-15 thousand years and that this age of this soil approximates or slightly postdates the timing of the MRE given that Unit 5 in trench Q1 is unfaulted.

### **Paleoearthquake Scenarios**

Cottonwood Canyon is near the southern end of the Anderson Junction segment of the Hurricane fault, a few kilometers north of the State Line geometric bend. Scarps with a height of about one meter or less in young fan deposits are present along the fault for 7 kilometers in either direction from Cottonwood Canyon, and likely formed in the same earthquake that displaced the Q1 surface at Cottonwood Canyon. As of yet, we have documented no clear evidence of similarly young scarps farther north along the Anderson Junction segment or immediately to the south on the Shivwitz segment. If the Anderson Junction geometric segment is also a seismologic rupture segment, then the MRE at Cottonwood Canyon may have been near the end of a segment rupture, increasing in slip to the north. Or, it could have been part of a rupture that 'spilled' around the boundary from an earthquake rupturing the Shivwitz segment. A third alternative is that the MRE may have been a small rupture limited to about 15 kilometers of the segment near the boundary zone. Perhaps the Anderson Junction geometric segment is not a seismological segment. In that case, the most recent rupture as recorded at Cottonwood Canyon need not have been constrained by the State Line segment boundary, and may have extended in both directions from the canyon mouth for some distance. It is likely that more small scarps existed beyond the 14 kilometers where we have observed them, but they have not been preserved. Using empirical relations from historical ruptures (Wells and Coppersmith, 1994), and assuming that the 60-centimeter-displacement was an average for the rupture, the earthquake may have been a M 6.3-7.0, and may have ruptured about 30 kilometers in length (Stenner and others, 1999).

From this stop we will continue driving north on the main road.

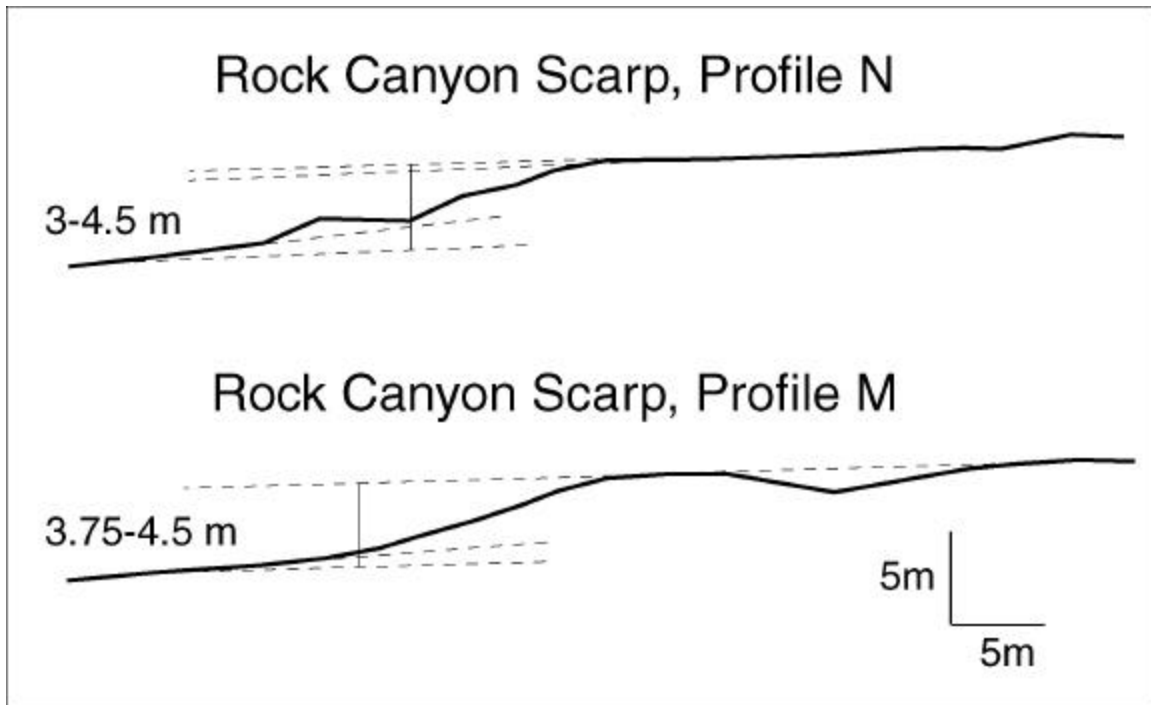
- 2.7 134.4 **Bear right**, cross Fort Pierce Wash. This is a major stream system that heads in Utah north of Colorado City and drains the western Vermillion Cliffs and much of the Uinkaret Plateau.
- 0.8 135.2 **Turn hard right** onto a small dirt track.
- 0.2 135.4 Take the left track. This track is rather rough, and 4-wheel drive is strongly recommended. Proceed south across two small hills.

0.6 136.0 Park on top of the third hill for a nice view of Rock Canyon.

**STOP 1-5. Rock Canyon Site Overlook** (Rock Canyon 7.5' quadrangle, T41N, R10W, section 1)

At this stop we can look to the east where Rock Canyon has incised through the Hurricane Cliffs, about 4 kilometers along the fault north of Cottonwood Canyon. The drainage that flows through Rock Canyon, known as Short Creek above the Hurricane Cliffs and Fort Pierce Wash through this area, is much larger than Cottonwood Wash. This drainage has had sufficient stream power to erode a large canyon through the Hurricane Cliffs and downcut extensively in the hanging wall as well (note the bouldery bedload deposited by the wash). We are currently standing on an eroded remnant of a Pleistocene terrace of Ft. Pierce Wash, and a higher terrace remnant is apparent immediately to the east of our position. Extensive exposures of the Triassic Petrified Forest Member of the Chinle Formation in this area clearly indicate that the thickness of Quaternary alluvium on the hanging wall is not great.

An alluvial fan on the north edge of the mouth of Rock Canyon is faulted, resulting in an approximately 30-meter-long fault scarp. Two profiles across this scarp reveal that the surface has probably been displaced at least 3-4.5 meters (figure 22). Based on surface character, we think it is possible that the hanging-wall side of the alluvial fan is preserved, and the 3-4.5 meters



**Figure 22. Topographic scarp profiles showing displacement of a tributary alluvial fan on the north side of Rock Canyon. Other evidence from this area indicates that displacement in the MRE may have been less than about 1 meter, this scarp likely formed in multiple faulting events.**

may be the true vertical displacement. This displacement is likely the result of more than one earthquake, based on the smaller fault scarps we observed at Cottonwood Canyon and elsewhere along this part of the fault. We estimate the faulted fan is likely a latest Pleistocene surface, based on comparing the surface undulations, degree of dissection, and the relative elevation above the active stream channel to those investigated more thoroughly at Cottonwood Canyon.

We hope to trench this scarp in the spring of 2002 to address several questions about the recent faulting history along the southern part of the Anderson Junction segment. (1) Was the MRE at Rock Canyon part of the same rupture we found evidence for at Cottonwood Canyon? (2) If the timing was the same, can we refine the timing of that MRE? (3) How does the amount of slip during the MRE at Rock Canyon compare to the 60 centimeters observed at Cottonwood Canyon? (5) What does that displacement imply about the last event along the southern Anderson Junction section? For example, if Rock Canyon's MRE is the same event but with a larger slip than at Cottonwood Canyon, it could mean that the slip generally decreased toward the State Line bend and perhaps the event did not initiate within that geometric segment boundary or along the Shivwitz section to the south.

Exposures of the faulting within the Rock Canyon fan may also provide information about earthquakes previous to the MRE. If we can recognize the signature of previous events, we may be able to tell if the size of the MRE was typical for the fault at that location. If we can estimate the timing of the previous event(s), we can improve our understanding of the recurrence interval for this section of the fault.

Head back to the main road after this stop.

- 0.6 136.6 **Turn right** at T onto small track.
- 0.2 136.8 Merge right onto graded gravel road.
- 2.2 139.0 Two tracks turn off to the right, do not turn, continue straight on main road.
- 0.2 139.2 This is an area of multiple fault strands where the Hurricane Cliffs are less precipitous. The Mormon pioneers, who carved the Honeymoon Trail up and over the escarpment here, exploited this fact.
- 0.2 139.4 Arizona/Utah state line.
- 4.9 144.3 Pull off to the side of the road

**STOP 1-6. Lava Cascade.** (The Divide 7.5' quadrangle, T43S, R13 W, section 3)

To the east is a lava cascade where dark-colored lava of The Divide flow (Higgins, 2000) flowed down the upper part of the Hurricane Cliffs. The source of the basalt flow is a volcanic center on the plateau east of the Hurricane Cliffs (Sanchez, 1995). The rock is fine grained, black in color, contains small olivine phenocrysts, and is classified as a basanite with less than 46 percent silica (Sanchez, 1995). The flow still has a relatively fresh surface morphology. Higgins (2000) obtained a  $^{40}\text{Ar}/^{39}\text{Ar}$  age of  $0.41 \pm 0.08$  Ma from near the top of the cascade.

The Hurricane fault was active and the Hurricane Cliffs existed as essentially a fault escarpment, at least in part, prior to the eruption of the lava in the cascade because the flow conforms to the topography showing that it flowed down the cliff. The flow ends part way down the cliff. Primary structures within the flow suggest the present end of the flow is near the original terminus of the flow. The cliffs are about 300 meters high here and the flow ends about 150 meters down the cliff, which implies that at least one half of the total scarp height formed prior to eruption of the flow. However, more of the scarp may have existed and the flow was just not voluminous or liquid enough to flow to the bottom.

Higgins (2000) mapped the lava flows exposed in the hill west of the road as the Grass Valley flow, which is a very dark gray, fine- to medium-grained basalt. Based on surface morphology and position, this flow is considerably older than The Divide flow, and was erupted from a volcanic center located to the west (Sanchez, 1995; Higgins, 2000).

**Remnants Flow in Grass Valley**

Near the north end of Grass Valley approximately 4 kilometers north of the lava cascade, Higgins (2000) mapped the Remnants basalt flow on both the up- and downthrown sides of the

Hurricane fault. Geochemical data (Higgins, 2000; Lund and others, 2001) confirm that the flows are correlative across the fault. Higgins (2000) reported two whole-rock  $^{40}\text{Ar}/^{39}\text{Ar}$  ages for the Remnants basalt, one from the footwall ( $0.94 \pm 0.04$  Ma) and one from the hanging wall ( $1.06 \pm 0.03$  Ma). Lund and others (2001) obtained a third  $^{40}\text{Ar}/^{39}\text{Ar}$  age of  $1.47 \pm 0.34$  Ma from a Remnants flow outcrop in the hanging wall. The two-sigma errors reported for the three ages do not overlap, indicating that they are discrete and non-correlative. Nevertheless, the two ages obtained by Higgins (2000) are relatively close in time and could represent a reasonable suite of ages from a single eruptive episode. Conversely, the Lund and others (2001) age from the Remnants flow on the hanging wall is approximately 500 thousand years older than the Higgins (2000) ages. The Lund and others (2001) age estimate came from the same basalt-capped hill as the Higgins (2000)  $1.06 \pm 0.03$  Ma age. The difference between the two age estimates remains unexplained.

The paleomagnetic data from the Remnants basalt flow are highly erratic, probably due to local remagnetization of the rock by lightning strikes (Lund and others, 2001, appendix C). As a result, those data were of no use in evaluating back-tilting of the hanging wall. Visual examination showed that the hanging-wall basalt is tilted toward the Hurricane fault, but the nearest Remnant flow outcrops are approximately 750 meters west of the fault (Higgins, 2000). Given those constraints, Lund and others (2001) used the elevation difference between the top of the Remnants flow on the footwall and the highest elevation on the least tilted basalt in the hanging wall as a best approximation of net slip. The elevation difference is 440 meters.

Because of the discrepancy in the radiometric ages, Lund and others (2001) calculated two slip rates for the Grass Valley site, the first using an average of the two Higgins (2000) ages and the second using their own older age estimate. The slip rates at Grass Valley are:

$$440,000 \text{ mm}/(0.94 + 1.06/2) \text{ Ma} = 0.44 \text{ mm/yr}$$

and

$$440,000\text{mm}/1.47 \text{ Ma} = 0.30 \text{ mm/yr}$$

Because of the relatively close correspondence in time of the Higgins ages, Lund and others (2001) consider the 0.44 mm/yr slip rate to be the preferred long-term slip rate at Grass Valley.

Continue north on the main road after this stop.

- 1.5     145.8    Cross cattle guard and continue on pavement. Sky Ranch subdivision and airport on the left (W). This road generally parallels the Hurricane fault for a few miles.
- 3.8     149.6    Volcano Mountain (Stop 2-1) at 10:00.
- 0.5     159.1    **Turn left** (~NW) onto 700 West at T intersection and enter Hurricane, Utah. Note cluster of homes that are on or near the Hurricane fault and at the mouth of a canyon, which is subject to flash flooding. Optional stop, if time and light are available.
- 2.1     152.2    Stop light. **Turn right** (E) onto State Route (SR) 9.
- 0.3     152.5    Pass straight through light at 300 West and very shortly **turn left** (N) into the parking lot of the Lamplighter Motel.

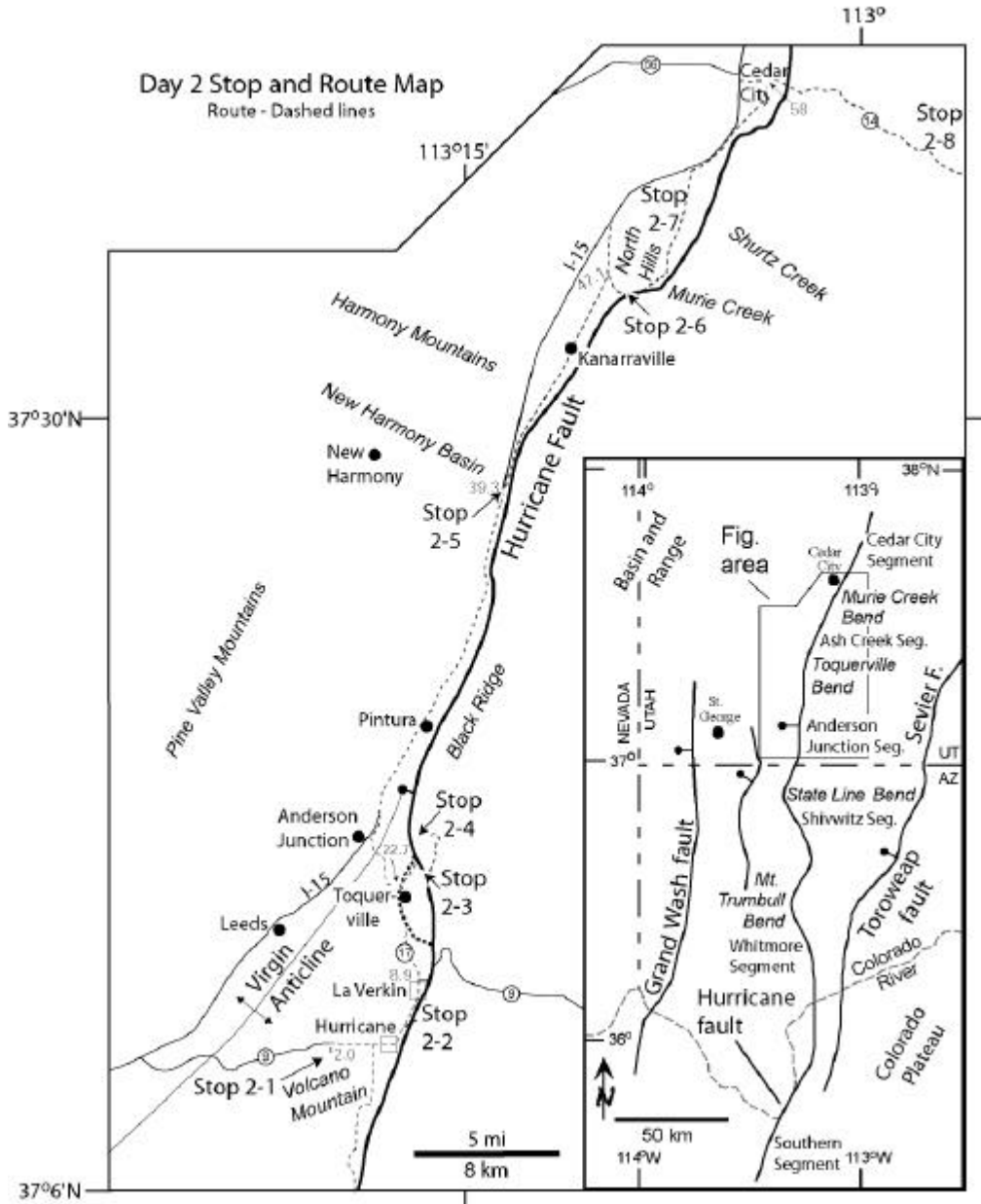
**End Day 1.**



*The Hurricane fault near Hurricane, Utah, with the Jurassic Moenkopi Formation (hanging wall) juxtaposed against the Permian Kaibab Formation (footwall).*

## SECOND DAY ROAD LOG

### The Northern Anderson Junction, Ash Creek, and Cedar City Segments Hurricane Fault Zone Utah



**Figure 23. Day 2 Route Map.** The dashed line shows the route of our trip on Day 2. Some key mileage values also are shown along the route. Words in italics are geographic locations noted in the road log. Inset shows trip map in a regional context.

## SECOND DAY ROAD LOG

### **The Northern Anderson Junction, Ash Creek, and Cedar City Segments Hurricane Fault Zone Utah**

The second day of this field trip begins in the parking lot of the Lamplighter Motel at the intersection of State Street and 300 West Street in Hurricane, Utah. We will spend today examining the northern part of the Anderson Junction segment and the Ash Creek and proposed Cedar City segments of the Hurricane fault in Utah. First we will proceed west from Hurricane to Volcano Mountain, which provides an overview of the northern part of the Anderson Junction segment. From Volcano Mountain, we will travel northward along the Anderson Junction segment, stopping to observe the fault in the walls of Timpoweap Canyon where the Virgin River cuts through the Hurricane Cliffs and also where a dated basalt flow is displaced across the fault, providing a good mid-Quaternary slip rate for the fault. Continuing north to the Toquerville geometric bend, we will examine structural evidence for the boundary between the Anderson Junction and Ash Creek segments and a dated basalt flow at the boundary that records nearly 370 meters of net slip across the fault and provides another long-term Quaternary slip rate. Farther north we will observe more displaced basalt flows, visit the proposed boundary between the Ash Creek and Cedar City segments near Coyote Gulch and Murie Creek, and make an overview stop at the Shurtz Creek scarp and trench site. Finally, we will cross the Hurricane fault at Cedar City and drive up Cedar Canyon to observe a basalt flow stranded high on the canyon wall that provides a surrogate long-term slip rate for the Cedar City segment.

The eight stops today provide information that shows that: (1) long-term slip rates on the northern Anderson Junction and Ash Creek segments are higher than late Quaternary rates, (2) the long-term slip rate for the Ash Creek segment is higher than the long-term rate for the northern Anderson Junction segment and the increase is at or near the Toquerville geometric bend, (3) a difference in timing of the MRE north and south of the Murie Creek geometric bend between Kanarraville and Cedar City argues for the presence of a previously unrecognized seismogenic segment boundary, (4) the proposed Cedar City segment has a long-term slip rate generally comparable to the Ash Creek segment and higher than the Anderson Junction segment, but shows no comparable evidence of latest Pleistocene or Holocene surface faulting.

#### **Mileage**

#### **Inc. Cum.**

0.0	0.0	Begin trip in parking lot of the Lamplighter Motel. Exit from northwest corner of lot. <b>Turn left (S)</b> onto 300 West.
0.1	0.1	Stop light. <b>Turn right (W)</b> at intersection with State Street.
0.3	0.4	Continue straight through stop light at State Street (SR-9) and 700 West. Volcano Mountain at 10:00.
0.5	0.9	Continue straight through stop light at SR-9 and 1150 West.
1.1	2.0	<b>Turn left (S)</b> into Painted Hills subdivision onto Rlington Parkway.
0.2	2.2	Continue straight at stop sign at Rlington and Ridge View Drive. Parallel rock wall to T intersection with Valley View Drive.
0.1	2.3	<b>Turn right (W)</b> onto Valley View Drive, just past end of rock wall.
0.1	2.4	<b>Turn left (S)</b> onto Ridge View Drive and proceed uphill.

- 0.1 2.5 **Turn right (S)** onto Panorama Drive, this road quickly turns to dirt.
- 0.2 2.7 Park by gate. Walk to rock promontory on spur to the northeast.

**STOP 2-1. Volcano Mountain Overview** (Hurricane 7.5' quadrangle, T42S, R13W, section 5)

Volcano Mountain is the largest of several volcanic vents in and near the town of Hurricane. Volcano Mountain still preserves its classic cinder cone shape and has moderately well developed rill weathering on its flanks (Biek, 1998) indicating a late Quaternary age. The cone is breached on its north side by a flow that rafted cinders associated with the breach downslope for a distance of at least a mile. The basaltic rocks here and visible from here are part of the western Grand Canyon basaltic field in southwestern Utah and adjacent northwestern Arizona (Hamblin, 1970a; Best and Brimhall, 1974). Although relatively small in volume when compared to other volcanic regions in the western United States, the flows of the Grand Canyon field provide important constraints on local tectonic and geomorphic development (Biek, 1998); we will examine several examples today.

Volcano Mountain provides a grand vista across a broad swath of southwestern Utah, and is an excellent location from which to orient ourselves for the morning portion of today's field trip. Looking to the southwest over our parked vehicles, in the far distance we can see the Beaver Dam Mountains, a metamorphic core complex flanked by Paleozoic sedimentary rocks. If we set the Beaver Dams at 9:00, we can begin a clockwise rotation through the vista before us. At 10:00 in the middle distance is the east limb of the Virgin anticline held up here by the resistant, east-dipping Shinarump Conglomerate Member of the Chinle Formation. Quail Creek reservoir occupies the breached core of the anticline. Beyond the anticline are the red-colored Jurassic Kayenta and Navajo Formations, which are capped by the lighter colored Cretaceous Iron Springs Formation. In the near distance along SR-9, we can see basalt flows associated with Volcano Mountain. At 11:00 are the Pine Valley Mountains, cored by the Tertiary Pine Valley laccolith, which intrudes the Clarion Formation, more about that at Stop 2-4 later today. At 12:00 we see craggy outcrops of the Navajo Sandstone in the east limb of the Virgin anticline. Black Ridge, the site of stops 2-3 and 2-4, is at 1:00. Black Ridge represents the east limb of the Kanarra anticline; the anticline's west limb has been displaced down-to-the-west and out of our view by the Hurricane fault. The Toquerville geometric bend and the proposed boundary between the Anderson Junction and Ash Creek segments of the Hurricane faults is near the south end of the ridge. In the far distance just east of Black Ridge, the Kolob Fingers (Navajo Sandstone) are visible in Zion National Park. At 2:00 in the near distance we can see the Cinder Pits and Radio Towers volcanic vents, which, along with Volcano Mountain, are the principal volcanic cones in the Hurricane volcanic field. The red cliffs in the middle distance expose nearly 470 meters of the Triassic Moenkopi Formation capped by the resistant Shinarump Conglomerate Member of the Chinle Formation, which we last saw behind us holding up the east limb of the Virgin anticline. Clearly a structure of major down-to-the-west displacement lies between our current vantage point and those cliffs. In the far distance are the white sandstone spires of Zion National Park. The structure that separates the topographically high, nearly undeformed Shinarump capping the cliff to the east from the steeply east-dipping Shinarump outcrops behind and below us in the east limb of the Virgin anticline is the Hurricane fault, which lies at the base of the Hurricane Cliffs in the middle distance between about 12:00 and 3:00. The portion of the Hurricane Cliffs within our view represents the central part of the Anderson Junction segment of the Hurricane fault. The basalt flow stranded at about the midpoint of the cliffs originated from Ivans Knoll just to the south of us, and will be the topic of discussion at our next stop at the mouth of Timpoweap Canyon (2:00 low) where the Virgin River cuts through the Hurricane Cliffs.

Return to SR-9 via the same route.

- 0.6 3.3 **Turn right (E)** at intersection with SR-9, toward the town of Hurricane.
- 1.1 4.4 Continue straight through the stop light at 1150 West.



- 0.5    4.9    Continue straight through the stop light at 700 West.
- 0.4    5.3    Continue straight through the stop light at 300 West, near the Lamplighter Motel.
- 0.3    5.6    Continue straight through the stop light at Main Street. Follow SR-9 (Main Street), staying left ahead.
- 0.3    5.9    Main strand of the Hurricane fault lies to the left (E) near the base of the basalt cliffs.
- 0.8    6.7    **Turn right (E)** just before the bridge over the Virgin River onto Enchanted Way. Follow tree-lined road to the bottom of the hill.
- 0.4    7.1    Park near the small bridge across the Virgin River.

**STOP 2-2. Exposures of the Hurricane fault in the walls of Timpoweap Canyon**  
(Hurricane 7.5' quadrangle, T41S, R13W, section 25)

At this stop, the Anderson Junction segment of the Hurricane fault consists of two easily visible fault strands and a third strand down the canyon to the west. At least two strands offset the Quaternary basalt at the top of the section, much of which contains well-developed columnar joints. On the south side of the canyon, the gray rocks on the left (E) are part of the Permian Kaibab and Toroweap Formations. These rocks lie in the footwall of the easternmost strand of the Hurricane fault. The eastern strand is in the steep side canyon. In the hanging wall of that strand (to the right), the brown, red, and green-gray layers are Triassic Moenkopi Formation that dips steeply (~60-80°W). This block of Moenkopi Formation is bounded on the right (W) by another fault strand that is exposed up the road and juxtaposes Chinle and Moenkopi Formations. These beds are overlain by Cenozoic basalt. The Moenkopi beds were steeply tilted prior to emplacement of the overlying basalt as evidenced by the strong angular unconformity between them and the overlying basalt. Thus, this site provides evidence that the Hurricane fault was active both before and after emplacement of the basalt.

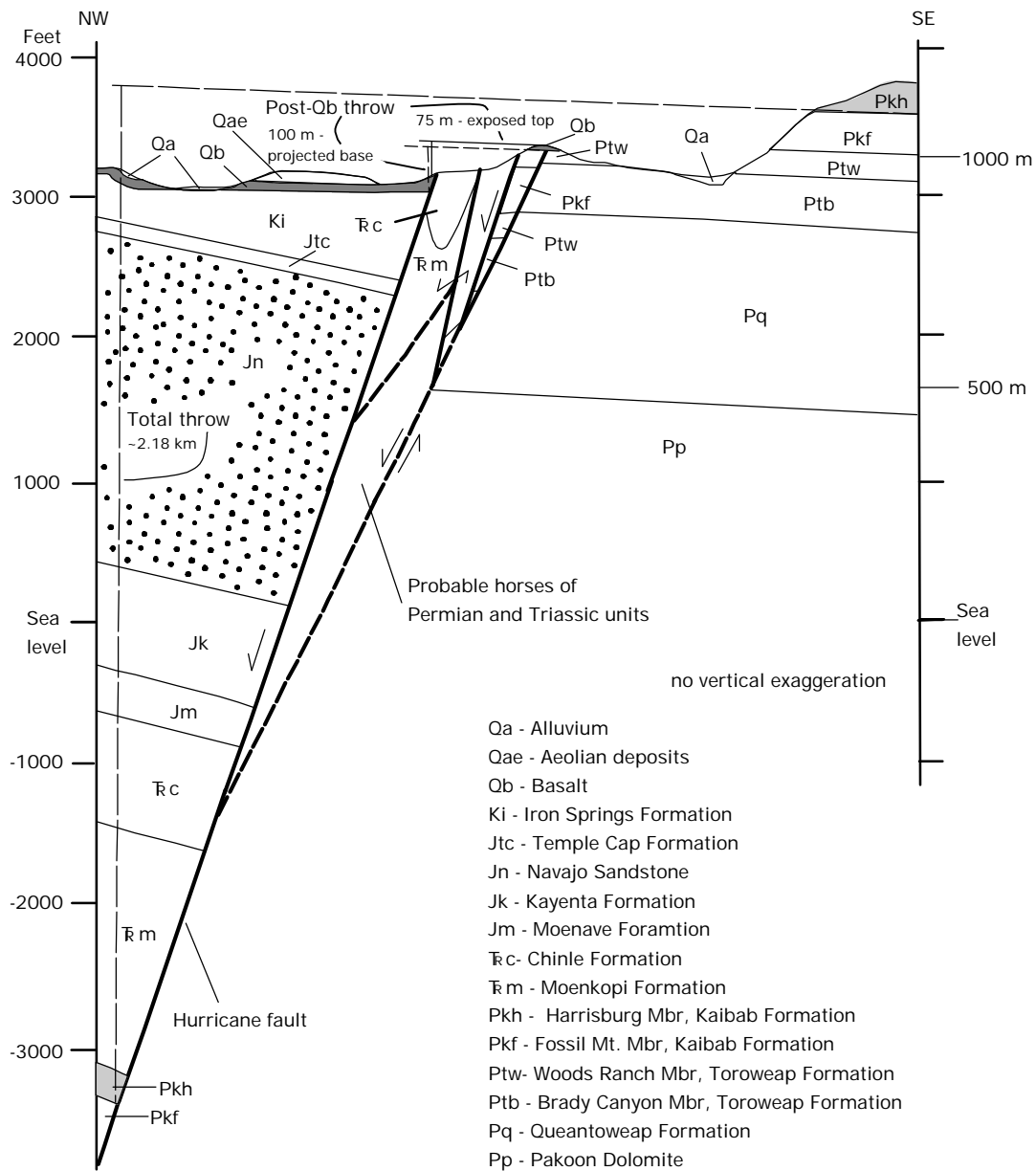
The easternmost fault strand splays under the river and appears as two fault strands on the north side of the canyon. These splays lie just to the east of the north end of the bridge. The eastern splay, which is visible around the corner to the east from the end of the bridge, juxtaposes Permian Kaibab and Toroweap Formations. The western splay is apparent near the end of the bridge where it juxtaposes siliciclastic layers of the Moenkopi Formation (some of which is green-gray) in the hanging wall against the gray limestone of Permian Kaibab Formation in the footwall. The obvious gypsum is in the Moenkopi Formation.

To view the other two fault strands on the north side of the canyon, re-cross the bridge and look north. The middle strand juxtaposes the western part of the Moenkopi Formation against the purple-brown Triassic Chinle Formation on the west. The westernmost strand is evident where it places Quaternary basalt next to the western part of the Chinle exposure. As we continue to the north along the Anderson Junction segment, the number of strands increases. The increase in the number of strands stops at the Toquerville geometric bend.

Up stream of the bridge, hot springs feed into Virgin River from the river bottom and from the rocks along the edge of the stream. In 1981 the spring discharge was estimated to be 4,700 gpm (Cordova, 1981). The springs discharge directly from the Kaibab Formation. The water from these springs contains high concentrations of dissolved solids (2,270 ppm Na, 3,250 ppm Cl, 775 ppm Ca, 1,891 ppm SO<sub>4</sub>, 907 ppm HCO<sub>3</sub>; Yelken, 1996). Consequently, the water quality in the Virgin River degrades downstream from Pah Tempe hot springs. The spring area is presently privately owned and used a mineral-spa resort.

**Mid-Quaternary Slip Rate from Displaced Basalt**

The basalt flow displaced here occupies an intermediate position part way up the Hurricane Cliffs. The flow originated from Ivans Knoll to the southwest (Sanchez, 1995; Biek, 1998) and ponded along the base of the Hurricane Cliffs. Subsequent movement of the Hurricane fault displaced the basalt 73 meters down-to-the-west (Biek, 1998). Sanchez (1995) obtained a



**Figure 24. This cross section represents the geology just north of the bridge across the Virgin River at Stop 2-2. Total throw is ~ 7,770 feet (2,370 m). Post Quaternary basalt throw is ~240 feet (73 m).**

$^{40}\text{Ar}/^{39}\text{Ar}$  whole-rock age of  $353 \pm 45$  ka for the basalt. Mapping and geochemical sampling by Biek (1998) shows that the basalts on either side of the fault are correlative. Paleomagnetic data from the basalt on both sides of the fault indicate that the basalt is normally magnetized and that the basalt in the hanging wall is tilted less than 10 degrees toward the fault, if it is tilted at all (Lund and others, 2001, appendix C). Visual examination confirms a lack of back tilting except in a very narrow zone immediately adjacent to the fault zone. The 73-meter difference in elevation (net slip) between the basalts in the footwall and hanging wall was measured outside of the deformation zone.

Using Sanchez's (1995) age estimate and a net slip of 73 meters (Biek, 1998), the slip rate at Pah Tempe Hot Springs for the past 353 thousand years is:

$$73,000 \text{ mm}/353,000 \text{ yrs} = 0.21 \text{ mm/yr}$$

The Pah Tempe slip rate is approximately one-half the preferred slip rate at Grass Valley (0.44 mm/yr), which is also on the Anderson Junction segment. The difference between the two sites may represent a difference in long-term rates on two independent fault segments, with an as yet unrecognized segment boundary between them. However, based on new geologic mapping by Biek (1998), the presence of an unrecognized seismogenic boundary along this part of the fault is considered doubtful. Because the age of the displaced basalt flow at Pah Tempe Hot Springs is only about one-third the age of the basalt at Grass Valley, the lower slip rate at Pah Tempe more likely reflects a change in slip rate through time on a single seismogenic segment.

Return to main road at top of hill.

- |     |      |                                                                                                                                                                                                                                                                                          |
|-----|------|------------------------------------------------------------------------------------------------------------------------------------------------------------------------------------------------------------------------------------------------------------------------------------------|
| 0.2 | 7.3  | <b>Turn right (N)</b> onto SR-9 and proceed north crossing the Virgin River bridge.                                                                                                                                                                                                      |
| 0.1 | 7.4  | Enter the town of LaVerkin. The road parallels the Hurricane Cliffs and the Hurricane fault.                                                                                                                                                                                             |
| 0.3 | 7.7  | A large landslide covered with basalt talus is visible at 9:00 along the canyon wall above the Virgin River. Quaternary basalt flows here are being undercut by slope failures in the underlying Cretaceous Iron Springs Formation, which locally contains abundant bentonitic mudstone. |
| 0.5 | 8.2  | School crossing, <b>drivers watch for flashing lights</b> . In LaVerkin SR-9 is also called State Street.                                                                                                                                                                                |
| 0.7 | 8.9  | Stop light at intersection with SR-17. <b>Proceed straight ahead (N), which is along SR-17</b> . The Toquerville geometric bend is visible at 12:00.                                                                                                                                     |
| 0.3 | 9.2  | Road cut through basin-fill sedimentary units.                                                                                                                                                                                                                                           |
| 0.4 | 9.6  | Cross LaVerkin Creek. To the right (E), the Hurricane fault comprises several strands. In this area, a Quaternary conglomerate is offset by the Hurricane fault (Stewart and others, 1997).                                                                                              |
| 0.2 | 9.8  | Enter Toquerville. Quaternary basalt overlying the Shinarump Conglomerate crops out from 9:00 to 12:00.                                                                                                                                                                                  |
| 0.5 | 10.3 | Hurricane Mesa is at 9:00. The mesa consists of the red, brown and white Triassic Moenkopi Formation with the cliff-forming Shinarump Member of the Chinle Formation at the top. The water tower at the skyline is part of a former U.S. Air Force rocket sled research facility.        |
| 1.3 | 11.6 | The northern end of the Virgin anticline, exposed in Jurassic Navajo Sandstone, lies at 10:00. Current thinking is that the Virgin anticline dies out northward as two different anticlines, the Pintura on the west and the Kanarra on the east, pick up.                               |
| 0.2 | 11.8 | Enter Toquerville, westernmost strand of the Hurricane fault parallels the basalt-covered ridge on the right.                                                                                                                                                                            |
| 0.6 | 12.4 | <b>Turn right (~E)</b> onto Spring Drive, just before bridge crossing Ash Creek, the western strand of the fault makes a similar bend here, still paralleling the basalt-covered ridge.                                                                                                  |

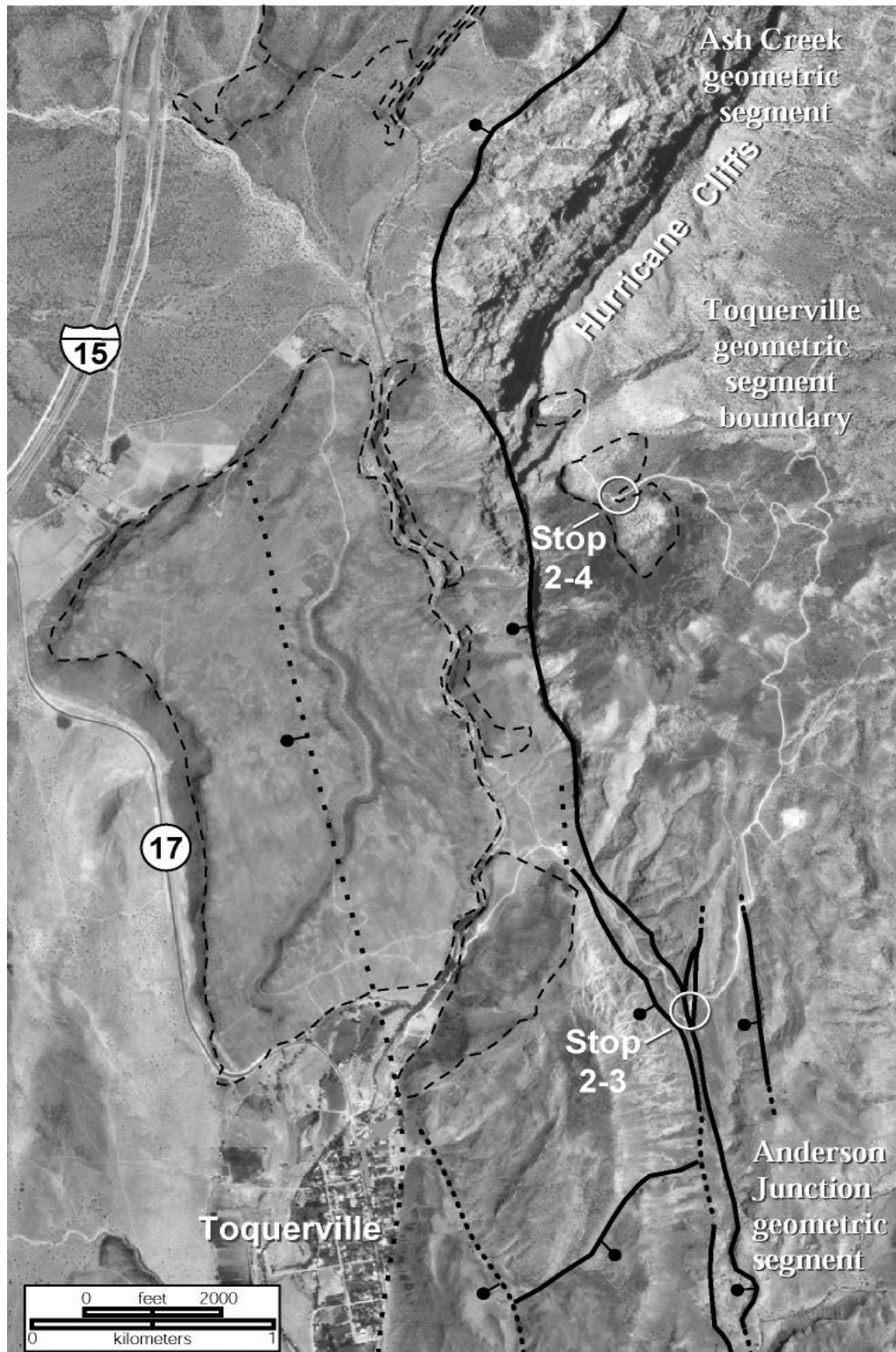
- 0.5    12.9    Toquerville spring, to the left (~N), surfaces along the Hurricane fault and supplies culinary water to the town of Toquerville.
  
- 0.2    13.1    From the water tank, look toward 10:00, the Hurricane fault is easily visible where dark-colored basalt is juxtaposed against the gray Permian Kaibab Formation. We are in the Toquerville geometric bend at the boundary between the Anderson Junction and Ash Creek seismogenic segments. At the top of the footwall cliff, Quaternary basalt crops out where it fills former embayments in the Hurricane Cliffs. This basalt at the cliff top is geochemically equivalent to the basalt at 10:00.
  
- 0.3    13.4    Stay on main road as it curves to the right (~S).
  
- 0.2    13.6    Road parallels and lies between two strands of the Hurricane fault in the eastern part of the Toquerville bend. The eastern strand is exposed in several places a few meters to the left (~E). The hill of Triassic Moenkopi Formation to the right lies in the hanging wall of the western strand.
  
- 0.5    14.1    Pull out to left (~E) and park.

**STOP 2-3. Toquerville Geometric Bend** (Pintura, 7.5' quadrangle, T40S, R13W, section 36)

This stop is in the Toquerville geometric bend, which separates the Anderson Junction and Ash Creek geometric segments of the Hurricane fault (figure 25). To the north, the main trace of the Hurricane fault lies along the base of the Hurricane cliffs, concealed by Quaternary deposits; a secondary strand lies to the west. Just to the north of the visible part of the fault, a scarp cuts Quaternary alluvium. Along this dirt road to the north are slickenlines exposed on the Permian Kaibab Formation. South of the gravel quarry the main fault trace splits into at least three west-side-down normal faults displacing sandstone and mudstone of the Triassic Moenkopi and Chinle Formations. These rocks are also deformed by a complex array of normal faults subsidiary to the Hurricane fault. This complex zone lies within the salient in the fault zone.

The footwall of the Hurricane fault zone consists here of the Fossil Mountain and Harrisburg Members of the Permian Kaibab Limestone and the Timpoweap Member of the Moenkopi Formation. These units are folded in the Kanarra anticline, a Late Cretaceous-Paleocene (?) fold of the Cordilleran fold and thrust belt. Near the fault zone, these strata dip ~10-30 degrees west. About 0.5 kilometers and farther to the east of here, these units dip 30 to 80 degrees east in the eastern limb of the anticline. The Fossil Mountain Member forms a prominent cliff of cherty limestone that is repeated by a west-directed thrust fault in the eastern limb of the Kanarra anticline.

We suggest that the Toquerville bend is a zone where two faults linked for a number of reasons. The fault strike across the Toquerville geometric bend changes from approximately N15°W on the south side of the salient to N25°E on the north side. The number of fault strands changes from several south of the bend to one or few north of the bend. The basalt in the hanging wall contains a gentle anticline that trends nearly perpendicular to the strike of the fault, a classic geometry for extensional folds. Hanging wall anticlines with this geometry are common at or near fault segment boundaries (Schlische, 1993). Note that this gentle anticline is superimposed on a rollover anticline that also folds the basalt. The displacement-distance profile along the relatively symmetric Toquerville bend shows relatively smooth decreases in throw to a minimum just adjacent to the apex of the bend. This pattern resembles the expected pattern for linkage of underlapping faults (figure 5). The displacement-distance profile and strike change of 35-40 degrees around the bend are interpreted to result from originally underlapping faults that curved to link with each other. In addition, the map geometry of the fault at the bend is relatively symmetric, which is consistent with that expected at a site of symmetrical linkage as can occur with underlapping faults. The decrease in stratigraphic separation at this bend and then an



**Figure 25 . Hurricane fault in the vicinity of the Toquerville bend between the Anderson Junction and Ask Creek geometric segments. Heavy-weight lines are faults; dotted where concealed. Light-weight lines outline Quaternary basalt fields. Modified from Reber and others (2001).**



increase in displacement toward the south mimics relief profiles for the same section of the fault (Taylor and others, 2001), and also points to the probable linkage of two originally isolated faults (figure 5). The Ash Creek and Anderson Junction geometric segments are inferred to have propagated laterally and linked as underlapping faults forming the Toquerville geometric bend (figure 5; Taylor and others, 2001).

At the next stop we will discuss the problems posed by the spatial coincidence between the Hurricane fault and the Kanarra anticline for reconstructing both features.

Continue uphill along the dirt road.

- 0.8 14.9 Well drill pad at ~3:00 (~S). At 12:00, view of the Moenkopi Formation capped by the Shinarump Conglomerate. These nearly flat-lying rocks are in the footwall of the Hurricane fault. The red cliffs in the distance are composed of Jurassic Navajo Sandstone in Zion National Park.
- 0.8 15.7 Outcrops to the right (E) are the Moenkopi Formation, which is capped by the resistant, tan-colored Shinarump Conglomerate Member of the Triassic Chinle Formation.
- 0.3 16.0 Road to right (NE), continue on main road (left fork). Down the hill in the light-colored Virgin Limestone Member of the Moenkopi Formation, is a small thrust fault with 15 meters of stratigraphic separation. This is the southern exposure of the Taylor Creek thrust fault (Lovejoy, 1964). The average strike and dip is N15°E, 30°E. Farther north in Zion National Park, this fault has more than 600 meters of vertical and 760 meters of horizontal displacement (Kurie, 1966).
- 0.1 16.1 To the right (~N) a high-angle fault is visible. Kaibab Limestone is in the footwall and Moenkopi Formation is in the hanging wall.
- 0.2 16.3 The red mudstone unit that we are driving across is the upper red member of the Moenkopi Formation.
- 0.4 16.7 Look down to the right (southeast), and see the Taylor Creek thrust fault again.
- 1.0 17.7 Radio towers at the south end of Black Ridge

**STOP 2-4. South Black Ridge Radio Towers** (Pintura 7.5' quadrangle, T40S, R13W, section 23)

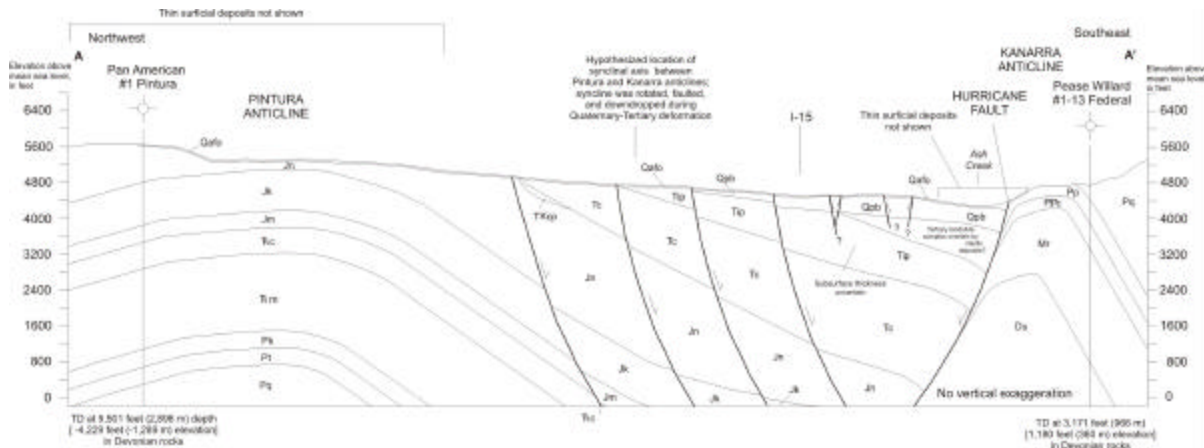
The radio towers are on the southern end of Black Ridge, in the hanging wall of the Hurricane fault. The Ash Creek valley lies below us, and the Pine Valley Mountains, reaching elevations over 10,000 feet, form the western skyline. Pre-Quaternary features visible from this site formed along the southwestern margin of the Late Cretaceous-Paleocene Cordilleran fold and thrust belt, and during Tertiary normal faulting prior to initiation of the Hurricane fault (and/or on the Hurricane fault prior to eruption of the Quaternary basalts). Here we briefly describe these structures and their geometric relation to, and possible influences on, the structural development of the Hurricane fault.

**Pre-Quaternary Structure and Stratigraphy**

Southwest of the radio towers, hogbacks of the Shinarump Member of the Triassic Chinle Formation define the form of the Late Cretaceous-Paleocene Virgin anticline. Much of the Anderson Junction geometric segment, exposed to the south, parallels the trend of the Virgin anticline. However, the fault generally lies to the east of the axial surface. The parallelism between the fault strike and anticlinal trend along this segment suggests the possibility that the Hurricane fault formed along or reactivated a fracture that formed during the formation of the Virgin anticline. Northeast of these hogbacks the Virgin anticline plunges out and shortening

transfers northeastward to the Kanarra anticline and possibly northwestward to the Pintura anticline. The Hurricane Cliffs expose the eastern limb and, locally, the hinge zone of the north-trending Kanarra anticline from here to Cedar City, 45 kilometers to the north.

The Pintura anticline occupies the hanging wall of the Hurricane fault; the southern end of its 4-kilometer-long, north-striking hinge zone is just north of the Toquerville geometric segment boundary. Along the hinge zone of the Pintura anticline, the Maastrichtian-Paleocene Canaan Peak Formation and the Oligocene-Eocene Claron Formation depositionally overlie the Jurassic Navajo Sandstone (Goldstrand, 1994; Hurlow and Biek, 2000), indicating erosion of about 1,200 meters of stratigraphic section along a Late Cretaceous-early Tertiary structural culmination. The geometry of the Pintura anticline is, however, difficult to ascertain because it is mainly exposed in the trough-cross-bedded Navajo Sandstone and is overprinted by younger normal faults. Based on detailed mapping, Hurlow and Biek (2000) interpreted the Pintura anticline as a broad, poorly defined, composite fold that originally formed during Late Cretaceous-Paleocene time, and was modified by Tertiary normal faulting and folding in the axis of a large, reverse-drag fold related to displacement on the Hurricane fault and/or earlier west-side-down normal faults (figure 26).

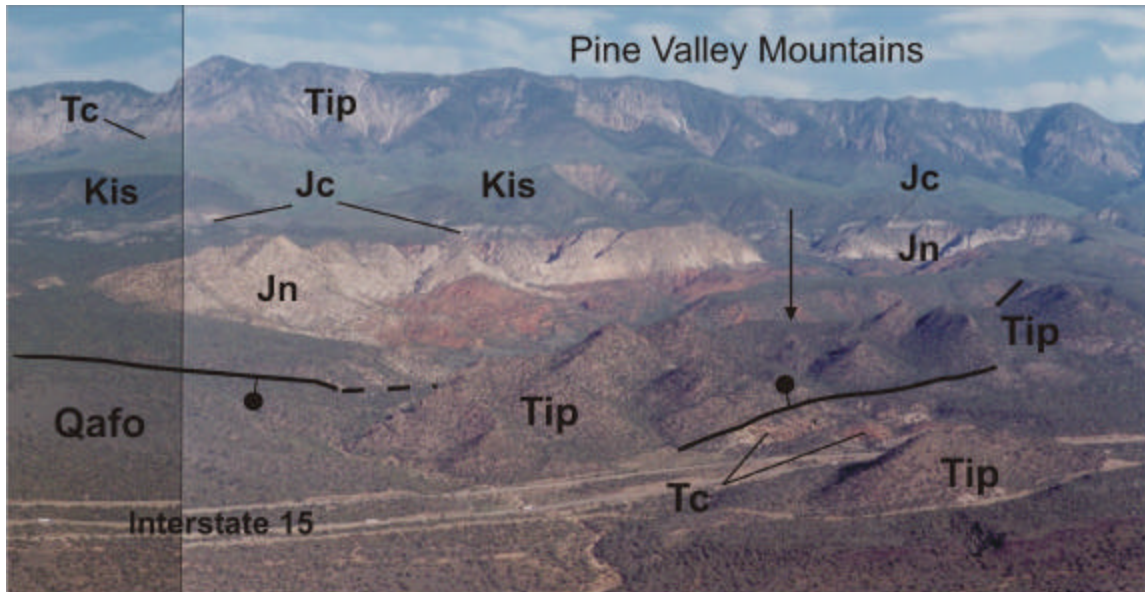


**Figure 26. Cross section across the Ash Creek segment of the Hurricane fault modified from Hurlow and Biek (2000). Units from youngest to oldest: Qafo – early quaternary alluvial-fan deposits; Qpb – basalt flows of the Pintura field (about 830 ka); Tip – quartz monzonite porphyry of the Pine Valley Mountains (21 Ma); Tc – Claron Formation (Oligocene-Eocene); TKcp – Canaan Peak Formation (Late Cretaceous-Paleocene); Jn – Navajo Sandstone (Jurassic); Jk – Kayenta Formation (Jurassic); Jm – Moenave Formation (Jurassic); Trc – Chinle Formation (Triassic); TRm – Moenkopi Formation (Triassic); Pk – Kaibab Formation (Permian); Pi – Toroweap Formation (Permian); Pq – Queantoweap Formation (Permian); Pp – Pakoon Formation (Permian); PPc – Callville Limestone (Permian-Pennsylvanian); Mr – Redwall Limestone (Mississippian); Du – Devonian rocks undivided.**

The western limb and most of the hinge zone of the Kanarra anticline, the eastern limb of the Pintura anticline, and the intervening syncline are concealed below younger deposits in the hanging wall of the Hurricane fault, and few subsurface data are available for this area. Despite this lack of information, some preliminary interpretations on the possible role of structural inheritance on the development of the Hurricane fault can be made. The spatial coincidence between the Hurricane fault and the Kanarra anticline implies localization of the Hurricane fault by a pre-existing structure, perhaps a blind thrust ramp (Grant and others, 1995). Interpretation of seismic-reflection data from the Cedar City area (Stop 2-6) permits a similar conclusion. The Toquerville geometric segment boundary occupies the transfer zone between the Virgin and

Kanarra anticlines. This fold-transfer zone may have localized the Toquerville geometric segment boundary, although the subsurface geometry and localization mechanism are uncertain.

Quartz monzonite porphyry of the 21-million-year-old Pine Valley laccolith forms the precipitous cliffs of the southwestern front of the Pine Valley Mountains (figure 27). Several masses of the Pine Valley laccolith also crop out near Interstate 15 northwest of this stop. These outcrops are enigmatic because: (1) their basal contacts are about 915 meters lower than in the main laccolith body and are structurally discordant with bedding in underlying units, and (2) one of



**Figure 27.** View to the northwest from southern Black Ridge near stop 2-4. The body of quartz monzonite porphyry of Pine Valley (Tip) west of Interstate 15 is about 915 meters below the main mass of the laccolith (visible in the background) and may be a satellitic intrusion or an erosional remnant of a once continuous sheet. The structurally low position of this body of quartz monzonite porphyry is due to the combined effects of: (1) normal faults bounding either side of the body (shown by solid lines where visible; the trace of the western fault is concealed behind the main body – the arrow shows its position), (2) reverse drag in the hanging wall of the Hurricane fault and/or other west-side-down normal faults. The base of the quartz monzonite porphyry here is discordant with bedding in the underlying Clarion Formation, indicating faulting during or prior to intrusion. Qafo = early Quaternary alluvial-fan deposits; Tip = quartz monzonite porphyry of Pine Valley; Tc = Clarion Formation (Oligocene-Eocene); Kis = Iron Springs Formation (Cretaceous); Jc = Carmel Formation (Jurassic); Jn = Navajo Sandstone (Jurassic). Photograph by Robert Biek, UGS.

these masses locally overlies the Cretaceous Iron Springs Formation. In contrast, the main mass of the Pine Valley laccolith consistently intrudes the middle part of the Claron Formation parallel to bedding, which dips gently toward the center of the laccolith (Cook, 1957, 1960; Hacker, 1998). These anomalous masses of quartz monzonite porphyry are either satellitic intrusions of the Pine Valley laccolith or erosional remnants of the once-continuous laccolith. The angular discordance between the intrusion base and bedding in the underlying Claron Formation and the local intrusion of the Iron Springs Formation reflect pre-intrusion faulting and related tilting. The masses owe their low structural position to the combined effects of pre-Quaternary normal faults and large-scale reverse drag in the hanging wall of the Hurricane fault. The largest body occupies a graben between two pre-Quaternary normal faults (figure 27), and covers a pre-intrusion, west-side-down normal fault that tilted and repeated section of the Claron Formation.



The western fault has stratigraphic separation of about 150 meters. A splay of this fault displaces early Quaternary alluvial-fan deposits by approximately 30 to 45 meters, indicating continued motion or reactivation during early Quaternary time (see discussion of Ash Creek graben above).

### **Structural Relations**

To the north along much of the Ash Creek geometric segment, the strike of the Hurricane fault is ~N21°E. To the south along much of the Anderson Junction geometric segment, the fault strikes ~N12°W. Stratigraphic separation decreases markedly across this segment boundary (figure 18), which is indicative of a boundary that has been a persistent barrier to slip (King, 1986).

Near the Toquerville bend (figure 25), it is clear that the Hurricane fault had significant offset prior to emplacement of the Quaternary basalt flows. In the footwall, the basalt occupies a paleochannel (visible here) in the (gray) Permian rocks. In the hanging wall (near the last stop), a section of basalt that is geochemically identical to that visible on the footwall overlies Triassic – Jurassic strata (Schramm, 1994; Stewart and Taylor, 1996). This stratigraphic difference indicates that the hanging-wall block was down-dropped relative to the footwall and that significant erosion of the footwall took place prior to basalt emplacement. The stratigraphic separation of the basalt across the fault is presently ~ 450 meters. The stratigraphic separation of the Navajo Sandstone is in the range of 1,740 – 2,070 meters (Stewart and Taylor, 1996). Therefore, only about one-quarter of the total stratigraphic separation in this area occurred since emplacement of the basalt.

The basalt can be used as a wide line to form a broad piercing point, because it had a limited original distribution. Using the geochemically identical basalt sections here and just to the SSW on the hanging wall, Stewart and Taylor (1996) determined a post-basalt slip vector ranging between 73°, N70°W and 75°, S18°W. This vector range is consistent with the limited number of slickenlines observed on the fault surface.

### **Long-Term Slip Rate Determined from Displaced Quaternary Basalt**

The basalt flows here exhibit reverse magnetization, and paleomagnetic vector analysis shows the hanging-wall basalt tilts 25 degrees toward the fault around a northeasterly trending axis, with little or no tilting of the footwall basalt (Lund and others, 2001, appendix C). Visual examination and dip measurements of the basalts in the hanging wall showed a pronounced tilt toward the fault in a relatively narrow zone - a few hundred meters wide - adjacent to the fault. Basalts west of the zone of back-tilting dip as much as 7 degrees toward the fault, but those dips mimic the slope of the alluvial-fan surfaces on which the flows were extruded.

Lund and Everitt (1998) recognized a zone of relatively small-displacement synthetic and antithetic faults in the basalts and alluvial-fan units in the hanging wall of the Hurricane fault below the radio towers and extending north from the Toquerville geometric bend. Hurlow and Biek (2000) mapped these faults at 1:24,000-scale in the Pintura quadrangle, which includes the Radio Towers site. Pairs of antithetic and synthetic faults in the hanging wall form several small grabens that roughly parallel the main Hurricane fault and define a zone of extensional stress along the axis of an asymmetric anticline created by reverse-drag folding in the hanging wall. Dip measurements in the basalt confirm the presence of the anticline, the axis of which defines the western limit of pronounced back-tilting toward the Hurricane fault.

Lund and others (2001) sampled the uppermost basalt flow in the hanging wall at the base of the Hurricane Cliffs directly below the Radio Towers site. The basalt yielded an  $^{40}\text{Ar}/^{39}\text{Ar}$  whole-rock age of  $0.81 \pm 0.1$  Ma.

The highest elevation on basalt west of the zone of back-tilting in the hanging wall is approximately 1,217 meters. The highest elevation on top of the correlative basalt in the footwall is approximately 1,585 meters. For their slip-rate calculation, Lund and others (2001) used the difference between those two elevations (368 m) as their value for net slip.

The slip rate at South Black Ridge for the past 810 thousand years is:

$$368,000 \text{ mm}/810,000 \text{ yr} = 0.45 \text{ mm/yr}$$

Because this slip rate is at a structural and possibly seismogenic fault boundary (Stewart and Taylor, 1996; Reber and others, 2001), it may or may not be typical of the long-term slip history of the proposed fault segments on either side of the boundary.

Turn around and return along same route to SR-17.

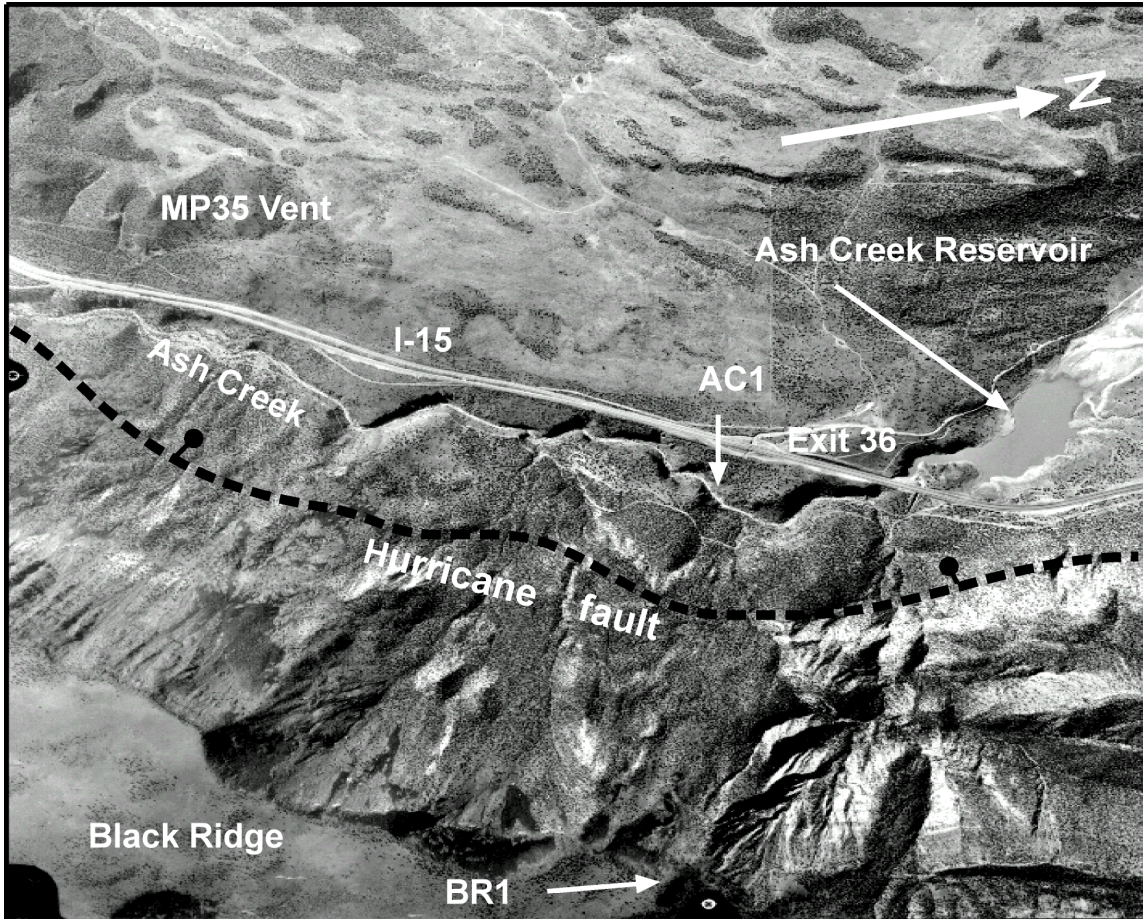
- 1.7 19.4 Pass fork on left (east) and continue along dirt road.
- 3.0 22.4 Cross cattle guard and continue southwest.
- 0.6 23.0 **Turn right (N)** off Spring Drive back onto SR-17 and immediately cross bridge over Ash Creek.
- 0.6 23.6 Road cut through the red Jurassic Navajo Sandstone. Near here dark-colored Quaternary basalt and bright orange-tan Quaternary dunes are visible.
- 1.8 25.4 **End SR-17, enter on ramp to I-15N.** Proceed north on I-15 paralleling the Hurricane Cliffs (Black Ridge). Hurricane fault is near the base of the cliffs, this is the Ash Creek segment of the Hurricane fault.
- 1.8 27.2 Quartz monzonite of the Pine Valley laccolith and orange and white Tertiary Claron Formation flank I-15 here. Both of these units are in the hanging wall of the Hurricane fault.
- 1.3 28.5 Hurricane fault at 2:00 between the dark-colored Quaternary basalt and the gray Permian rocks. This hanging wall basalt is geochemically distinct from Quaternary basalt in the footwall on the cliff top to the north. Because the basalts here are not correlative they were not used to calculate a long-term slip rate for the Hurricane fault.
- 4.3 32.8 Tree-covered hill at 9:00 is a cinder cone. Lund and Everitt (1998) designated this the MP-35 (milepost 35) cinder cone. This cone is the only known volcanic vent in the hanging wall of the Ash Creek segment, and is the likely source of much of the basalt in this area.
- 1.8 34.6 **Take Exit 36, Ranch Exit, to the right.**
- 0.1 34.7 Park near stop sign at bottom of off ramp.

**STOP 2-5. North Black Ridge** (Kolob Arch 7.5' quadrangle, T39S, R12W, section 16)

This stop is at about the midpoint of the proposed Ash Creek fault segment. Looking to the east, the Black Ridge (Hurricane Cliffs) in the Hurricane fault footwall consists of grayish tan Permian (Kaibab Formation) and reddish brown Mesozoic (Moenkopi and Chinle Formations) rocks capped by Quaternary basalt at the skyline. The sedimentary units and the Hurricane fault are covered by basalt talus, and in many places by hummocky topography that represents landslide deposits. The basalt exposed in road cuts here and in the walls of Ash Creek Gorge a few tens of meters west of this stop are in the fault hanging wall and are geochemically correlative with the basalt at the skyline (Lund and others, 2001, appendix B).

Lund and Everitt (1998) sampled the basalts in the footwall and the hanging wall and obtained  $^{40}\text{Ar}/^{39}\text{Ar}$  age estimates of  $0.84 \pm 0.03$  Ma and  $0.88 \pm 0.05$  Ma, respectively (figure 28). The two-sigma age uncertainties overlap and the two ages are considered analytically indistinguishable. Lund and others (2001) averaged the two age estimates for their slip rate calculation, and used 860 thousand years for the age of the basalts at this location.

Magnetic vectors obtained from the basalts in the footwall and hanging wall document 10 degrees of back-tilt toward the fault in the hanging wall around a northeasterly trending axis (Lund



**Figure 28. Oblique aerial view of North Black Ridge showing the location of the MP35 vent and  $^{40}\text{Ar}/^{39}\text{Ar}$  isotopic age sample locations BR1 and AC1. Ages: BR1 = 0.84 myr; AC1 = 0.88 myr.**

and others, 2001; appendix C). There is no indication of tilting in the footwall basalt. Visual examination of the basalts in the hanging wall showed that the zone of near-fault deformation is relatively narrow (a few hundred meters). Within a short distance west of the Exit 36 off ramp, the dip of the basalt toward the fault is generally less than 3 degrees, corresponding to the slope of the ground surface over which the basalt was extruded.

West of Exit 36 the basalt is displaced by a number of small synthetic and antithetic faults (Grant, 1995; Lund and Everitt, 1998). The displacement across these faults ranges from a few meters to possibly as much as ten meters. However, the faults are generally paired creating small graben; therefore, Lund and others (2001) consider the total net slip across this zone of secondary faulting minimal and of little net effect on slip-rate calculations.

Because the zone of near-fault deformation in the hanging wall is relatively narrow (a few hundred meters at most), Lund and others (2001) chose a basalt location at an elevation of 1,475 meters which, based on paleomagnetic analysis, visual observation, and dip measurements, is clearly west of the zone of near-fault deformation. They projected the basalt from that point at a dip of 3 degrees approximately 200 meters to the estimated location of the Hurricane fault, which at this site is buried by young landslide deposits. The resulting elevation of the basalt in the hanging wall at the Hurricane fault is 1,465 meters. Using that elevation and an elevation of 1,951 meters on top of the basalt in the footwall, results in a net slip across the fault at the north end of Black Ridge of 486 meters.

The slip rate at the north end of Black Ridge for the past 860 thousand years is:

486,000 mm/860,000 yr = 0.57 mm/yr

This slip rate is substantially higher than those obtained for the Anderson Junction segment at Grass Valley and Pah Tempe Hot Springs, and at the proposed segment boundary at the Toquerville geometric bend (table 1). It is also higher than Lund and Everitt's (1998) estimated slip rate of 0.39 mm/yr, but is based on information that was not available to them at the time of their earlier estimate.

- 1.9 36.6 Rounded peak at ~11:00 is the Tertiary Stoddard Mountain stock/laccolith, one of a series of Miocene intrusions that continues from the Pine Valley laccolith ~NE into the Colorado Plateau. These Miocene intrusions form the "iron axis", named for the abundant hematite-magnetite replacement bodies and veins formed within and adjacent to the intrusions. The iron deposits comprise the Iron Springs mining district, which was exploited from 1923 until the late 1970s.
- 1.5 38.1 Pass exit to Kolob entrance to Zion National Park. A strand of the Ash Creek segment of the Hurricane fault lies near the base of the cliff to the right (E).
- 1.5 39.6 **Take Exit 42 to the right (E).**
- 0.5 40.1 **Turn right (E)** at bottom of off ramp. Follow signs to Kanarraville.
- 0.1 40.2 **Turn left (~N).**
- 2.0 42.2 The Hurricane Cliffs on the right are formed mostly by gray Permian carbonates.
- 1.9 44.1 Enter Kanarraville.
- 0.8 44.9 Leave Kanarraville. At 2:00, the stratigraphic section is overturned in the footwall of the Hurricane fault. The Triassic Moenkopi Formation (red and tan) lies beneath the gray Permian Kaibab Limestone.
- 2.5 47.4 **Turn right (~SE)** onto Murie Creek road (dirt).
- 1.0 48.4 Park on the right side of the road.

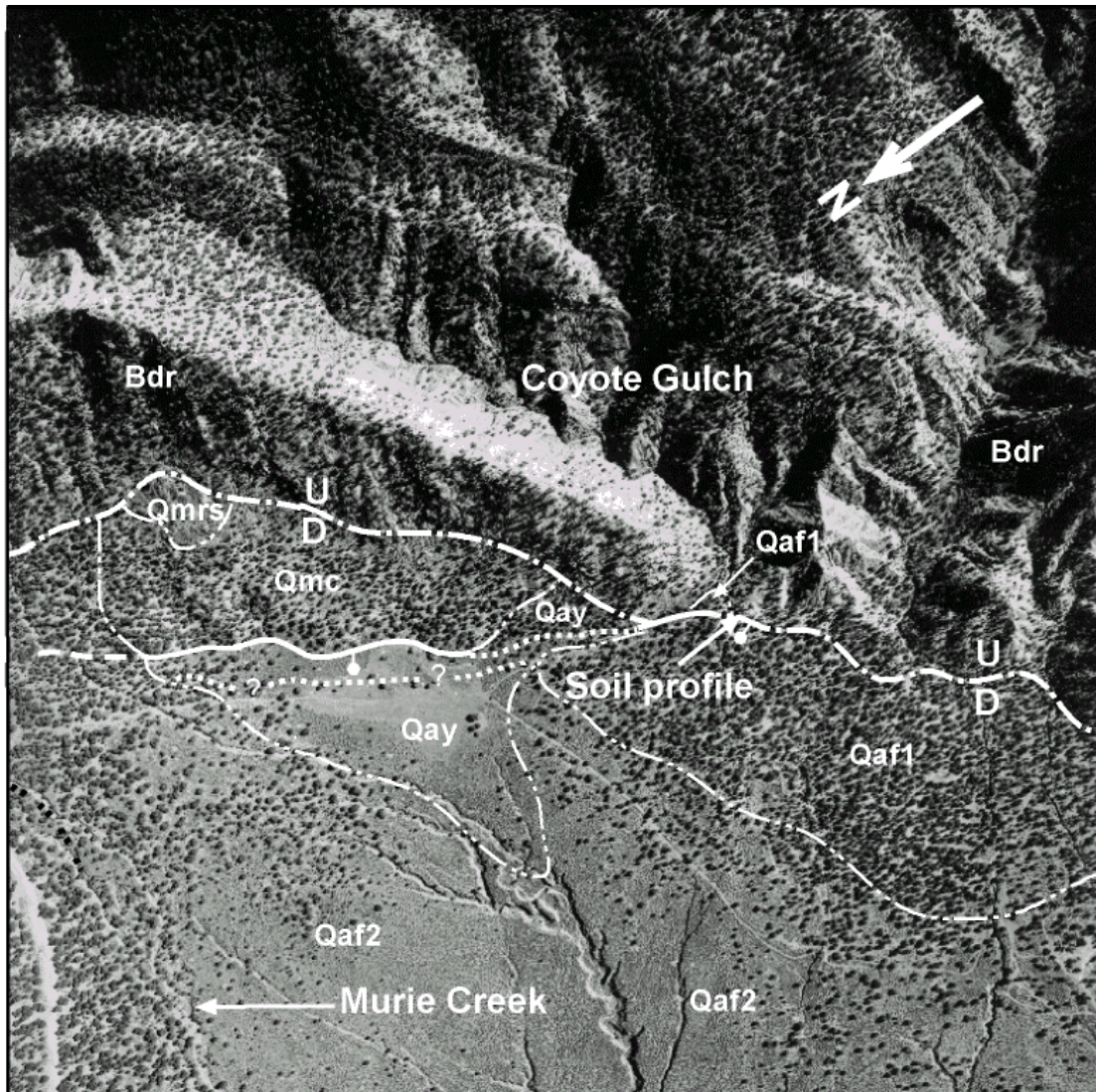
**STOP 2-6. Coyote Gulch** (Kanarraville 7.5' quadrangle, T37S, R12W, section 25)

Coyote Gulch is at the north end of the Ash Creek segment at the mouth of a small ephemeral drainage issuing from the Hurricane Cliffs about 1 kilometer southwest of Murie Creek. We will walk south along the Hurricane Cliffs to the best fault scarps formed on unconsolidated deposits on the Ash Creek segment. As we do, notice the rock units exposed in the cliff face in the fault footwall, the grayish tan Kaibab Formation and reddish brown Moenkopi Formation, which are overturned in the east limb of the Sevier-age Kanarra anticline.

The intermittent stream that flows from Coyote Gulch has deposited a young alluvial fan at the base of the Hurricane Cliffs (figure 29). The fan surface is displaced down-to-the-west across a partially buried approximately 3-meter-high, probable single-event fault scarp (Lund and Everitt, 1998). A few tens of meters north of the alluvial fan, a colluvial deposit at the base of the Hurricane Cliffs is also faulted and is displaced 10 meters down-to-the-west on a single fault strand. The two scarps at Coyote Gulch represent the best opportunity for developing detailed paleoseismic information at the north end of the Hurricane fault; however, the site is on private land and is not available for trenching.

Because they were unable to trench, Lund and others (2001) attempted to determine a maximum limiting age for the timing of the MRE at Coyote Gulch by dating the displaced alluvial-fan sediments. The fan is incised about 1.5 meters by the intermittent stream issuing from the gulch. The soil formed on the fan is very weakly developed, exhibiting minor rubification in a thin





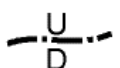
### EXPLANATION

**GEOLOGIC UNITS**  
 Qay Young alluvium  
 Qaf1 Young alluvial-fan deposits  
 Qaf2 Older alluvial-fan deposits  
 Qmc Slope colluvium  
 Qmrs Rock slide deposit (?)  
 Bdr Bedrock, undifferentiated

1/4 Mile

### SYMBOLS

 Geologic contact

 Main trace Hurricane fault, approximately located; U = upthrown side, D = downthrown side of fault.


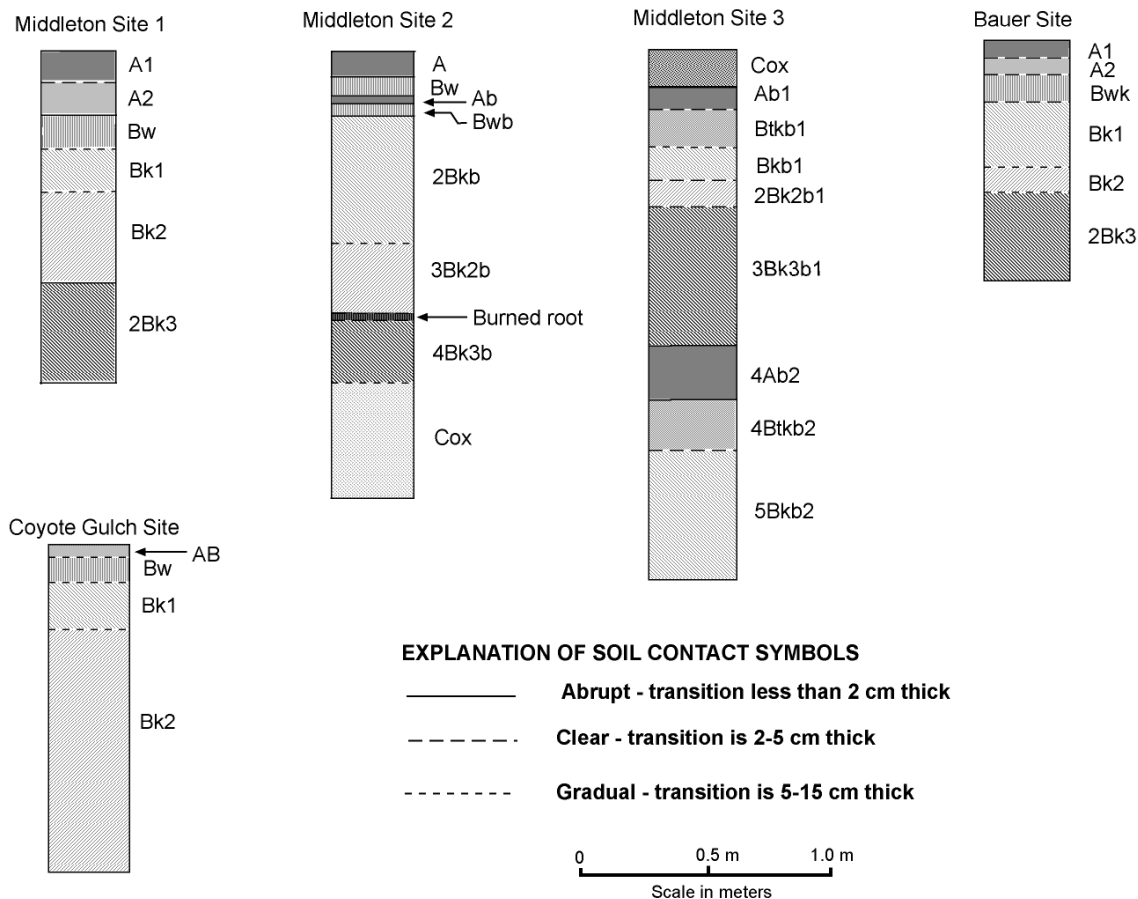
 Normal fault, bar and ball on downthrown side, dashed where approximately located, dotted where buried or inferred

Figure 29. Photo-geologic map of the Coyote Gulch site on the Hurricane fault, Utah, showing soil profile location.

Btw horizon, a weak Bk horizon that shows Stage I or Stage I-minus carbonate development, and generally weak or absent soil structure (figure 30).

A bulk sediment sample collected from an interval 15 to 128 centimeters below the fan surface yielded three very small fragments of detrital charcoal. None of the fragments were individually large enough for accelerator mass spectrometer (AMS) radiocarbon dating, so they were combined for dating. The combined sample yielded a conventional AMS radiocarbon age of  $1,220 \pm 40$  yr B.P. (Beta-140468), which calendar calibrates to 1,260 to 1,055 cal B.P. (cal A.D. 690 to 895). The calibrated age represents a maximum limiting age on the timing of the MRE at Coyote Gulch. The MRE occurred after 1,055 to 1,260 cal B.P., but how long after is unknown, nor is the actual age of the fan known, other than it is younger than the detrital charcoal contained within it.



**Figure 30. Soil profiles measured at the Coyote Gulch, Bauer, and Middleton sites, Hurricane fault, Utah.**

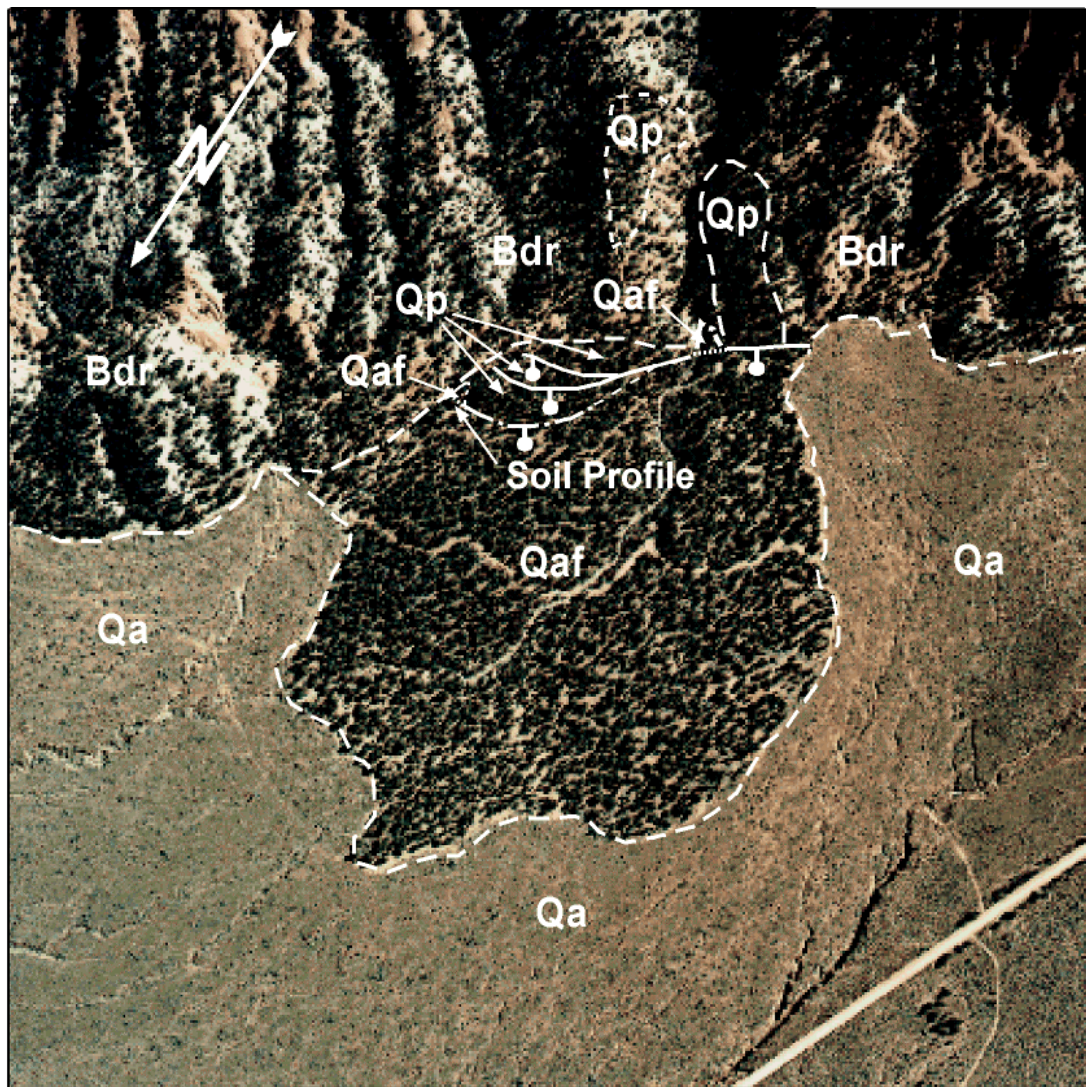
A scarp profile recorded a net slip of 2.75 meters across the single-event scarp at Coyote Gulch (Lund and Everitt, 1998). Data on event displacement are limited for the Hurricane fault in Utah, but the 2.75 meters measured here is the largest observed on the proposed Ash Creek segment, and if not the maximum value, it is likely a close approximation. Employing Wells and Coppersmith's (1994) regression of displacement and moment magnitude for maximum displacement on a normal fault, and assuming that the 2.75 meters represents the maximum displacement during the MRE, Lund and others (2001) estimated a moment magnitude of M 6.9 for the event that displaced the fan surface. If the 2.75 meters represents the average

displacement, using the appropriate Wells and Coppersmith (1994) regression for average displacement on a normal fault produces a moment magnitude of M 7.1.

Return to cars and proceed approximately east along the Murie Creek road.

- 0.6 49.0 The Hurricane fault displaces Quaternary basalt at 2:00. Basalt in the footwall is found on the cliffs at 1:00. Source of the basalt is a cinder cone at the top of the cliffs. This is Lund and others (2001) Section 19 site. Anderson and Mehnert (1979) also studied this site. Lund and others (2001) best estimate for a slip rate here is 0.37-0.51 mm/yr (table 1), depending on which basalt in the footwall is selected as being "in place."
- 0.2 49.2 Stay left at fork in the road by corrals (~ straight).
- 0.3 49.5 T intersection with a road from the right (~SE). Stay left (~ straight).
- 0.4 49.9 Y intersection, take the right fork (~ E).
- 0.1 50.0 Continue straight (left) toward wooden structure that is part of an old coal tram and tipple. Coal mined on Cedar Mountain was trammed to the valley floor here during the 1930s and 1940s.
- 0.2 50.2 At base station for coal tram, stay left (~NW).
- 0.3 50.5 Bauer Site at 1:00 (Lund and others, 2001)  
The Bauer site is in section 17, T. 37 S., R. 11 W. (Cedar Mountain 7.5' quadrangle), at the mouth of two small unnamed ephemeral drainages issuing from the Hurricane Cliffs about 2.6 kilometers southwest of Shurtz Creek. The drainages dissect a late Quaternary alluvial fan. The pediment/fan surface is displaced 5.5 meters down-to-the-west across three strands of the Hurricane fault (figure 31). The unnamed ephemeral streams have combined to deposit a young alluvial fan at the base of the Hurricane Cliffs where they enter the valley. The fan apex extends up the northernmost drainage a short distance, burying the western fault strand where it crosses the stream channel.  
Lund and others (2001) described the soil formed on the young alluvial fan. The soil is poorly developed, exhibiting some rubification in a thin Btw horizon, a weak Bk horizon expressed as Stage I or Stage I-minus carbonate development, and generally weak soil structure (figure 30). A bulk sediment sample collected from the soil 13 to 60 centimeters below the ground surface yielded several small fragments of detrital charcoal. Only one charcoal fragment was large enough to permit AMS radiocarbon dating. The charcoal fragment provided a conventional AMS radiocarbon age of 420±40 yr B.P. (Beta-140469), which calendar calibrates to both cal A.D. 1425 to 1515 (cal B.P. 525 to 435) and cal A.D. 1590 to 1620 (cal B.P. 360 to 330). Because the alluvial-fan deposit is not displaced, the calibrated age represents a minimum limiting age on the timing of the MRE at the Bauer site. The MRE occurred sometime before ~360 to 525 cal B.P., but how much before is not known, and because the charcoal was detrital, the deposit is younger than the AMS age estimate.
- 1.6 52.1 Pull off on the right side of the road.





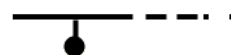
### EXPLANATION

**GEOLOGIC UNITS**  
 Qa Valley-fill alluvium  
 Qaf Alluvial-fan deposit  
 Qp Pediment-mantle deposit  
 Bdr Bedrock, undifferentiated

**SYMBOLS**  
 Geologic contact, dashed where approximately located

0 6000 12,000  
 Feet

Normal fault, bar and ball on downthrown side, dashed where approximately located, dotted where buried.



**Figure 31. Photo-geologic map of the Bauer site, Hurricane fault, Utah. Showing soil profile location (geology after Averitt, 1962).**



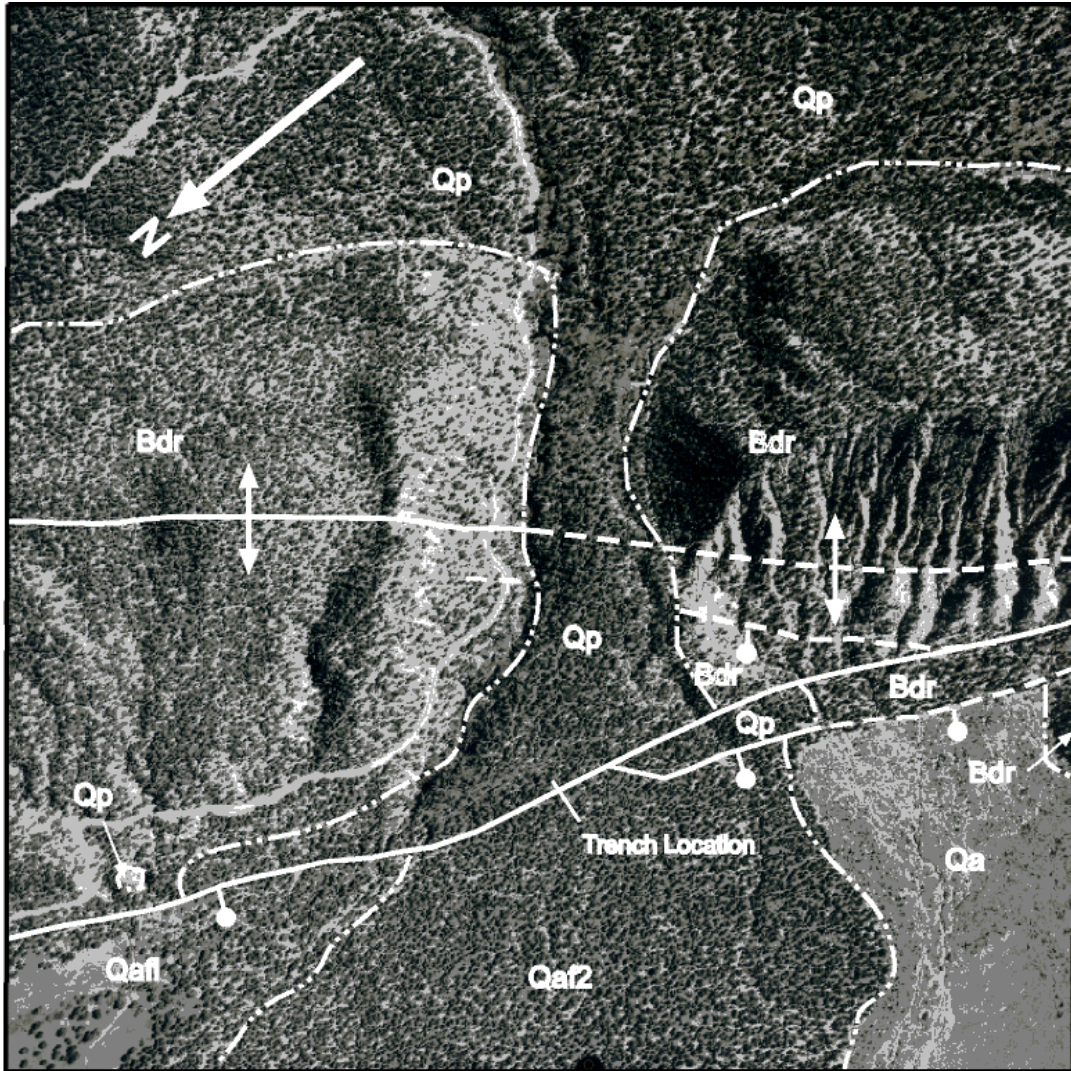
**STOP 2-7. Shurtz Creek Overview** (Cedar Mountain 7.5' quadrangle, T37S, R11W, section 9)

Shurtz Creek is on the newly proposed Cedar City seismogenic fault segment (figure 6). In the Hurricane Cliffs to the east, Mesozoic sedimentary rocks crop out in the Shurtz Creek drainage basin. Formations include the relatively soft Moenkopi and Chinle Formations with the more resistant Moenave, Kayenta, and Navajo Formations cropping out at higher elevations. The Sevier orogeny has deformed these units, and the axis of the Shurtz Creek (Kanarra) anticline (Averitt, 1962) is just east of and parallels the Hurricane fault, which lies at the base of the Hurricane Cliffs. Above these deformed units lie relatively undeformed Cretaceous and Cenozoic rocks including Quaternary basalt at the skyline. The Shurtz Creek pediment (Averitt, 1962) developed in the Shurtz Creek amphitheater, an area of relatively low elevation (middle distance) formed in the Hurricane Cliffs on the softer Mesozoic rock units.

The pediment is covered with large basalt boulders and is displaced across a 13-meter-high scarp (figure 32). Two ages of alluvial deposits are on the downthrown side of the fault; an active alluvial fan along Shurtz Creek, and an older alluvial deposit south of and a few meters higher than the young alluvial fan. This older alluvial surface is also covered with large basalt boulders. Lund and Everitt (1998) hypothesized that the older alluvial surface is correlative with the pediment surface in the footwall. Test pits showed that soils on both surfaces have moderate to well-developed argillic and calcic horizons, and gypsum is leached from both profiles confirming they are both older than Holocene. Soil colors are lighter (indicating more  $\text{CaCO}_3$ ), moist consistence is firmer (indicating higher secondary clay content), and clay films are more abundant in the pediment soil. Additionally, pH is  $< 8$  to a depth of 26 centimeters on the upthrown side, but  $< 8$  only to a depth of 8 centimeters for the soil on the downthrown block, indicating that  $\text{CaCO}_3$  removal has been more extensive on the upthrown side of the fault. The pediment soil exhibited Stage III carbonate development, while the soil on the downthrown block only reached Stage II. Based on these differences, the soil on the upthrown block is estimated to be up to twice as old as the soil on the downthrown block and therefore the surfaces are not correlative (Lund and Everitt, 1998).

Lund and Everitt (1998) sampled both surfaces at Shurtz Creek for  $^{26}\text{Al}$  (sandstone) and  $^{36}\text{Cl}$  (basalt) isotope abundances. The  $^{26}\text{Al}$  abundances clustered around 15,000 to 18,000 years. The  $^{36}\text{Cl}$  samples clustered at about 25,000 years. These young ages conflict with the soil-profile data, which argue for significantly older surface ages. Based on soil-profile development, the age of the upper surface is estimated at 80,000 to 100,000 years, and the age of the lower surface is estimated at about 50,000 years (Lund and Everitt, 1998). These estimates are in general agreement with ages assigned by Machette (1985a, 1985b) to soils with similar  $\text{CaCO}_3$  accumulations in the Beaver Basin 90 kilometers north of Shurtz Creek. The difference between the estimated soil ages and the cosmogenic isotope data is difficult to explain, but likely reflects the effect of presently poorly understood ongoing geomorphic processes on the two surfaces.

The Shurtz Creek scarp has a maximum slope angle of 28 degrees, and a minimum net vertical tectonic displacement (NVTD) of 10.5 meters (Lund and Everitt, 1998). Because the surfaces on either side of the fault are not correlative, the scarp height and NVTD are minimum values, and a slip rate calculated using the NVTD data would also be a minimum value. Additionally, neither the time interval since the most recent surface-faulting earthquake, nor the interval between development of the pediment surface and the first surface-faulting earthquake are known. Together those two intervals could represent several thousand years, and combine to leave the pediment surface age open ended across two seismic cycles (the first and the most recent events). A slip rate calculated using the age of the pediment surface would therefore be a minimum value because the slip actually occurred over a shorter time interval than the age of the surface. Because both the net-slip data and the pediment surface age tend to produce minimum values, a slip rate calculated using the combination of those data would give a minimum "best



**EXPLANATION**

- GEOLOGIC UNITS**
- Qa Valley-fill alluvium
  - Qaf1 Young alluvial-fan deposit
  - Qaf2 Older alluvial-fan deposit
  - Qp Pediment-mantle deposit
  - Bdr Bedrock, undifferentiated

1/4 Mile

**SYMBOLS**

--- Geologic contact

--- Shurtz Creek anticline

--- Normal fault, bar and ball on downthrown side, dashed where approximately located

Figure 32. Photo-geologic map of the Shurtz Creek site, Hurricane fault, Utah, showing trench location (geology after Averitt, 1962).

approximation” of late Quaternary fault slip at Shurtz Creek. The wide variation in age estimates for the pediment surface (cosmogenic versus geomorphic and soils) makes it possible to significantly change the slip rate value obtained by changing the time interval selected for the age of the surface. Choosing a younger age would give a higher slip rate, while selecting an older age would give a slower slip rate. Based on geomorphic expression and a lack of young appearing scarps north and south of Shurtz Creek, Lund and others (2001) chose 100,000 years as a “best estimate” for the age of the pediment surface, resulting in a minimum late Quaternary slip rate at Shurtz Creek of 0.11 mm/yr.

Trenching at Shurtz Creek (see figure 32 for trench location) to better constrain the slip rate and determine other paleoseismic parameters for the proposed Cedar City segment was hampered by large basalt boulders in the subsurface that limited the trench depth to less than 1.5 meters, preventing exposure of the fault zone (Lund and others, 2001). Because basalt boulders are ubiquitous along the scarp, Lund and others (2001) concluded that the chances of successful trenching anywhere on the Shurtz Creek scarp were low and rejected further excavation there. The remaining scarps on the Cedar City segment were also rejected because of access problems and equally prohibitive geologic constraints.

### **Mobil Shurtz Creek Seismic Reflection Line**

A seismic-reflection line by Mobil Exploration and Production Services U.S., Inc. (now part of ExxonMobil) crosses the Hurricane fault here (figure 33). Mobil collected this and several other seismic-reflection lines during a 1979-1981 data-acquisition program; the UGS recently obtained several of these lines as part of a hydrogeologic study of the Cedar City area (Hurlow, 2000; Hurlow, 2001).

Interpretation of the Mobil Shurtz Creek seismic-reflection line (figure 32) suggests that the Hurricane fault merges downward with a Late Cretaceous-Paleocene thrust ramp. The Hurricane fault may reactivate the listric thrust plane, or it may be relatively planar, departing from the thrust plane as its dip shallows to the northwest. This unresolved question has important implications for the seismic-hazard potential of the Hurricane fault in this area; the risk of a large earthquake is significantly greater in the planar-fault interpretation.

A Late Cretaceous-Paleocene anticline occupies the hanging wall of the Hurricane fault, as revealed by the geometry of reflectors and nearby outcrops and exploration wells. South of the Shurtz Creek line, the Oligocene-Eocene Claron Formation depositionally overlies the Jurassic Navajo Sandstone (Averitt, 1967; Anderson and Mehnert, 1979), as observed along the axis of the Pintura anticline to the south (Stop 2-3). The angular unconformity between the Claron Formation and underlying Mesozoic rocks shows that the anticline is at least in part pre-Tertiary. Normal displacement of the Permian-Triassic boundary is substantial. Refinement of the geologic interpretation of the Shurtz Creek seismic-reflection line and depth conversion would permit construction of a retrodeformable cross section, yielding substantial new information about the structural evolution of this area.

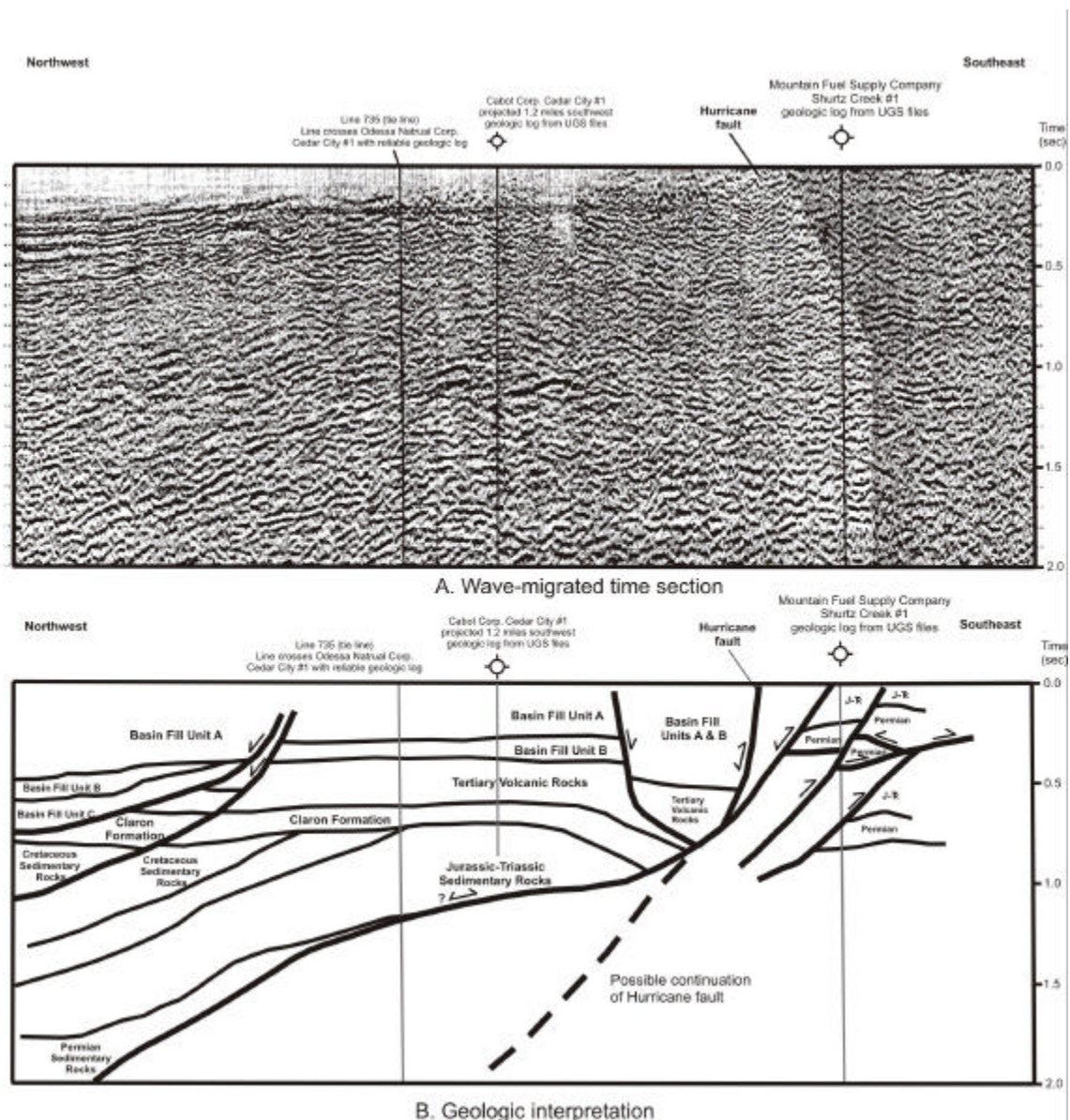
Continue north along the same road.

0.8 52.9 Bulldog fault expressed in basalt at 9:00 (Averitt, 1962).

0.5 53.4 Middleton site at ~ 1:00 (Lund and others, 2001).

The Middleton site is in section 4, T37S, R11W (Cedar Mountain 7.5' quadrangle) at the mouth of an unnamed drainage issuing from the Hurricane Cliffs about 1.3 kilometers northeast of Shurtz Creek. The drainage dissects a late Quaternary surface mapped by Averitt (1962) as “pediment deposits in the Shurtz Creek amphitheater.” The pediment surface is displaced 12.7 meters down-to-the-west across three strands of the Hurricane fault (Lund and Everitt, 1998; figure 34). The stream has deposited a young alluvial fan at the base of the cliffs where it enters the valley. The alluvial fan and an alluvial terrace that extends up the drainage from the fan apex combine to bury all three of the fault strands where they cross the stream and are not displaced.

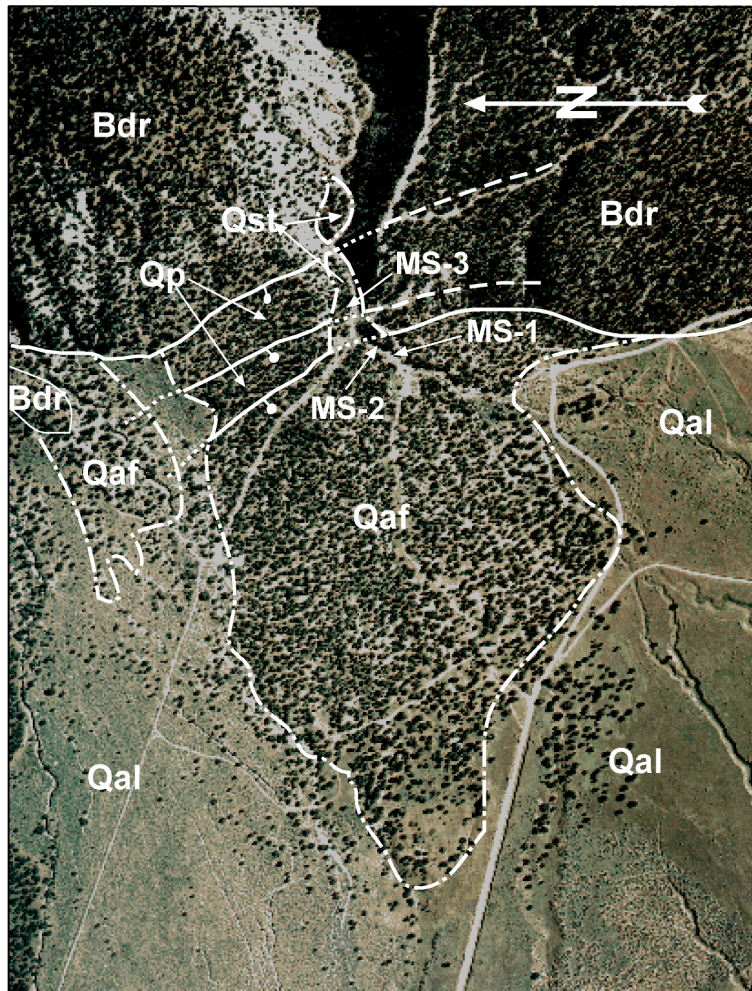




**Figure 33. Wave-migrated time section(A) and geologic interpretation (B) of Mobil Shurtz Creek seismic-reflection line 81MM-738. The geologic interpretation was made on a 1:12,000-scale plot of the wave-migrated time section. The image shown in (A) is a scanned and reduced version of that plot, and is of considerably lower quality than the original plot.**

Lund and others (2001) described three soil profiles at the Middleton site (figure 30), two on the young alluvial-fan deposit, and the third on the stream terrace. The profiles on alluvial-fan deposits consisted chiefly of coarse-grained debris-flow and debris-flood sediment. The stream terrace profile consisted chiefly of coarse fluvial and debris-flow material.

Lund and others (2001) submitted charcoal collected from the stream terrace profile for AMS radiocarbon dating. The charcoal came from the A horizon of a buried paleosol formed on a debris-flow/flood deposit at a depth of



EXPLANATION

GEOLOGIC UNITS  
 Qal Valley-fill alluvium  
 Qaf Alluvial-fan deposit  
 Qst Stream-terrace deposit  
 Qp Pediment-mantle deposit  
 Bdr Bedrock, undifferentiated

SYMBOLS  
 Geologic contact

0 6000 12,000  
 Feet

Normal fault, bar and ball  
 on downthrown side, dashed  
 where approximately located,  
 dotted where buried.

**Figure 34. Photo-geologic map of the Middleton site, Hurricane fault, Utah showing the locations of soil profiles MS-1, Ms-2, and MS-3 (geology after Averitt, 1962).**

117-139 centimeters. They selected this charcoal sample for dating because charcoal obtained from a soil A horizon is likely primary, accumulating during the soil-forming process, rather than detrital, having been entrained within a debris flow or flood and carried to the site from another location. The charcoal from the paleosol A horizon yielded a conventional AMS radiocarbon age of 1,710±40 yr B.P. (Beta-140470), which calendar calibrates to cal A.D. 240 to 420 (cal B.P. 1,710 to 1,530). This calibrated age represents a minimum limiting age for the timing of the MRE at Middleton.

The timing of the MRE at the Middleton site is older than the MRE at Coyote Gulch a few kilometers to the south. This difference in MRE timing is the principal evidence for the newly proposed Cedar City segment of the Hurricane fault.

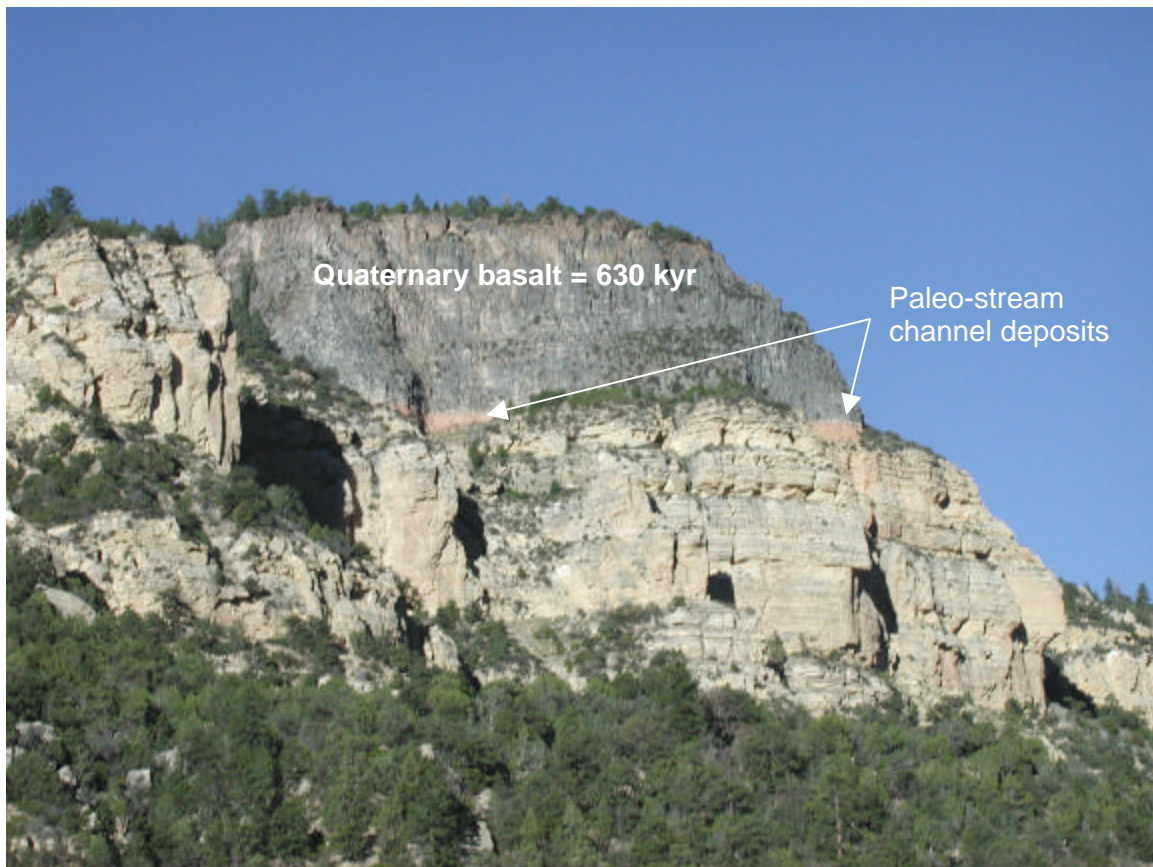
- 1.0 54.4 **Turn right (N)** onto paved road at T intersection and proceed toward Cedar City.
- 2.1 56.5 Late Pleistocene Green Hollow landslide at 9:00.
- 0.3 56.8 **Turn right (~N)** at intersection with Main Street and proceed into Cedar City. After the turn, note the Cedar City-Parowan monocline at 12:00.
- 0.9 57.7 Continue straight on Main (N) through stop light at 800 South.
- 0.3 58.0 Continue straight on Main (N) through stop light at 600 South.
- 0.2 58.2 Lupita's Mexican restaurant is on the right (E). Highly recommended by Bill. I bought Wanda her lunch there when we did our dry run of this trip and I think she agrees.
- 0.4 58.6 Continue straight on Main (N) through stop light at 200 South.
- 0.2 58.8 **Turn right (E)** at the intersection of Main and Center Streets. Proceed toward the Hurricane Cliffs following SR-14 up Cedar Canyon. The close bluffs are formed on Triassic Moenkopi Formation and Jurassic Navajo Sandstone.
- 0.5 59.3 We are crossing the Hurricane fault and entering the structural transition zone between the Basin and Range and the Colorado Plateau physiographic provinces.
- 0.3 59.6 At 9:00, the steeply dipping red to brown Moenkopi Formation is in the east limb of the Kanarra anticline.
- 0.3 59.9 Tan-gray Shinarump Conglomerate is on the left (N) with the purple-brown Petrified Forest Member of the Triassic Chinle Formation just beyond.
- 0.3 60.2 Contact between the Navajo Sandstone and the underlying Kayenta Formation is visible here.
- 0.5 60.7 Deformed Jurassic Carmel Formation containing thick deposits of white gypsum on the left (N). Several high-grade gypsum claims have been staked in this area.
- 1.6 62.3 Anticline on the right (S).
- 1.0 63.3 Cliffs on the left (N) are composed of Cretaceous sandstone.
- 0.4 63.7 Continue up canyon past road to the right that leads to Right Hand Canyon.
- 1.9 65.6 On the right (S) is a fault in Cretaceous units, just before milepost 7. On the east side of the fault, green and red mudstones of the nonmarine middle member of the Dakota Formation are flat lying. On the west (down) side of the fault, sandstone with interbedded thin coal seams of the Tibbet Canyon Member of the Straight Cliffs Formation are dragged nearly vertical (Eaton and others, 2001). At 10:00 the orange-colored Tertiary Claron Formation can be seen up a side canyon.



0.8 66.4 Pull off in wide spot on left side of the road.

**STOP 2-8. Cedar Canyon Basalt** (Flanigan Arch 7.5' quadrangle, T36S, R10W, section 25)

At this site, 12 kilometers east of Cedar City in the footwall of the Hurricane fault, erosion on Coal Creek has left a basalt remnant isolated high on a cliff above the stream on the north side of Cedar Canyon (figure 35). Coal Creek is graded to Cedar Valley and crosses the Hurricane fault at the mouth of Cedar Canyon. Lund and others (2001) believe that the rate of downcutting on Coal Creek is directly related to the rate of displacement on the Hurricane fault, which changes the stream's base level following each surface-faulting earthquake. Therefore, the rate of stream downcutting provides a surrogate slip rate for the Hurricane fault at Cedar City. However, because Cedar Valley is a closed basin, this slip rate is considered a minimum value due to the simultaneous filling of the valley, which slows the rate of downcutting from the maximum it would achieve if the sediment were carried away by a through-going drainage system.



**Figure 35. Remnant of 0.63 Ma basalt flow occupying a paleo-stream channel high on the north side of Cedar Canyon near milepost 7 on SR-14 east of Cedar City, Utah.**

Lund and others (2001) sampled the base of the basalt remnant in Cedar Canyon for both geochemistry and  $^{40}\text{Ar}/^{39}\text{Ar}$  age analysis. Because the remnant is well outside the influence of near-fault deformation in the fault footwall, back-tilting is not an issue. The basalt flow (possibly two stacked flows) occupies a narrow paleo-valley in Cretaceous bedrock and rests directly on paleo-channel deposits of Coal Creek. Diverted from its course by the basalt flow, Coal Creek eroded the soft Cretaceous sandstone adjacent to the basalt, and now occupies a new channel 335 meters below its former valley. The geochemical data show that the basalt

remnant is unrelated to any of the other basalt flows analyzed along the Hurricane fault. The  $^{40}\text{Ar}/^{39}\text{Ar}$  analysis yielded an age of  $0.63 \pm 0.10$  Ma.

The rate of downcutting by Coal Creek, which provides a surrogate minimum slip rate for the Hurricane fault, is:

$$335,000 \text{ mm}/630,000 \text{ yr} = 0.53 \text{ mm/yr}$$

Although considered a minimum value, this slip rate is generally comparable with the other rates obtained from displaced basalts north of the proposed seismogenic boundary between the Anderson Junction and Ash Creek segments at the Toquerville geometric bend.

Turn around and return to Cedar City (W) on SR-14.

- 3.4 69.8 Fault at 1:00 in Moenkopi Formation (red next to yellow-tan)
- 3.6 73.4 Enter Cedar City on SR-14/Center Street.
- 0.6 74.0 Continue straight on Center Street (W) through stop light at intersection between Center and Main streets.
- 0.3 74.3 Continue straight on Center Street (W) through stop light at intersection with 300 West.
- 0.4 74.7 Continue straight on Center Street (W) through stop light at intersection with 800 West.
- 0.2 74.9 **Turn left (S)** onto 1150 West.
- 0.2 75.1 **Turn right (W)** into parking lot on SUU campus.

**End trip.**

## REFERENCES

- Amoroso, Lee, Pearthree, P.A., and Arrowsmith, J.R., 2002, Paleoseismology and neotectonics of the Shivwitz section of the Hurricane fault, Mohave County, northwestern Arizona: Arizona Geological Survey Open-File Report 02-05, 92 p., 1 sheet, scale 1:24,000.
- Anderson, R.E., and Christenson, G.E., 1989, Quaternary faults, folds, and selected features in the Cedar City 1°x2° quadrangle, Utah: Utah Geological and Mineral Survey Miscellaneous Publication 89-6, 29 p.
- Anderson, R.E., and Mehnert, H.H., 1979, Reinterpretation of the history of the Hurricane fault in Utah, *in* Newman, G. W., and Goode, H. D., editors, 1979 Basin and Range Symposium: Rocky Mountain Association of Geologists, p. 145-165.
- Arabasz, W.J., and Julander, D.R., 1986, Geometry of seismically active faults and crustal deformation within the Basin and Range-Colorado Plateau transition in Utah, *in* Meyer, Larry, editor, Cenozoic Tectonics of the Basin and Range Province: A Perspective on Processes and Kinematics of an Extensional Origin: Boulder, Geological Society of America, Special Paper 208, p. 43-74.
- Armstrong, R.L., 1968, Sevier orogenic belt in Nevada and Utah: Geological Society of America Bulletin, v. 79, p. 429-458.
- Averitt, Paul, 1962, Geology and coal resources of the Cedar Mountain quadrangle, Iron County, Utah: U.S. Geological Survey Professional Paper 389, 71 p., 3 plates, scale 1:24,000.
- \_\_\_\_\_, 1964, Table of post-Cretaceous geologic events along the Hurricane fault, near Cedar City, Iron County, Utah: Geological Society of America Bulletin, v. 75, p. 901-908.



- \_\_\_\_\_, 1967, Geology of the Kanarrville quadrangle, Iron County, Utah: U.S. Geological Survey Map GQ-694, 1 plate, scale 1:24,000.
- Best, M.G., and Brimhall, W.H., 1974, Late Cenozoic alkalic basaltic magmas in the western Colorado Plateaus and Basin and Range transition zone, U.S.A., and their bearing on mantle dynamics: *Geological Society of America Bulletin*, v. 85, no. 11, p. 1677-1690.
- Best, M.G., McKee, E.H., and Damon, P.E., 1980, Space-time composition patterns of late Cenozoic mafic volcanism, southwestern Utah and adjoining areas: *American Journal of Science*, v. 280, p. 1035-1050.
- Biek, R.F., 1997, Interim geologic map of the Harrisburg Junction quadrangle, Washington County, Utah: Utah Geological Survey Open-file Report 353,123 p., scale 1:24,000.
- \_\_\_\_\_, 1998, Interim geologic map of the Hurricane quadrangle, Washington County, Utah: Utah Geological Survey Open-File Report, scale 1:24,000.
- Billingsley, G.H., 1991, Geologic map of the Sullivan Draw North quadrangle, northern Mohave County, Arizona: U.S. Geological Survey Open-File Report 91-558, scale 1:24,000.
- \_\_\_\_\_, 1992a, Geologic map of the Gyp Pocket quadrangle, northern Mohave County, Arizona: U.S. Geological Survey Open-File Report 92-412, scale 1:24,000.
- \_\_\_\_\_, 1992b, Geologic map of the Rock Canyon quadrangle, northern Mohave County, Arizona: U.S. Geological Survey Open-File Report 92-449, scale 1:24,000.
- \_\_\_\_\_, 1993a, Geologic map of the Wolf Hole Mountain and vicinity, Mohave County, northwestern Arizona, U.S. Geological Survey Map I-2296, scale 1:31,680.
- \_\_\_\_\_, 1993b, Geologic map of the Russell Spring quadrangle, northern Mohave County, Arizona: U.S. Geological Survey Open-File Report 93-717, scale 1:24,000.
- \_\_\_\_\_, 1993c, Geologic map of the Dutchman Draw quadrangle, northern Mohave County, Arizona: U.S. Geological Survey Open-File Report 93-587, scale 1:24,000.
- \_\_\_\_\_, 1993d, Geologic map of the Grandstand quadrangle, northern Mohave County, Arizona: U.S. Geological Survey Open-File Report 93-588, scale 1:24,000.
- \_\_\_\_\_, 1994a, Geologic map of the Antelope Knoll quadrangle, northern Mohave County, Arizona: U.S. Geological Survey Open-File Report 94-449, scale 1:24,000.
- \_\_\_\_\_, 1994b, Geologic map of the Moriah Knoll quadrangle, northern Mohave County, Arizona: U.S. Geological Survey Open-File Report 94-634, scale 1:24,000.
- Billingsley, G.H., and Workman, J.B., 2000, Geologic map of the Littlefield 30'x60' quadrangle, Mohave County, northwestern Arizona, with accompanying 25 page booklet: U.S. Geological Survey Miscellaneous Investigation Series Map I-2628, scale 1:100,000.
- Birkeland, P.W., 1984, *Soils and geomorphology*: New York, Oxford University Press, 372 p.
- Burgmann, R., Pollard, D.D., and Martel, S.J., 1994, Slip distributions on faults - Effects of stress gradients, inelastic deformation, heterogeneous host-rock stiffness, and fault interaction: *Journal of Structural Geology*, v. 16, p. 1675 -1690.
- Cartwright, J.A., Mansfield, C.S., and Trudgill, B. D., 1996, The growth of normal faults by segment linkage, *in* Buchanan, P.G., and Nieuwland, D.A., editors, *Modern developments in structural interpretation, validation, and modeling*: Geological Society of America Special Publication, v. 99, p. 163-177.
- Cartwright, J.A., Trudgill, B.D., and Mansfield, C.S., 1995, Fault growth by segment linkage; an explanation for scatter in maximum displacement and trace length data from the Canyonlands grabens of SE Utah: *Journal of Structural Geology*, v. 17, p. 1319-1326.
- Childs, C., Watterson, J., and Walsh, J.J., 1995, Fault overlap zones within developing normal fault systems: *Journal of the Geological Society of London*, v. 152, pt. 3, p. 535-549.
- Christenson, G.E., 1992, Geologic hazards of the St. George area, Washington County, Utah, *in* Harty, K.M., editor, *Engineering and environmental geology of southwestern Utah*: Utah Geological Association Publication 21, p. 99-107.
- Christenson, G.E., editor, 1995, The September 2, 1992 M<sub>L</sub> 5.8 St. George earthquake: Utah Geological Survey Circular 88, 41 p.
- Christenson, G.E., and Deen, R.D., 1983, *Engineering geology of the St. George area, Washington County, Utah*: Utah Geological and Mineral Survey Special Studies 58, 32 p., 2 plates.
- Christenson, G.E., Harty, K.M., and Hecker, Suzanne, 1987, Quaternary faults and seismic hazards in western Utah, *in* Kopp, R.S., and Cohenour, R.E., 1987, *Cenozoic geology of*

- western Utah - Sites for precious metal and hydrocarbon accumulation: Utah Geological Association Publication 16, p. 389-400.
- Christenson, G.E., and Nava, S.J., 1992, Earthquake hazards of southwestern Utah, *in* Harty, K.M., editor, Engineering and environmental geology of southwestern Utah: Utah Geological Association Publication 21, p. 123-137.
- Cook, E.F., 1953, Pine Valley laccolith, Washington County, Utah: Geological Society of America Bulletin, v. 64, p.1543.
- \_\_\_\_\_, 1957, Geology of the Pine Valley Mountains, Utah: Utah Geological and Mineralogical Survey Bulletin, v. 58, 111 p.
- \_\_\_\_\_, 1960, Geologic atlas of Utah, Washington County: Utah Geological and Mineralogical Survey Bulletin, v. 70, 119 p., 1 plate, scale 1:125,000.
- Cordova, R.M., 1981, Ground-water conditions in the upper Virgin River and Kanab Creek basins area, Utah, with emphasis on the Navajo Sandstone: State of Utah, Department of Natural Resources, Technical Publication No. 70, 87 p.
- Cowie, P.A., 1998, A healing-reloading feedback control on the growth rate of seismogenic faults: Journal of Structural Geology, v. 20, p. 1075-1087.
- Cowie, P.A., and Roberts, G.P., 2001, Constraining slip rates and spacings for active normal faults: Journal of Structural Geology, v. 23, p. 1901-1915.
- Cowie, P.A., and Scholz, C.H., 1992a, Displacement-length scaling relationship for faults; data synthesis and discussion: Journal of Structural Geology, v. 14, p. 1149-1156.
- \_\_\_\_\_, 1992b, Growth of faults by accumulation of seismic slip: Journal of Geophysical Research, v. 97, p. 11,085-11,095.
- Cowie, P.A., Sornette, D., and Vanneste, C., 1995, Multifractal scaling properties of a growing fault population: Geophysical Journal International, v. 122, p. 457-469.
- Dawers, N.H., Anders, M.H., and Scholz, C.H., 1993, Growth of normal faults - Displacement-length scaling: Geology, v. 21, p. 1107-1110.
- dePolo, C.M., Clark, D.G., Slemmons, D.B., and Ramallie, A., 1991, Historical Basin and Range Province surface faulting and fault segmentation: Journal of Structural Geology, v. 13, p. 123-136.
- Downing, R.F., Smith, E.I., Orndorff, R.I., Spell, T.L., and Zanetti, K.A., 2001, Imaging the Colorado Plateau – Basin and Range transition zone using basalt geochemistry, geochronology and geographic information systems, *in* Erskine, M.C., Faults, J.E., Bartley, J.M., and Rowley, P.D., editors, The geologic transition, High Plateaus to Great Basin – A symposium and field guide (The Mackin Volume): Utah Geological Association Publication 30 and Pacific Section American Association of Petroleum Geologists Publication GB 78, p. 127-154.
- DuBois, S.M., Smith, A.W., Nye, N.K. and Nowak, T.A., 1982, Arizona earthquakes, 1776-1980: Arizona Bureau of Geology and Mineral Technology Bulletin 193, 456 p.
- Dutton, C.E., 1880, Report on the geology of the high plateaus of Utah: Washington D.C., Department of the Interior, U.S. Geographical and Geological Survey of the Rocky Mountain Region (Powell), 307 p., atlas.
- Earth Sciences Associates, 1982, Seismic safety investigation of eight SCS dams in southwestern Utah: Portland, Oregon, unpublished consultant's report for the U.S. Soil Conservation Service, 2 vols.
- Eaton, J.G., Laurin, J., Kirkland, J.I., Tibert, N.E., Leckie, R.M., Sageman, B.B., Goldstrand, P.M., Moore, D.W., Straub, A.W., Cobban, W.A., and Dalebout, J.D., 2001, Cretaceous and early Tertiary geology of Cedar and Parowan Canyons, western Markagunt Plateau, Utah, *in* Erskine, M.C., Faults, J.E., Bartley, J.M., and Rowley, P.D., editors, The geologic transition, High Plateaus to Great Basin - A symposium and field guide (The Mackin Volume): Utah Geological Association Publication 30 and Pacific Section of the American Association of Petroleum Geologists Guidebook GB 78, p. 337-364.
- Fenton, C.R., Webb, R.H., Pearthree, P.A., Cerling, T.E., and Poreda, R.J., 2001, Displacement rates on the Toroweap and Hurricane faults - Implications for Quaternary downcutting in the Grand Canyon, Arizona: Geology, v. 29, p. 1035-1038.

- Gile, L.H., 1994, Soils, geomorphology, and multiple displacements along the Organ Mountains fault in southern New Mexico: New Mexico Bureau of Mines and Mineral Resources Bulletin 133, 91 p.
- Gile, L.H., and Grossman, R.B., 1979. The Desert Project soil monograph - Soils and landscapes of a desert region astride the Rio Grande Valley near Las Cruces, New Mexico: Soil Conservation Service Monograph, Department of Agriculture, 984 p.
- Goldstrand, P.M., 1994, Tectonic development of Upper Cretaceous to Eocene strata of southwestern Utah: Geological Society of America Bulletin, v. 106, p. 145-154.
- Grant, S. K., 1995, Geologic map of the New Harmony quadrangle, Washington County, Utah: Utah Geological Survey Miscellaneous Publication 95-2, 2 plates, scale 1:24,000.
- Grant, S.K., Fielding, L.W., and Noweir, M.A., 1994, Cenozoic fault patterns in southwestern Utah and their relationships to structures of the Sevier orogeny, *in* Blackett, R.E., and Moore, J.N., editors, Cenozoic geology and geothermal systems of southwestern Utah: Utah Geological Association Publication 23, p. 139-153.
- Gupta, S., Cowie, P.A., Dawers, N.H., and Underhill, J.R., 1998, A mechanism to explain rift-basin subsidence and stratigraphic patterns through fault-array evolution: *Geology*, v. 26, p. 595-598.
- Hacker, D.B. 1998, Catastrophic gravity sliding and volcanism associated with the growth of laccoliths - examples from early Miocene hypabyssal intrusions of the Iron Axis magmatic province, Pine Valley Mountains, southwestern Utah: Kent, Ohio, Kent State University, Ph.D. thesis, 258 p., 5 plates.
- Hamblin, W.K., 1963, Late Cenozoic basalts of the St. George basin, Utah, *in* Heylman, E.B., editor, Geology of the southwestern transition between the Basin-Range and Colorado Plateau, Utah: Intermountain Association of Petroleum Geologists, Guidebook to the Geology of Southwestern Utah, p. 84-89.
- \_\_\_\_\_, 1965a, Tectonics of the Hurricane fault zone, Arizona-Utah: Geological Society of America Special Paper 82, 83 p.
- \_\_\_\_\_, 1965b, Origin of "reverse drag" on the downthrown side of normal faults: Geological Society of America Bulletin, v. 76, p. 1145-1164.
- \_\_\_\_\_, 1970a, Late Cenozoic basalt flows of the western Grand Canyon, *in* Hamblin, W.K., and Best, M.G., editors, The western Grand Canyon region: Utah Geological Society Guidebook to the Geology of Utah, no. 23, p. 21-37.
- \_\_\_\_\_, 1970b, Structure of the western Grand Canyon region, *in* Hamblin, W.K., and Best, M.G., editors, The western Grand Canyon region: Utah Geological Society Guidebook to the Geology of Utah, no. 23, p. 3-20.
- \_\_\_\_\_, 1984, Direction of absolute movement along the boundary faults of the Basin and Range - Colorado Plateau margin: *Geology*, v. 12, p. 116-119.
- \_\_\_\_\_, 1987, Late Cenozoic volcanism in the St. George Basin, Utah: Geological Society of America Centennial Field Guide - Rocky Mountain Section, p. 291-294.
- Hamblin, W.K., and Best, M.G., 1970, The western Grand Canyon District: Utah Geological Society, Guidebook to the Geology of Utah, no. 23, 156 p.
- Hamblin, W.K., Damon, P.E., and Bull, W.B., 1981, Estimates of vertical crustal strain rates along the western margin of the Colorado Plateau: *Geology*, v. 9, p. 293-298.
- Hanks, T.C., 2000, The age of scarp-like landforms from diffusion-equation analysis, *in* Noller, J. S., Sowers, J. M., and Lettis, W.R., editors, Quaternary geochronology: Methods and applications: Washington D.C., American Geophysical Union, p. 313-338.
- Hanks, T.C., Bucknam, R.C., Lajoie, K.R., and Wallace, R.E., 1984, Modification of wave-cut and faulting-controlled landforms: *Journal of Geophysical Research*, v. 89, p. 5771-5790.
- Hecker, Suzanne, 1993, Quaternary tectonics of Utah with emphasis on earthquake-hazard characterization: Utah Geological Survey Bulletin 127, 157 p., 2 plates.
- Higgins, J.M., 1998, Interim geologic map of the Washington Dome quadrangle, Washington County, Utah: Utah Geological Survey Open-file Report 363, 106 p., scale 1:24,000.
- \_\_\_\_\_, 2000, Interim geologic map of The Divide 7.5' quadrangle, Washington County, Utah: Utah Geological Survey Open-File Report 378, 61 p., scale 1:24,000.
- Huntington, Ellsworth, and Goldthwait, J.W., 1904, The Hurricane fault in southwestern Utah: *Journal of Geology*, v. 11, p. 45-63.

- \_\_\_\_\_, 1905, The Hurricane fault in the Toquerville district, Utah: Harvard College, Bulletin of the Museum of Comparative Zoology, v. 42, p.199-259.
- Huntoon, P., 1990, Phanerozoic structural geology of the Grand Canyon, *in* Beus, S. S., and Morales, M., editors, Grand Canyon Geology: New York, Oxford University Press/Museum of Northern Arizona, p. 261-309.
- Hurlow, H.A., 1998, The geology of the central Virgin River basin, southwestern Utah, and its relation to ground-water conditions: Utah Geological Survey Water-Resources Bulletin 26, 53 p., 6 plates.
- \_\_\_\_\_, 2000, Complex evolution of Neogene extensional faulting and basin subsidence in the eastern Basin and Range Province, Cedar Valley, southwestern Utah – Evidence from seismic reflection data [abs]: Geological Society of America Abstracts with Programs, v. 32, no. 7, p. A-506.
- \_\_\_\_\_, 2001, Influence of Neogene extensional structure and stratigraphy on the hydrogeology of Cedar Valley, southwestern Utah [abs]: Geological Society of America Abstracts with Programs, v. 33, no. 5, p. A-16.
- Hurlow, H.A., and Biek, R.F., 2000, Interim geologic map of the Pintura quadrangle, Washington County, Utah: Utah Geological Survey Open-File Report 375, 67 p., scale 1:24,000.
- Jackson, J., and Leeder, M., 1994, Drainage systems and the development of normal faults - An example from Pleasant Valley, Nevada: Journal of Structural Geology, v. 16, p. 1041-1059.
- King, G.C.P., 1986, Speculations on the geometry of the initiation and termination processes of earthquake rupture and its relation to morphology and geological structure: Pageoph, v. 124, p. 567–583.
- Kurie, A. E., 1966, Recurrent structural disturbance of the Colorado Plateau margin near Zion National Park, Utah: Geological Society of America Bulletin, v. 77, p. 867-872.
- Larsen, P.H., 1988, Relay structures in a Lower Permian basement-involved extension system, east Greenland: Journal of Structural Geology, v. 10, p. 3-8.
- Lay, Thorne, Ritsema, J., Ammon, C.J., and Wallace, T.C., 1994, Rapid source mechanism analysis of the April 29, 1993 Cataract Creek (Mw 5.3), northern Arizona earthquake: Bulletin of the Seismological Society of America, v. 84, p. 451-457.
- Lovejoy, E.M.P., 1964, The Hurricane fault zone and the Cedar Pocket-Shebit-Gunlock fault complex, southwestern Utah and northwestern Arizona: Tucson, Arizona, University of Arizona Ph.D. dissertation, 195 p., scale 1:125,000.
- Lund, W.R., and Everitt, B.L., 1998, Reconnaissance paleoseismic investigation of the Hurricane fault in southwestern Utah, *in* Pearthree and others, 1998, Paleoseismic investigations of the Hurricane fault in southwestern Utah and northwestern Arizona - Final Project Report: Arizona Geological Survey (Tucson) and Utah Geological Survey (Salt Lake City), Final Technical Report to the U.S. Geological Survey National Earthquake Hazard Reduction Program, Award No. 1434-HQ-97-GR-03047, p. 8-48.
- Lund, W.R., Pearthree, P.A., Amoroso, Lee, Hozik, M.J., and Hatfield, S.C., 2001, Paleoseismic investigation of earthquake hazard and long-term movement history of the Hurricane fault, southwestern Utah and northwestern Arizona: Utah Geological Survey (Salt Lake City) and Arizona Geological Survey (Tucson), Final Technical Report to the U.S. Geological Survey National Earthquake Hazard Reduction Program, Award No. 99HQGR0026, 71 p., 5 appendices.
- Machette, M.N., 1985a, Calcic soils of the southwestern United States, *in* Weide, D.L., Farber, M.L., editors, Soils and Quaternary geology of the southwestern United States: Geological Society of America Special Paper 203, p. 1-21.
- \_\_\_\_\_, 1985b, Late Cenozoic geology of the Beaver basin, southwestern Utah: Brigham Young University Geology Studies, v.32, pt. 1, p. 19-37.
- Machette, M.N., Personius, S.F., and Nelson, A.R., 1992, Paleoseismology of the Wasatch fault zone – A summary of recent investigations, interpretations, and conclusions, *in* Gori, P.L., and Hays, W.W., editors, Assessment of regional earthquake hazard and risk along the Wasatch Front, Utah: U.S. Geological Survey Professional Paper 1500, p. A1-A59.
- Maerten, L., Gillespie, P., and Pollard, D.D., 2002, Effects of local stress perturbation on secondary fault development: Journal of Structural Geology, v. 24, p. 145-153.

- Mansfield, C., and Cartwright, J., 2001, Fault growth by linkage: Observations and implications from analogue models: *Journal of Structural Geology*, v. 23, p. 745 – 763.
- Mayer, L., 1985, Tectonic geomorphology of the Basin and Range-Colorado Plateau boundary in Arizona, *in* Morisawa, M., and Hack, J.T., editors, *Tectonic geomorphology - Proceedings of the 15th Annual Binghamton Geomorphology Symposium, September 1984*: Boston, Allen and Unwin, p. 235-259.
- McCalpin, J.P., and Nelson, A.R., 1996, Introduction to Paleoseismology, *in* McCalpin, J.P., editor, *Paleoseismology*: San Diego, Academic Press, p. 1-32.
- McCalpin, J.P., Zuchiewicz, W., and Jones, L.C.A., 1993, Sedimentology of fault-scarp derived colluvium from the Borah Peak rupture, central Idaho: *Journal of Sedimentary Petrology*, v. 63, no. 1, p. 120-130.
- McDuffie, S., and Marsh, B.D., 1991, Pine Valley Mountain laccolith; a thick, dacitic, phenocryst-rich body [abs]: *Eos, Transactions, American Geophysical Union*, v. 72, p. 316.
- Menges, C.M., and Pearthree, P.A., 1983, Map of neotectonic (latest Pliocene-Quaternary) deformation in Arizona: Arizona Bureau of Geology and Mineral Technology Open-File Report 83-22, 48 p. booklet, 2 plates.
- Nash, D. B., 1980, Morphologic dating of degraded normal fault scarps: *Journal of Geology*, v. 88, p. 353-360.
- Ostenaar, Dean, 1984, Relationships affecting estimates of surface fault displacement based on scarp-derived colluvium deposits [abs]: *Geological Society of America Abstracts with Programs*, v. 16, no. 5, p. 327.
- Peacock, D.C.P., 1991, Displacements and segment linkage in strike-slip fault zones: *Journal of Structural Geology*, v. 13, p. 1025-1035.
- Peacock, D.C.P., and Sanderson, D.J., 1991, Displacements, segment linkage, and relay ramps in normal fault zones: *Journal of Structural Geology*, v. 13, p. 721-733.
- \_\_\_\_\_, 1994, Geometry and development of relay ramps in normal fault zones: *American Association of Petroleum Geologists Bulletin*, v. 78, p. 147-165.
- \_\_\_\_\_, 1996, Effects of propagation rate on displacement variations along faults: *Journal of Structural Geology*, v. 18, p. 311-320.
- Pearthree, P.A., 1998, Quaternary fault data and map for Arizona: Arizona Geological Survey Open-File Report 98-24, 122 p., scale 750,000.
- Pearthree, P.A., and Bausch, D.B., 1999, Earthquake hazards in Arizona: Arizona Geological Survey Map M-34, scale 1:1,000,000.
- Pearthree, P.A., Lund, W.R., Stenner, H.D., and Everitt, B.L., 1998, Paleoseismic investigation of the Hurricane fault in southwestern Utah and northwestern Arizona - Final project report: Arizona Geological Survey (Tucson) and Utah Geological Survey (Salt Lake City), Final Technical Report to the U.S. Geological Survey National Earthquake Hazard Reduction Program, Award No. 1434-HQ-97-GR-03047, 131 p.
- Pearthree, P.A., Menges, C.M., and Mayer, Larry, 1983, Distribution, recurrence, and possible tectonic implications of late Quaternary faulting in Arizona: Arizona Bureau of Geology and Mineral Technology Open-File Report 83-20, 36 p.
- Pechmann, J.C., Arabasz, W.J., and Nava, S.J., 1995, Seismology, *in* Christenson, G.E., editor, *The September 2, 1992 M<sub>L</sub> 5.8 St. George earthquake, Washington County, Utah*: Utah Geological Survey Circular 88, p. 1.
- Pollard, D.D., and Aydin, A., 1984, Propagation and linkage of oceanic ridge segments: *Journal of Geophysical Research*, v. 89, p. 10,017-10,028.
- Pollard, D.D., and Segall, P., 1987, Theoretical displacements and stresses near fractures in rock - With applications to faults, joints, veins, dikes, and solution surfaces, *in* Atkinson, B.K., editor, *Fracture Mechanics of Rock*: London, Academic Press, p. 277-349.
- Reber, S., Taylor, W.J., Stewart, M., and Schiefelbein, I.M., 2001, Linkage and reactivation along the northern Hurricane and Sevier faults, southwestern Utah, *in* Erskine, M.C., Faults, J.E., Bartley, J.M., and Rowley, P.D., editors, *The geologic transition, High Plateaus to Great Basin – A symposium and field guide (The Mackin Volume)*: Utah Geological Association Publication 30 and Pacific Section American Association of Petroleum Geologists Publication GB 78, p. 379-400.

- Reynolds, S.J., Florence, F.P., Welty, J.W., Roddy, M.S., Currier, D.A., Anderson, A.V., and Keith, S.B., 1986, Compilation of radiometric age determinations in Arizona: Arizona Bureau of Geology and Mineral Technology Bulletin 197, 258 p., 2 sheets, scale 1:1,000,000.
- Sanchez, Alexander, 1995, Mafic volcanism in the Colorado Plateau/Basin and Range transition zone, Hurricane, Utah: Las Vegas, Masters thesis, Department of Geoscience, University of Nevada, 92 p.
- Schlische, R.W., 1993, Anatomy and evolution of the Triassic-Jurassic continental rift system, eastern North America: *Tectonics*, v. 12, p.1026-1042.
- Schlische, R.W., and Anders, M.H., 1996, Stratigraphic effects and tectonic implications of the growth of normal faults and extensional basins, *in* Beratan, K.K., editor, *Reconstructing the history of Basin and Range extension using sedimentology and stratigraphy*: Geological Society of America Special Paper, v. 303, p. 183-203.
- Schramm, M.E., 1994, Structural analysis of the Hurricane fault in the transition zone between the Basin and Range Province and the Colorado Plateau, Washington County, Utah: Las Vegas, Masters thesis, Department of Geosciences, University of Nevada, 90 p.
- Schwartz, D.P., and Coppersmith, K.J., 1984, Fault behavior and characteristic earthquakes: Examples from the Wasatch and San Andreas fault zones: *Journal of Geophysical Research*, v. 89, p. 5681-5698.
- Schwartz, D.P., and Crone, A.J., 1985, The 1983 Borah Peak earthquake: A calibration event for quantifying earthquake recurrence and fault behavior on Great Basin normal faults, *in* Stein, R.S. and Bucknam, R.C., editors, *Proceedings of Workshop XXVIII on the Borah Peak, Idaho earthquake*: U.S. Geological Survey Open-File Report 85-290, p. 153-160.
- Segall, P., and Pollard, D.D., 1980, Mechanics of discontinuous faults: *Journal of Geophysical Research*, v. 85, p. 4337-4380.
- Shipton, Z.K., and Cowie, P.A., 2001, Damage zone and slip-surface evolution over  $\mu\text{m}$  to km scales in high-porosity Navajo Sandstone, Utah: *Journal of Structural Geology*, v. 23, p. 1825-1844.
- Smith, R.B., and Arabasz, W.J., 1991, Seismicity of the Intermountain seismic belt, *in* Slemmons, D.B., Engdahl, E.R., Zoback, M.D., and Blackwell, D.D., editors, *Neotectonics of North America*: Boulder, Colorado, Geological Society of America, Decade Map Volume, p. 185-228.
- Smith, R.B., and Sbar, M.L., 1974, Contemporary seismicity in the Intermountain seismic belt: *Geological Society of America Bulletin*, v. 85, p. 1205-1218.
- Sorauf, J.E., and Billingsley, G.H., 1991, Members of the Toroweap and Kaibab Formations, lower Permian, northern Arizona and southwestern Utah: *The Mountain Geologist*, v. 28, no. 1, p. 9-24.
- Spencer, J.E., and Reynolds, S.J., 1989, Middle Tertiary tectonics of Arizona and adjacent areas, *in* Jenney, J. P., and Reynolds, S. J., editors, *Geologic Evolution of Arizona*: Tucson, Arizona Geological Society Digest 17, p. 539-574.
- Stenner, H.D., Lund, W.R., Pearthree, P.A., and Everitt, B.L., 1999, Paleoseismologic investigations of the Hurricane fault in northwestern Arizona and southwestern Utah: Arizona Geological Survey Open-File Report. 99-8, 138 p.
- Stewart, M.E., and Taylor, W.J., 1996, Structural analysis and fault segment boundary identification along the Hurricane fault in southwestern Utah: *Journal of Structural Geology*, v. 18, p. 1017-1029.
- Stewart, M.E., Taylor, W.J., Pearthree, P.A., Solomon, B.J., and Hurlow, H.A., 1997, Neotectonics, fault segmentation, and seismic hazards along the Hurricane fault in Utah and Arizona: An overview of environmental factors in an actively extending region: *Brigham Young University Geologic Studies* 1997, v. 42, part II, p. 235-277.
- Taylor, W.J., Stewart, M.E., and Orndorff, R.L., 2001, Definition of fault segments from bedrock data - Segmentation of the Hurricane fault, southwestern Utah and Northern Arizona: *Utah Geological Association Publication* 30, p. 113-126.
- Timmons, J.M., Karlstrom, K.E., Dehler, C.M., Geissman, J.W., and Heizler, M.T., 2001, Proterozoic multistage (ca. 1.1 and 0.8 Ga) extension recorded in the Grand Canyon

- Supergroup and establishment of northwest- and north-trending tectonic grains in the Southwestern United States: *Geological Society of America Bulletin*, v.113, p.163-180.
- Trudgill, B., and Cartwright, J., 1994, Relay-ramp forms and normal-fault linkages, Canyonlands National Park, Utah: *Geological Society of America Bulletin*, v. 106, p. 1143-1157.
- Wallace, R. E., 1977, Profiles and ages of young fault scarps, north-central Nevada: *Geological Society of America Bulletin*, v. 88, p. 1267-1281.
- Walsh, J.J., and Watterson, J., 1987, Distributions of cumulative displacement and seismic slip on a single normal fault: *Journal of Structural Geology*, v. 9, p. 1039-1046.
- \_\_\_\_\_, 1991, Geometric and kinematic coherence and scale effects in normal fault systems: *Geological Society Special Publications*, v. 56, p.193-203.
- Walsh, J.J., Watterson, J., Bailey, W.R., and Childs, C., 1999, Fault relays, bends, and branch-lines: *Journal of Structural Geology*, v. 21, p. 1019-1026.
- Wells, D.L., and Coppersmith, K.J., 1994, New empirical relationships between magnitude, rupture length, rupture width, rupture area, and surface displacement: *Bulletin of the Seismological Society of America*, v. 84, p. 974-1002.
- Wenrich, K.J., Billingsley, G.H., Blackerby, B.A., 1995, Spatial migration and compositional changes of Miocene-Quaternary magmatism in the western Grand Canyon: *Journal of Geophysical Research*, v. 100, p.10,417-10,440.
- Willemse, E.J.M., 1997, Segmented normal faults: Correspondence between three-dimensional mechanical models and field data: *Journal of Geophysical Research*, v. 102, p. 675-692.
- Willemse, E.J.M, and Pollard, D.D., 2000, Normal fault growth; evolution of tipline shapes and slip distribution, *in* Lehner, F.K., and Urai, J.L., editors, *Aspects of tectonic faulting*: Springer,
- Willemse, E.J.M., Pollard, D.D., Aydin, A., 1996, Three-dimensional analyses of slip distributions on normal fault arrays with consequences for fault scaling: *Journal of Structural Geology*, v. 18, p. 295-309.
- Williams, J.S., and Trapper, M.L., 1953, Earthquake history of Utah: *Bulletin of the Seismological Society of America*, v. 43, p. 191-218.
- Willis, G.C., and Higgins, J.M., 1995, Interim geologic map of the Washington quadrangle, Washington County, Utah: *Utah Geological Survey Open-File Report 324*, 2 plates, scale 1:24,000.
- Yelken, M.A., 1996, Trace element analysis of selected springs in the Virgin River basin: M.S. thesis, University of Nevada, Las Vegas, 156 p.
- Young, M.J., Gawthorpe, R.L., and Hardy, S., 2001, Growth and linkage of a segmented normal fault zone; the Late Jurassic Murchison-Statfjord North Fault, northern North Sea: *Journal of Structural Geology*, v. 23, p.1933-1952.
- Zhang, P., Slemmons, D.B., and Mao, F., 1991, Geometric pattern, rupture termination, and fault segmentation of the Dixie Valley-Pleasant Valley active normal fault system, Nevada, U.S.A.: *Journal of Structural Geology*, v.13, no. 2, p. 165-176.